General Disclaimer

One or more of the Following Statements may affect this Document

- This document has been reproduced from the best copy furnished by the organizational source. It is being released in the interest of making available as much information as possible.

- This document may contain data, which exceeds the sheet parameters. It was furnished in this condition by the organizational source and is the best copy available.

- This document may contain tone-on-tone or color graphs, charts and/or pictures, which have been reproduced in black and white.

- This document is paginated as submitted by the original source.

- Portions of this document are not fully legible due to the historical nature of some of the material. However, it is the best reproduction available from the original submission.

Produced by the NASA Center for Aerospace Information (CASI)

November, 1975

Report ESL-R-632
Contract DOT-TSC-982
NASA/Ames Grant NGL-22-009-124

(NASA-CR-146127) DESIGN AND SIMULATION OF A DESCENT CONTROLLER FOR STRATEGIC FOUR-DIMENSIONAL AIRCRAFT NAVIGATION M.S. Thesis (Massachusetts Inst. of Tech.) 206 p HC $7.75 CSCL 17G G3/04 N76-16058 Unclas 08587

DESIGN AND SIMULATION OF A DESCENT CONTROLLER FOR STRATEGIC FOUR-DIMENSIONAL AIRCRAFT NAVIGATION

Frederick M. Lax

RECEIVED
NASA STI FACILITY
INPUT BRANCH

Electronic Systems Laboratory *Decision and Control Sciences Group*

MASSACHUSETTS INSTITUTE OF TECHNOLOGY, CAMBRIDGE, MASSACHUSETTS 02139

Department of Electrical Engineering and Computer Science

November, 1975 Report ESL-R-632

DESIGN AND SIMULATION OF A DESCENT CONTROLLER FOR STRATEGIC FOUR-DIMENSIONAL AIRCRAFT NAVIGATION

by

Frederick M. Lax

This report is based on the unaltered thesis of Frederick M. Lax, submitted in partial fulfillment of the requirements for the degree of Master of Science at the Massachusetts Institute of Technology in August, 1975. The research was conducted at the Decision and Control Sciences Group of the M.I.T. Electronic Systems Laboratory. Mr. Lax was supported in part as a research fellow by the Bell Telephone Laboratories, Inc. OYOC Education Program; also partial support was extended by the Department of Transportation, Transportation Systems Center, under contract DOT-TSC-982 and by NASA/Ames under grant NGL-22-009-124.

Electronic Systems Laboratory
Department of Electrical Engineering and Computer Science
Massachusetts Institute of Technology
Cambridge, Massachusetts 02139

DESIGN AND SIMULATION OF A DESCENT CONTROLLER FOR STRATEGIC FOUR-DIMENSIONAL AIRCRAFT NAVIGATION

by

Frederick Morgan Lax

BSEE, University of Notre Dame
(1974)

SUBMITTED IN PARTIAL FULFILLMENT OF THE

REQUIREMENTS FOR THE DEGREE OF

MASTER OF SCIENCE

at the

MASSACHUSETTS INSTITUTE OF TECHNOLOGY

September, 1975

Signature of Author.....Frederick M. Lax.....
Department of Electrical Engineering and
Computer Science, August 11, 1975

Certified by..Timothy L. Johnson.....
Thesis Supervisor

Accepted by.....
Chairman, Departmental Committee on Graduate Students

DESIGN AND SIMULATION OF A DESCENT CONTROLLER FOR STRATEGIC FOUR-DIMENSIONAL AIRCRAFT NAVIGATION

by

Frederick Morgan Lax

Submitted to the Department of Electrical Engineering and Computer Science on August 11, 1975, in partial fulfillment of the requirements for the Degree of Master of Science.

ABSTRACT

A time-controlled navigation system applicable to the descent phase of flight for airline transport aircraft has been developed and simulated. The design contained herein incorporates the linear discrete-time sampled-data version of the linearized continuous-time system describing the aircraft's aerodynamics. Using optimal linear quadratic control techniques, an optimal deterministic control regulator which is implementable on an airborne computer is designed. The navigation controller assists the pilot in complying with assigned times of arrival along a four-dimensional flight path in the presence of wind disturbances.

In this study, the strategic air traffic control concept is also described, followed by the design of a strategic control descent path. A strategy for determining possible times of arrival at specified waypoints along the descent path and for generating the corresponding route-time profiles that are within the performance capabilities of the aircraft is presented.

Using a mathematical model of the Boeing 707-320B aircraft along with a Boeing 707 cockpit simulator interfaced with an Adage AGT-30 digital computer, a real-time simulation of the complete aircraft aerodynamics was achieved. The strategic four-dimensional navigation controller for longitudinal dynamics was tested on the nonlinear aircraft model in the presence of 15, 30, and 45 knot head-winds. The results reported herein indicate that the controller preserved the desired accuracy and precision of a time-controlled aircraft navigation system.

THESIS SUPERVISOR: Timothy L. Johnson
TITLE: Associate Professor of Electrical Engineering

ACKNOWLEDGEMENT

The opportunity to conduct the research reported herein is the result of invaluable assistance and support from many people. The author wishes to gratefully acknowledge their contributions at this time:

first and foremost, to Bell Telephone Laboratories, Inc., for the opportunity to participate in their OYOC Education Program and for the financial support provided for this undertaking at the Massachusetts Institute of Technology;

to Professor Timothy Johnson for his continued guidance, supervision and interest throughout the course of this research;

to Wolf Kohn for his knowledgeable advice and encouragement during many fruitful and invaluable discussions;

to Charles Corley for his development of a precise and accurate mathematical model of the Boeing 707-320B aircraft used in this study;

to Mark Connelly, research engineer with experience and intimate knowledge in the field of air traffic control, for his constructive comments and suggestions during the course of this research;

to Captain Bud Vietor of American Airlines for his insight and interest in efficient aircraft navigation;

to Arye Ephrath for his computer programming assistance;

to the Department of Transportation-Transportation Systems

PRECEDING PAGE BLANK NOT FILMED

Center for funds providing computer time under the sponsorship of OSP #82439 for the Federal Aviation Administration-Office of Systems Engineering Management;

and certainly not least, to the students and faculty of M.I.T. whose cooperation and organizational support have helped to make this research effort successful.

The author is deeply appreciative to all of the above. These people and organizations have provided a truly invaluable educational experience.

TABLE OF CONTENTS

		page
ABSTRACT		2
ACKNOWLEDGEMENT		3
TABLE OF CONTENTS		5
LIST OF FIGURES		7
LIST OF TABLES		9
LIST OF SYMBOLS AND ABBREVIATIONS		10
CHAPTER I	INTRODUCTION	12
	1.1 STRATEGIC AIR TRAFFIC CONTROL	12
	1.1.1 RESEARCH OBJECTIVES AND DESIGN GOALS	15
	1.2 ASSIGNMENT OF FLIGHT PATHS AND ARRIVAL TIMES	17
	1.3 THE 4-D STRATEGIC NAVIGATION CONTROLLER	19
	1.4 THE AIRCRAFT SIMULATION	22
CHAPTER II	THE STRATEGIC AIR TRAFFIC CONTROL ENVIRONMENT	27
	2.1 STRATEGIC CONTROL DESCENT PROFILE	28
	2.2 ROUTE-TIME PROFILE GENERATION	32
	2.2.1 ASSIGNMENT OF ARRIVAL TIMES	33
	2.2.2 GROUNDSPEED PERFORMANCE ENVELOPE	35
	2.2.3 ROUTE-TIME PROFILE STRATEGY	36
	2.2.4 ROUTE-TIME PROFILE BOUNDARY CONDITIONS USED IN THIS STUDY	48
	2.3 CALCULATION OF ARRIVAL TIMES AND ROUTE-TIME PROFILES	49

page

CHAPTER III THE AIRCRAFT MODEL 54

3.1 REFERENCE FRAMES 56
3.2 EULER AND AERODYNAMIC ANGLES 58
3.3 EQUATIONS OF MOTION 59
3.4 AIRCRAFT PHYSICAL PARAMETERS 66
3.5 ATMOSPHERE MODEL 68
3.6 AERODYNAMIC FORCES 70
3.7 AERODYNAMIC MOMENTS 71
3.8 THE ENGINE MODEL 72
3.9 REAL-TIME SIMULATION OF NONLINEAR AIRCRAFT MODEL 81

CHAPTER IV DESIGN OF A 4-D NAVIGATION CONTROLLER . . . 82

4.1 LINEARIZATION 83
4.2 THE DISCRETE-TIME LINEAR MODEL 96
4.3 THE LINEAR FEEDBACK LAW AND RICCATI EQUATION 99
4.4 OUTLINE OF ALGORITHM FOR COMPUTING OPTIMAL FEEDBACK LAW 107

CHAPTER V EXPERIMENTAL RESULTS 108

5.1 NOMINAL STATE AND CONTROL TRAJECTORIES 108
5.2 WIND DISTURBANCES 109
5.3 PERFORMANCE WEIGHTING MATRICES 115
5.4 THE OPTIMAL FEEDBACK SOLUTION 118
5.5 TIME-CONTROLLED NAVIGATION EVALUATION 124
5.5.1 ACCURACY ACHIEVED 129
5.5.2 COMPARISON OF EXOGENOUS FEEDBACK COMPONENT SOLUTIONS . . . 135

CHAPTER VI ACCOMPLISHMENTS, RECOMMENDATIONS, AND CONCLUSION 137

6.1 ACCOMPLISHMENTS 137
6.2 RECOMMENDATIONS 138
6.3 CONCLUSION 139

APPENDIX A EVALUATION OF CONTINUOUS-TIME/DISCRETE-TIME LINEAR SYSTEM MATRICES AND OPTIMAL FEEDBACK LAW 141

APPENDIX B COMPUTER PROGRAMS 146

REFERENCES 202

LIST OF FIGURES

		page
1-1	STRATEGIC ARRIVAL CONTROL ALGORITHM STRUCTURE. . .	16
1-2	COCKPIT SIMULATOR	23
1-3	SIMULATOR INSTRUMENT PANEL.	25
1-4	SIMULATION FACILITY	26
2-1	STRATEGIC CONTROL DESCENT TRACK PROFILE	29
2-2	TYPICAL STANDARD DAY VELOCITY PROFILE	37
2-3	AIRCRAFT OPERATING ENVELOPE CORRECTIONS	38
2-4	GENERAL CONSTRUCTION OF GROUNDSPEED OPERATING ENVELOPE.	39
2-5	TYPICAL GROUNDSPEED OPERATING ENVELOPE.	40
2-6	VELOCITY PROFILE--BOEING 707-320B	41
2-7	EARTH COORDINATE SYSTEM MAP AND AIRCRAFT GROUND TRACK.	50
3-1	WIND AND BODY AXES AND AERODYNAMIC ANGLES	60
3-2	MASTER DIAGRAM OF AXIS SYSTEMS AND EULER ANGLES	61
3-3	NOTATION IN BODY AXES.	64
3-4	FLIGHT CONTROL SURFACES--BOEING 707.	67
3-5	SEA LEVEL THRUST FOR P&W JT3D-1 TURBOFAN ENGINE	74
3-6	MAXIMUM THRUST VARIATION	77
3-7	IDLE THRUST VARIATION.	78
3-8	THRUST RELATED TO THROTTLE POSITION.	80
5-1	NOMINAL FORWARD BODY VELOCITY-STATE u.	110
5-2	NOMINAL DOWNWARD BODY VELOCITY-STATE w	110
5-3	NOMINAL PITCH RATE-STATE q	111
5-4	NOMINAL PITCH ANGLE-STATE θ.	111
5-5	NOMINAL ALTITUDE-STATE h	112
5-6	NOMINAL RANGE-STATE r.	112
5-7	NOMINAL THRUST-CONTROL T	113
5-8	NOMINAL ELEVATOR DEFLECTION-CONTROL δ_E	113
5-9	δT^* THRUST CONTROL FEEDBACK GAINS.	120
5-10	$\delta\delta_E^*$ ELEVATOR CONTROL FEEDBACK GAINS	121
5-11	EXOGENOUS FEEDBACK THRUST COMPONENT.	123
5-12	EXOGENOUS FEEDBACK ELEVATOR COMPONENT.	123
5-13	DEVIATION IN FORWARD BODY VELOCITY - δu.	125
5-14	DEVIATION IN DOWNWARD BODY VELOCITY - δw	125
5-15	DEVIATION IN PITCH RATE - δq	126
5-16	DEVIATION IN PITCH ANGLE - $\delta\theta$.	126
5-17	DEVIATION IN ALTITUDE - δh	127
5-18	DEVIATION IN RANGE - δr	127

page

5-19 DEVIATION IN THRUST - δT^*. 128
5-20 DEVIATION IN ELEVATOR DEFLECTION - $\delta\delta_E^*$. 128
5-21 FORWARD VELOCITY RESPONSE. 134
5-22 THRUST RESPONSE. 134

LIST OF TABLES

		page
2-1	POSSIBLE TIMES OF ARRIVAL AT IAF FOR BOEING 707-320B.	51
2-2	ROUTE-TIME PROFILE--ATA = 19.73 MINUTES	53
3-1	AIRCRAFT AEROPERFORMANCE DATA	55
3-2	BOEING 707-320B PHYSICAL PARAMETERS	66
3-3	AIRCRAFT MANEUVERING CONTROL LIMITS	68
3-4	NOTATION USED IN EQUATIONS OF MOTION.	73
3-5	BOEING 707 NORMAL OPERATING RANGE	75
5-1	ACCEPTABLE STATE AND CONTROL DEVIATIONS	115
5-2	EFFECT OF EXOGENOUS FEEDBACK COMPONENT.	131
A-1	NOMINAL VALUES.	141

LIST OF SYMBOLS AND ABBREVIATIONS

ATA	ASSIGNED TIME OF ARRIVAL
ATC	AIR TRAFFIC CONTROL
CAS	CALIBRATED AIRSPEED
EAS	EQUIVALENT AIRSPEED
EF	ENTRY FIX
EPTA	EARLIEST POSSIBLE TIME OF ARRIVAL
FAA	FEDERAL AVIATION ADMINISTRATION
FDV	FINAL DESCENT VELOCITY
4-D	FOUR-DIMENSIONAL
IAF	INITIAL APPROACH FIX
IAS	INDICATED AIRSPEED
ICAO	INTERNATIONAL CIVIL AVIATION ORGANIZATION
IDV	INITIAL DESCENT VELOCITY
KCAS	KNOTS CALIBRATED AIRSPEED
KEAS	KNOTS EQUIVALENT AIRSPEED
KIAS	KNOTS INDICATED AIRSPEED
KTAS	KNOTS TRUE AIRSPEED
LPTA	LATEST POSSIBLE TIME OF ARRIVAL
M_{MO}	MAXIMUM OPERATING MACH NUMBER
OM	OUTER MARKER
RTP	ROUTE-TIME PROFILE
TH	RUNWAY THRESHOLD
3-D	THREE-DIMENSIONAL
T1	TIME AT WAYPOINT #1
T2	TIME AT WAYPOINT #2
T3	TIME AT WAYPOINT #3
TAS	TRUE AIRSPEED
TF	TURN FIX
V_{MO}	MAXIMUM OPERATING VELOCITY
VOR	VERY HIGH FREQUENCY OMNI-RANGE
WP1	WAYPOINT #1
WP2	WAYPOINT #2
WP3	WAYPOINT #3

Dedicated to my parents

Donald M. Lax

and

Teresa J. Lax

CHAPTER I

INTRODUCTION

The Federal Aviation Administration (FAA) is responsible for the control of air traffic within the United States. The FAA's objective is to provide a continued growth in air traffic control services by utilizing improved technology to satisfy the ever-increasing demand for safe, orderly and expeditious flow of aircraft within the airways system [1,2]. Four-dimensional (4-D) aircraft navigation is one concept proposed to solve this problem. Navigation incorporating the fourth dimension of time is categorized as a strategic air traffic control concept [3]. Time-controlled navigation is a concept whereby available airspace and airports are utilized more efficiently to achieve increased airport capacity.

1.1 STRATEGIC AIR TRAFFIC CONTROL

Strategic air traffic control is an organizational plan wherein the factors of space management, energy management and time management are integrated to determine a four-dimensional route-time profile to be assigned to each aircraft. Strategic control is a specific method whereby the air traffic control (ATC) system defines flight paths in four-dimensions (cross-track, along-track, altitude, and time) to resolve traffic conflicts [3].

Time control can be broadly defined as a guidance system which places an aircraft at a specified three-dimensional (3-D) geographical location at an assigned time. Three methods have been proposed to implement this type of control. The first method utilizes the ground-based air traffic control system to transmit a sequence of radar vectors to each aircraft. This is similar to present ATC procedures in which aircraft arrive randomly at the boundaries of the terminal area and are aligned in a string prior to landing by a series of controller-generated heading and speed commands. This method, primarily employing "path stretching" maneuvers, neither employs optimum energy management procedures, nor provides sufficient accuracy in the fourth dimension of time.

The second method of control could be achieved if pilots utilized an airborne guidance system to follow a predetermined assigned 3-D route while receiving speed commands from the ground-based air traffic controller. With this method, control is shared jointly by the airborne system and the ground-based system.

In the first two types of time control, a significant amount of controller-pilot communication is required. A third type of control, which reduces the communication workload requirement, could be entirely executed by the airborne system using precision four-dimensional navigation/guidance equipment [3] which requires the pilot to fly an assigned route-time

profile. The airborne system would be responsible for generating descent (or ascent) and speed commands which would ensure arrival at three-dimensional geographic locations at pre-assigned times.

The Federal Aviation Administration currently favors a totally centralized aircraft management system similar to the first type of time control. This concept utilizes a ground-based system to generate a 4-D schedule, to transmit a sequence of commands to each aircraft, and to monitor, detect and correct any deviations from the schedule. Those favoring "distributed management," employing the third type of time control, believe that the pilot should participate more actively in the air traffic control process [6]. This study is oriented toward the latter type of time control, whereby the pilot would utilize an airborne system to detect and correct for any deviations from the 4-D schedule.

In a strategic air traffic control system, aircraft would request entry into the system from the ground-based controller. The ground-based system would consider other traffic and measured or estimated values of winds aloft and temperature in generating a four-dimensional, conflict-free, route-time profile based on the aircraft's groundspeed performance envelope. The ground facility would then transmit this route-time profile to the aircraft. The aircraft's avionics and on-board navigation systems would be designed to achieve precise four-dimensional

control in the presence of actual environmental conditions encountered in flight such as unexpected winds.

The overall strategic control structure from entry into the system to execution of the assigned route-time profile is depicted in block diagram form in Figure 1-1. It is the execution of the route-time profile and adherence to the 4-D schedule that are the major concerns of this study.

1.1.1 RESEARCH OBJECTIVES AND DESIGN GOALS

The main objective in this research effort is to investigate the engineering feasibility of four-dimensional navigation using an optimal feedback controller which could be implemented by the airborne computer system. The development of a time-controlled navigation system is motivated by three general goals: to improve air traffic control performance and increase safety, to utilize available airspace more efficiently and increase airport capacity, and to reduce operating costs.

As strategic control is primarily designed for automatic operation [3], it is necessary to understand aircraft performance capabilities, the effects of wind and temperature, and the on-board computer requirements. With a comprehensive understanding of these issues, this study is directed toward the fundamental problem facing controllers and pilots--the problem of safe and efficient guidance and control of aircraft

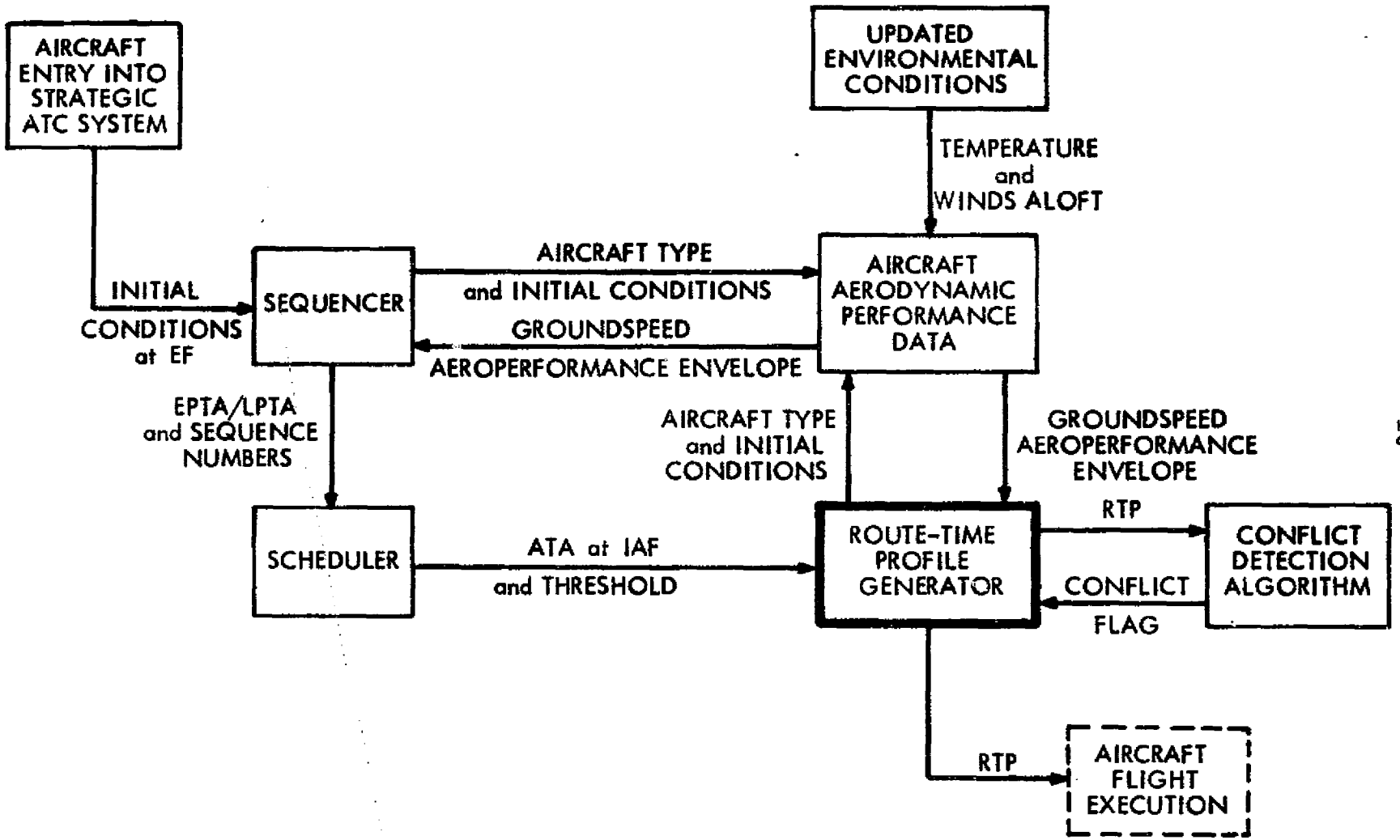

Fig. 1-1 Strategic Arrival Control Algorithm Structure [5]

within the air traffic control environment [17]. From this consideration evolves the two specific goals of this study: 1) determination of route-time profiles, and 2) design and evaluation of a four-dimensional navigation/guidance system controller that executes the route-time profile using real-time simulation capabilities.

1.2 ASSIGNMENT OF FLIGHT PATHS AND ARRIVAL TIMES

The precise control of aircraft using a 4-D concept is certainly a practical possibility for the air traffic control system of the 1980's and beyond. The ground-based air traffic computer would generate four-dimensional flight paths for all strategically controlled aircraft. The layout of these strategic flight paths must consider airspace geometry, environmental effects, and aircraft performance capabilities. It is desirable to define these flight paths in terms of horizontal position, altitude, and time such that they make the most efficient use of the available airspace. The routes and times assigned must be within the performance capabilities of each aircraft and must be assigned so as not to conflict with the routes and times of other aircraft. The Boeing Company has considered these aspects in detail in their study on strategic air traffic control [3,4,5].

The assignment of arrival times is constrained by aircraft performance, and thus, there is a finite range of arrival

times which each aircraft can achieve for a fixed 3-D route profile without holding. This range is lower bounded by the earliest possible time of arrival (EPTA) and upper bounded by the latest possible time of arrival (LPTA). The earliest possible time of arrival is that time at which the aircraft would arrive if it accelerated to its maximum airspeed, flew at that maximum, and then decelerated to comply with any airspeed constraints at the assigned waypoint (essentially a minimum time "bang-bang" control law). Likewise, the latest possible time of arrival is that time the aircraft would arrive if it decelerated to its minimum airspeed, flew at that minimum, and then accelerated to comply with airspeed constraints at the assigned waypoint. The complete set of possible arrival times can be computed by utilizing the entire aircraft performance envelope. Once an assignment of arrival time is made, it is desirable to determine a corresponding route-time profile that will guarantee aircraft arrival at designated waypoints at the assigned times. The route-time profiles are generated in terms of groundspeeds which are piecewise linear approximations to constant Mach and/or indicated airspeeds that have been corrected for wind and temperature [5]. These groundspeeds integrated over the descent route distances correspond to a particular time of arrival that may be assigned to the aircraft. Time-controlled navigation can be applied to the entire flight, from take-off to landing, but presently the greatest

need for this capability is within the descent phase of flight. The descent phase of flight, as referred to in this study, is defined to be that segment of flight where transition occurs between enroute altitudes and the outer boundary of the airport terminal area (at approximately 30-35 nautical miles from the airport at an altitude of 10,000 feet). It is within this phase of flight, between cruise altitudes and entry into the terminal area, where derandomization of aircraft in time can be achieved most efficiently to ensure proper separation between aircraft. Utilizing time-controlled navigation during the descent phase of flight would eliminate most delays now imposed inside into the terminal area.

In Chapter II, a strategic control descent route profile will be described in detail. In addition, a strategy for determining the possible times of arrival at specified waypoints along the descent path and for generating the corresponding route-time profiles for each type of aircraft will be presented.

1.3 THE 4-D STRATEGIC NAVIGATION CONTROLLER

The relationship between aircraft performance and the route-time profiles which are achievable is essential to the airborne navigation concept. A precise and accurate mathematical model of the Boeing 707-320B aircraft has been developed by Charles Corley in his study on aircraft time-

controlled navigation [6].

With the use of this aircraft model and the associated atmosphere model, a 4-D strategic navigation control regulator has been designed, simulated and evaluated. In the presence of winds, pilot error and inaccuracies in observing position and speed, an optimal solution for flight path regulation is desirable in order to best preserve the time precision inherent in 4-D navigation. The ultimate objective of the design is to obtain an optimal linear discrete-time feedback solution that will achieve the accuracy required for effective time-controlled navigation.

The design procedure requires linearization of the nonlinear aircraft equations of motion to obtain a linear continuous-time system. The linearization is performed about nominal trajectories which are acquired by "flying" the desired route-time profile using the complete nonlinear aircraft model in a real-time simulation. When considering the actual physical implementation of the 4-D navigation controller, it is desirable to implement the discrete-time equivalent to the continuous-time linear system. The discrete-time system was formulated as the sampled-data version of the continuous-time system. Using linear quadratic control techniques, a cost function was formulated and the discrete-time linear feedback solution was derived. In the derivation, the wind components of the system were formulated as exogenous variables. These

wind components were treated as known deterministic disturbances for purposes of this study.

The novelty of this approach leads to a feedback solution that consists of two parts. One part is dependent upon any deviations in the states of the system while the second part is an exogenous component dependent upon wind disturbances. Both the feedback gains and exogenous components are time-varying. When the wind is formulated as an exogenous variable to the system, the choice of the weighting matrices in the cost function becomes extremely important. The difficulty in choosing these weighting matrices arises from the fact that the performance of the feedback solution must be evaluated for each choice in a real-time simulation wherein the optimal discrete-time linear feedback law is implemented on the complete non-linear aircraft model.

The ability to evaluate the controller design during the real-time simulation was greatly facilitated by actual observation of the system responses as displayed on the aircraft's instruments in the cockpit simulator. The simulation facilities will be described in more detail in the following section.

The design of the 4-D navigation controller as discussed in this section will be presented in greater detail in Chapter IV. The formulation of the discrete-time linear system and the derivation of the appropriate optimal feedback law will be

thoroughly presented. The nominal state and control trajectories along with the performance weighting matrices will be presented in Chapter V. In addition, and most importantly, an evaluation of the 4-D navigation controller, based on its performance in real-time simulations when implemented on the complete nonlinear aircraft model, will be discussed in Chapter V. Finally, the accomplishments of this study, recommendations for further research, and the overall conclusion will be presented in Chapter VI.

1.4 THE AIRCRAFT SIMULATION

The simulation facilities of the Electronics Systems Laboratory, the Flight Transportation Laboratory, and the Man-Vehicle Laboratory at M.I.T. consists of a fixed-base cockpit simulator resembling a Boeing 707 aircraft. The cockpit simulator, with interior panels, switches, controls, and instrumentation facsimilies, was donated to M.I.T. by the Boeing Company. The cockpit simulator has been used extensively to study new technology applicable to future air traffic control systems. An interior view of the cockpit simulator is shown in Figure 1-2.

An Adage AGT-30 digital computer is interfaced with the cockpit simulator. The computer simulates the aircraft's aerodynamics and drives the simulator's flight instruments using three cathode ray tubes. The basic flight instruments

ORIGINAL PAGE IS
OF POOR QUALITY

Fig. 1-2 Cockpit Simulator

as shown in Figure 1-3 are simulated for the Captain and First Officer and the Airborne Traffic Situation Display [8] is also presented in the cockpit. A block diagram depicting the interface between the cockpit simulator, Adage computer, and associated peripheral equipment is shown in Figure 1-4.

ORIGINAL PAGE IS
OF POOR QUALITY

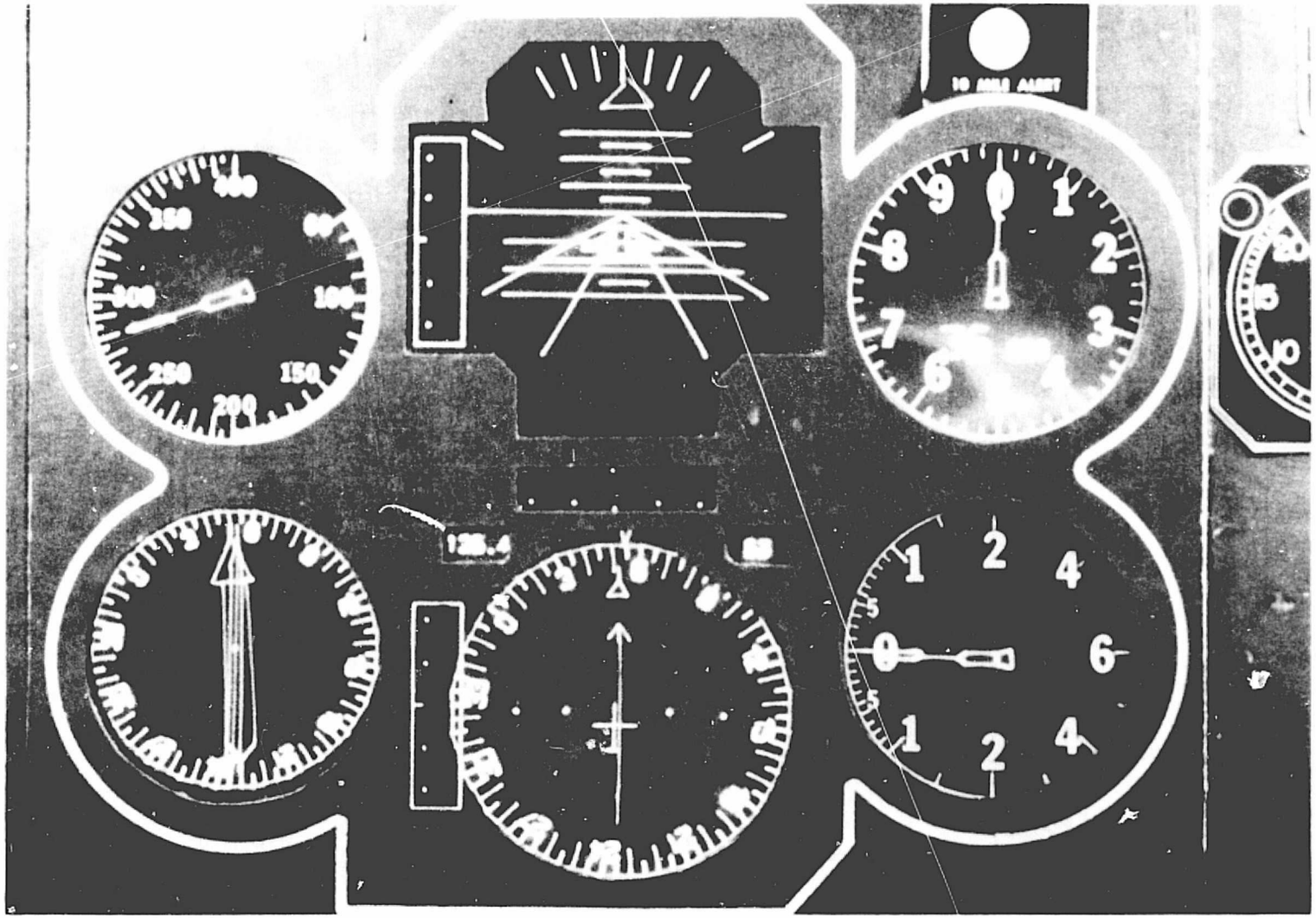

Fig. 1-3 Simulator Instrument Panel

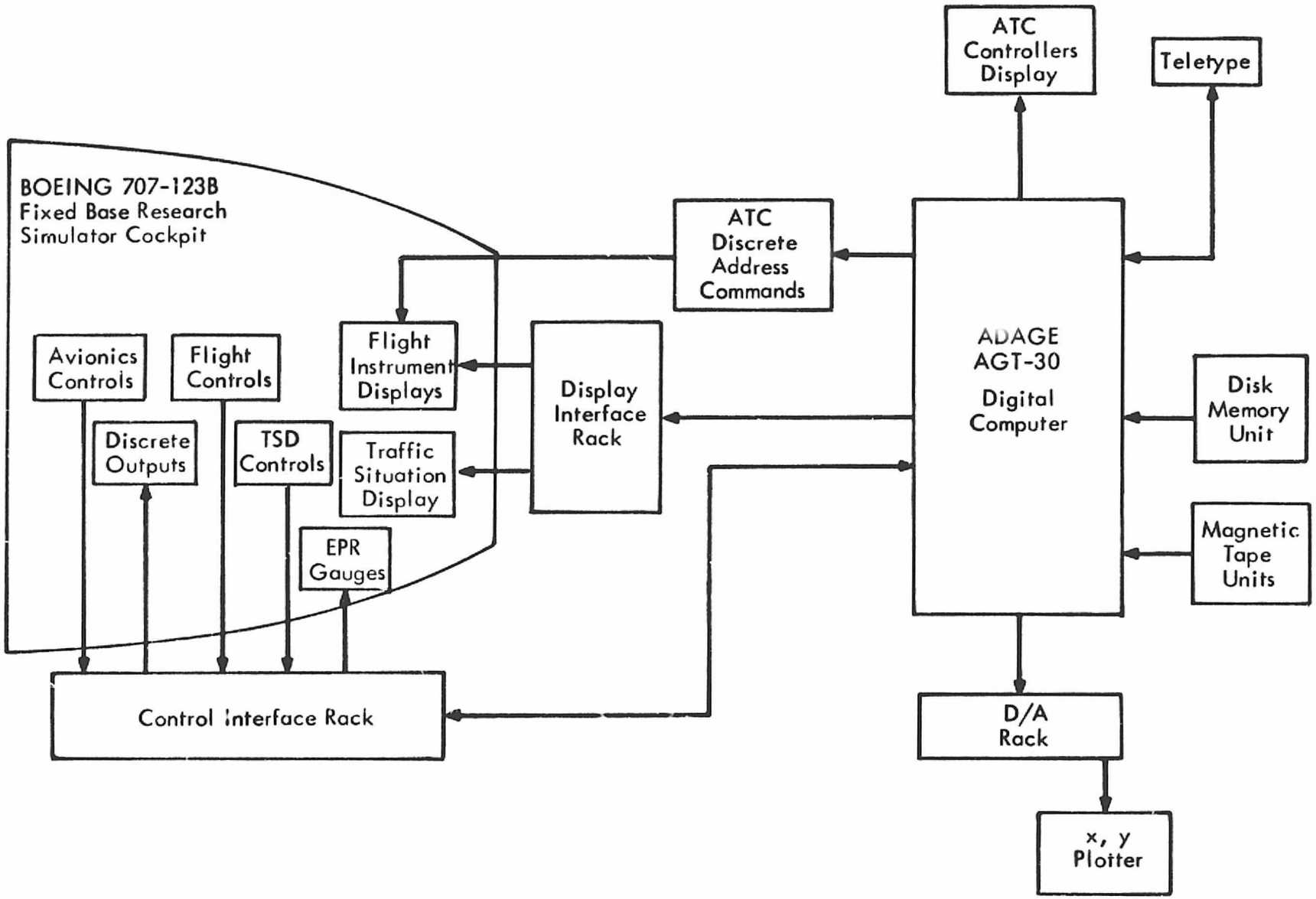

Fig. 1-4 Simulation Facility

CHAPTER II

THE STRATEGIC AIR TRAFFIC CONTROL ENVIRONMENT

A strategic air traffic control system has two basic components. The first component is the descent flight path which the aircraft is assigned to fly. The second component is the assignment of a velocity schedule to be executed along the descent flight path. These two components combine to determine a route-time profile which dictates the rate at which the flight path is to be traversed. Since there is a range of airspeeds that can be maintained along a given flight path, it is difficult for the pilot to decide what airspeed schedule will ensure arrival at certain waypoints at specified times. Thus, it is desirable for the pilot to have a predetermined route-time profile which will ensure arrival at waypoints at times specified by the ground-based air traffic controller.

The Boeing Company and the National Aeronautics and Space Administration have studied these issues pertaining to 4-D navigation and have proposed several methods of solution [3,4, 5,17]. In this chapter, a flight path applicable to the descent phase of flight is defined. A procedure for calculating possible times of arrival at various waypoints is also described along with a strategy for generating route-time profiles.

2.1 STRATEGIC CONTROL DESCENT PROFILE

The Boeing study points out that "airplane performance is probably the single most important criterion in the design of the terminal area descent profile." [4:p.63] The aerodynamic capabilities of the aircraft limit the flexibility available in the design of the descent track profile. For each type of aircraft, the available drag, lift, thrust, and gross weight combine to constrain and limit the flight path angle (slope of descent path) at which the aircraft can descent without accelerating due to gravity. For time-controlled navigation, it is desirable to design a descent profile with a flight path angle that preserves sufficient aircraft acceleration and deceleration capability in order to achieve the required time accuracy.

The Boeing study has suggested that fixed linear descent profiles be used. Such linear profiles are desirable from a scheduling point of view and provide well defined airspace structures that simplify conflict-free flight path design. The strategic control descent and arrival path used in this study is a modified version of one suggested by Boeing and is depicted as a function of altitude and distance in Figure 2-1.

When the aircraft is maintaining a constant flight path angle without accelerating or decelerating, the descent gradient (γ_d) is equal to the descent track slope (γ_t) [4] and is expressed by the following relationships:

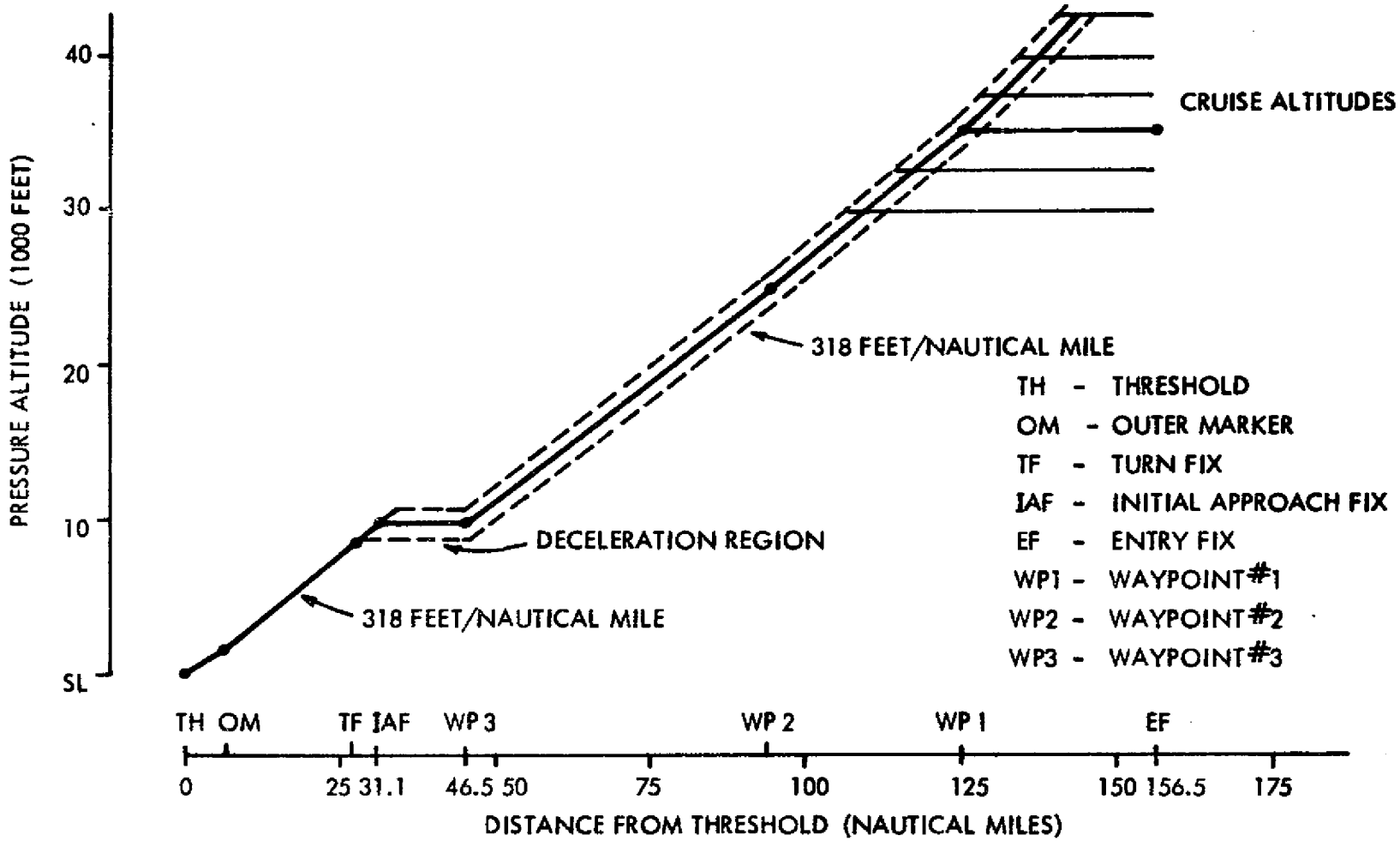

Fig. 2-1 Strategic Control Descent Track Profile

$$\gamma_d = \text{descent gradient} = \frac{\text{drag}}{\text{lift}} - \frac{\text{thrust}}{\text{weight}} \qquad 2\text{-}1$$

$$\gamma_t = \text{descent track slope} = \frac{\text{vertical distance}}{\text{horizontal distance}} \qquad 2\text{-}2$$

If the aircraft is in accelerated or decelerated flight along a fixed descent track, the descent gradient required for the aircraft is expressed as:

$$\gamma_{d_{req}} = \text{descent gradient required} = \gamma_t\left(1 + \frac{V}{g}\frac{dV}{dh}\right) \qquad 2\text{-}3$$

This required descent gradient must be within the performance capabilities of the aircraft if it is required to fly a constant descent path while descending at speeds other than constant true airspeed (TAS), such as constant Mach number or constant indicated airspeed (IAS), which require acceleration or deceleration. In a clean configuration (landing gear up and flaps retracted), the only method for increasing or decreasing gradient is by varying engine thrust. Additional gradient can be achieved by deploying aircraft spoilers when engines are at idle thrust.

The rate of vertical descent (dh/dt) required to maintain a constant flight path angle is a function of speed and is limited by cabin repressurization rate, anti-icing power requirements, and the effects of wind and temperature on the performance capabilities [3,5,17].

Choice of a vertical descent gradient must be within the performance capability of all aircraft utilizing fixed linear strategic control descent profiles. Boeing suggests a slope of 250 feet per nautical mile above 10,000 feet and 300 feet per nautical mile below that altitude, while others [7,18] have recommended slopes of 300 feet per nautical mile at all altitudes. The descent track slope chosen for use in this study is approximately 3° corresponding to a vertical descent gradient of 318 feet per nautical mile.

The descent route profile as shown in Figure 2-1 includes a level flight deceleration segment at 10,000 feet to provide for the transition from high descent speeds to a speed not exceeding 250 knots indicated, as required by the FAA for flight below 10,000 feet. The length of this deceleration segment has been chosen to be 15 nautical miles. This is sufficient to accommodate a level deceleration at idle thrust from the maximum operating true airspeed at 10,000 feet to 200 knots indicated airspeed with a 72 knot tailwind.† It is reasonable to assume that this deceleration segment is adequate for most flight situations.

The complete strategic control descent profile as depicted in Figure 2-1 is described geographically by the

---

† This calculation is based on actual flight measurements made by Captain Carl W. Vietor of American Airlines.

position of each waypoint along its linear path segments. This three-dimensional route is described by the following points:

1. ENTRY FIX. This point, approximately 150 to 175 nautical miles from the airport is fixed and defines the point at which the aircraft enters the strategic control system. Known entry fixes allow schedules and times to be determined over known distances.

2. INITIAL APPROACH FIX. Entry into the terminal area would occur at this point approximately 30 to 35 nautical miles from the airport. The desired spacing of aircraft is achieved by speed control between the entry fix and the initial approach fix with possible parallel paths to resolve conflicts.

3. TURN FIX. At this point, inside the initial approach fix, aircraft from several entry fixes would merge and be positioned on a common path within the terminal area.

4. OUTER MARKER. From the turn fix to the outer marker, all aircraft adhere to the same velocity profile along a common path.

5. RUNWAY THRESHOLD. Once inside the outer marker, each aircraft is flown at its appropriate final approach speed down to the runway threshold.

6. WAYPOINTS. These are additional points as required for any turns or descents or to insure time separation between aircraft along a common path.

With the additional assignment of arrival times at various points along the descent path, a velocity-route-time profile can be determined.

2.2 ROUTE-TIME PROFILE GENERATION

Strategic control is a concept which may be applied to

the entire flight, from departure to landing. However, this study is principally concerned with the descent phase of flight between the entry fix and the initial approach fix. It is assumed that all aircraft can fly a common path and airspeed profile from the initial approach fix to the outer marker. Therefore, it is within the descent phase of flight from cruise altitudes into the terminal area where the greatest need for the strategic control concept can be foreseen. It is within this phase of flight where the greatest amount of time control can be achieved, thus where derandomization of aircraft in time (sequencing and scheduling) must be accomplished in order to ensure proper merging of aircraft inside the initial approach fix and suitable separation of aircraft at the outer marker.

2.2.1 ASSIGNMENT OF ARRIVAL TIMES

The assignment of the desired time of arrival at the IAF and any intermediate waypoints is the responsibility of the ground-based strategic air traffic controller. The control algorithm must assign a time of arrival at the IAF that is within the earliest possible time of arrival (EPTA) and the latest possible time of arrival (LPTA) which are constrained by the groundspeed performance envelope along the descent route profile. The EPTA is based on the maximum groundspeeds that the aircraft can achieve along the descent path. These

speeds vary with altitude and are constrained by structural limitations, by maximum available thrust, by environmental conditions, or below 10,000 feet, by FAA directives. The LPTA is based on the minimum groundspeeds that the aircraft can achieve. These speeds are also a function of altitude and environmental effects, and are related to the airspeed at which the aircraft can perform a 1.3g maneuver without buffeting [4]. The difference between the LPTA and the EPTA is known as the delay spread and the relative position of the assigned time of arrival (ATA) within the delay spread is referred to as the time flexibility available [6]. Maximum time flexibility is achieved when LPTA-ATA = ATA-EPTA, thus the aircraft is capable of arriving earlier or later than the assigned time by the same amount [6]. This is certainly desirable in the event that the strategic controller would have to reschedule aircraft due to emergency or weather conditions.

Given fixed descent route profiles, desired times of arrival at various waypoints can be assigned to aircraft upon reaching the entry fixes. Whereas the aircraft's performance capabilities affect and limit the actual descent route profile, the aircraft's groundspeed envelope affects the range of achievable arrival times at selected waypoints.

The ground-based strategic controller would have knowledge of the groundspeed performance envelope for each type

of aircraft. The scheduling and conflict detection algorithms, with knowledge of the descent route profile, would sequence the aircraft and assign non-conflicting times of arrival [5] at the initial approach fix as well as any additional times of arrival at specified waypoints along the descent path. (See Figure 1-1 for the general structure of this procedure.)

Since the groundspeed performance envelope is ultimately used to compute the range of arrival times at the IAF and the corresponding route-time profiles, it is important to consider its formulation.

2.2.2 GROUNDSPEED PERFORMANCE ENVELOPE

True airspeed is the speed with which the airplane moves through the airmass. Groundspeed is the vector sum of the true airspeed and the wind. Thus knowledge of the wind vector along the geographical path is necessary to determine the groundspeed velocity profile that is within the aeroperformance capabilities of the aircraft along the pre-defined route.

True airspeed performance curves are commonly based on standard day conditions. Pressure altitude, the altitude measured with an altimeter set at 29.92 inches of mercury, is equal to the height above sea level for standard day temperatures (15°C at sea level). For non-standard day temperatures, there is a deviation between pressure altitude and the actual height above sea level. Therefore, an adjustment

in the aircraft's performance curves, which are based on pressure altitude, is necessary. This adjustment alters the true airspeed velocity profile and thus the groundspeed velocity profile.

A typical standard day aeroperformance velocity profile is shown in Figure 2-2. The general procedure, as suggested in the Boeing study [5], for modifying the standard day aeroperformance envelope to obtain an aeroperformance temperature and wind corrected groundspeed envelope is depicted in Figures 2-3 and 2-4. A complete typical transformation of the standard day operating envelope to obtain the corresponding groundspeed envelope is shown in Figure 2-5.

2.2.3 ROUTE-TIME PROFILE STRATEGY

The strategy used for generating the route-time profile is one suggested by the Boeing company [5] and modified in this study. The aircraft enters the strategic control system in level flight at the entry fix. The aircraft then accelerates or decelerates in level flight to its initial descent velocity (IDV). Upon intercepting the descent path, the aircraft will fly a velocity-altitude profile while descending. This velocity-altitude profile, referred to as a Mach/IAS profile [5], implies a particular Mach number and IAS, each corresponding to a specific airspeed to be maintained while descending through certain altitudes along the descent path.

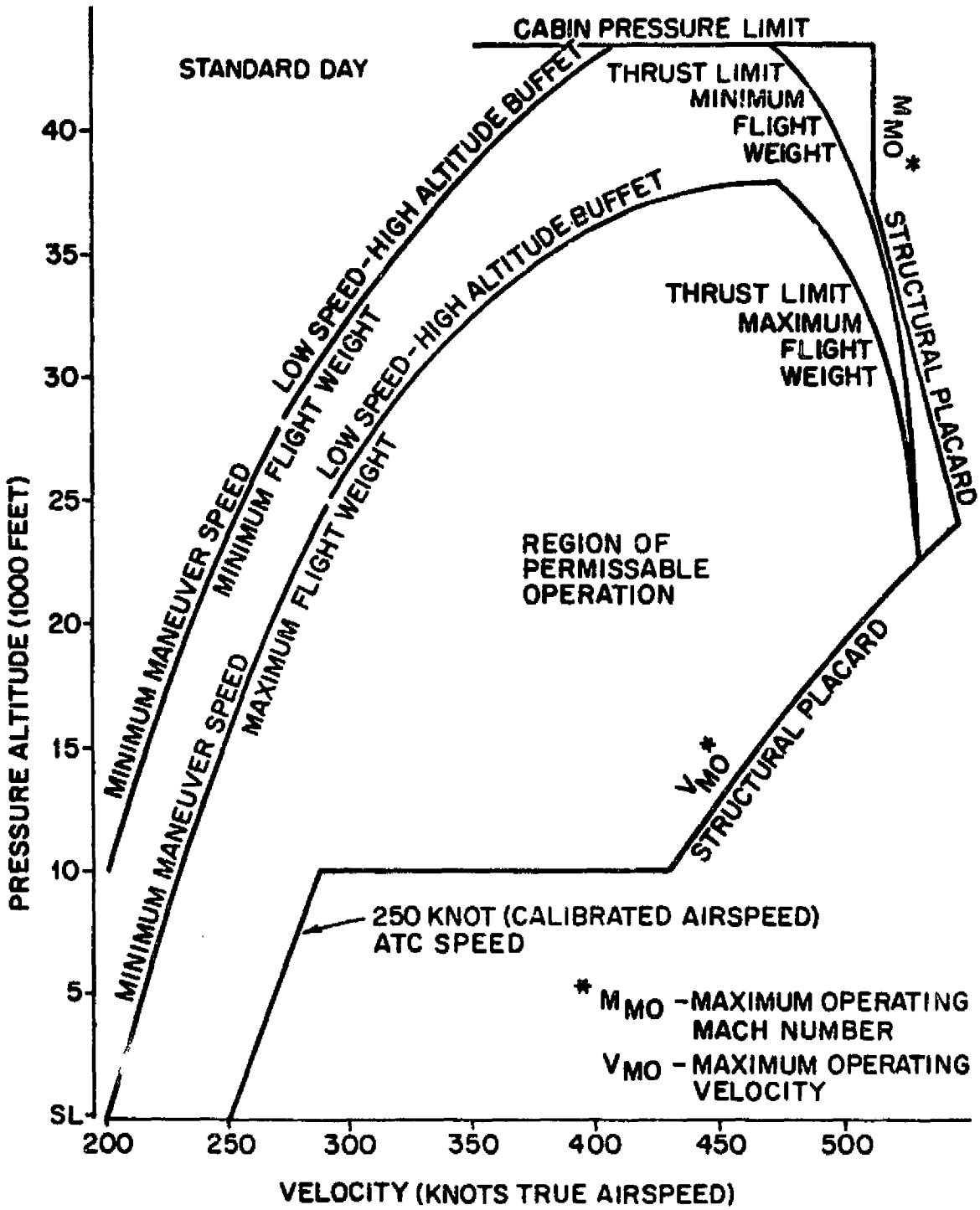

Fig. 2-2 Typical Standard Day Velocity Profile

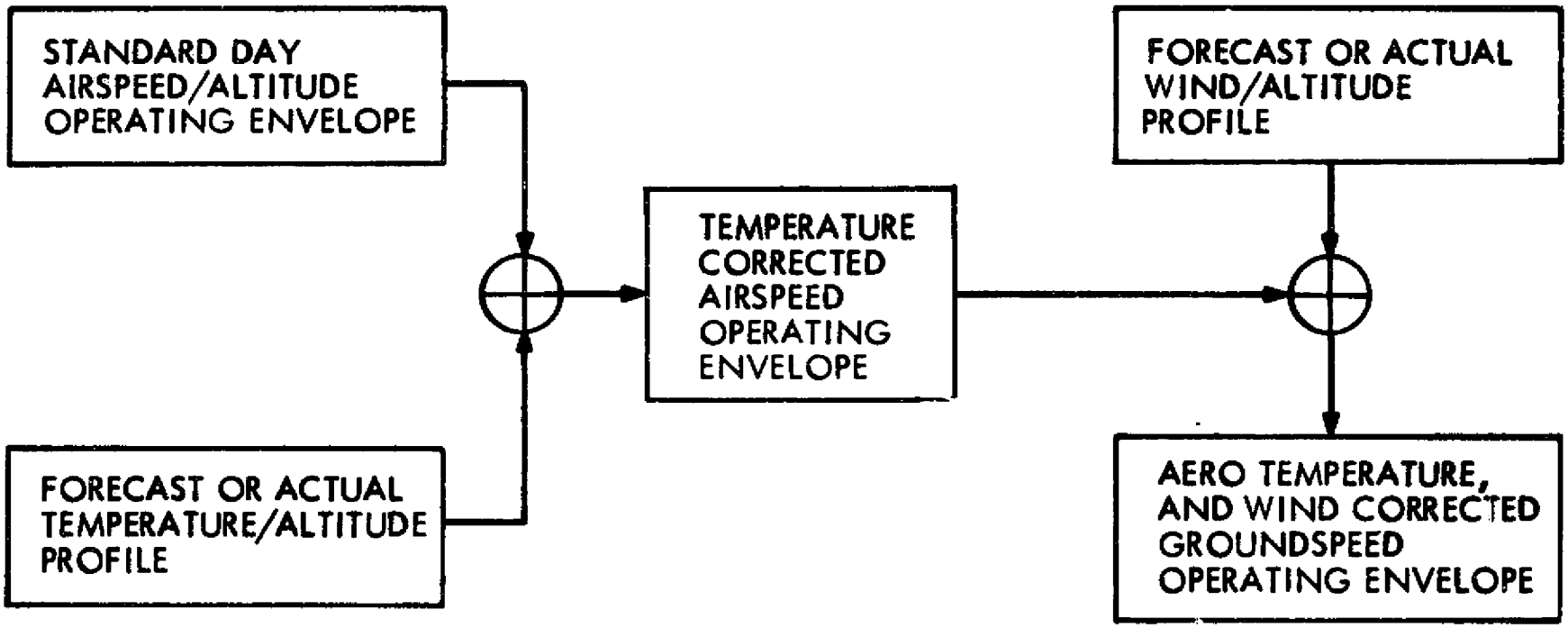

Fig. 2-3 Aircraft Operating Envelope Corrections

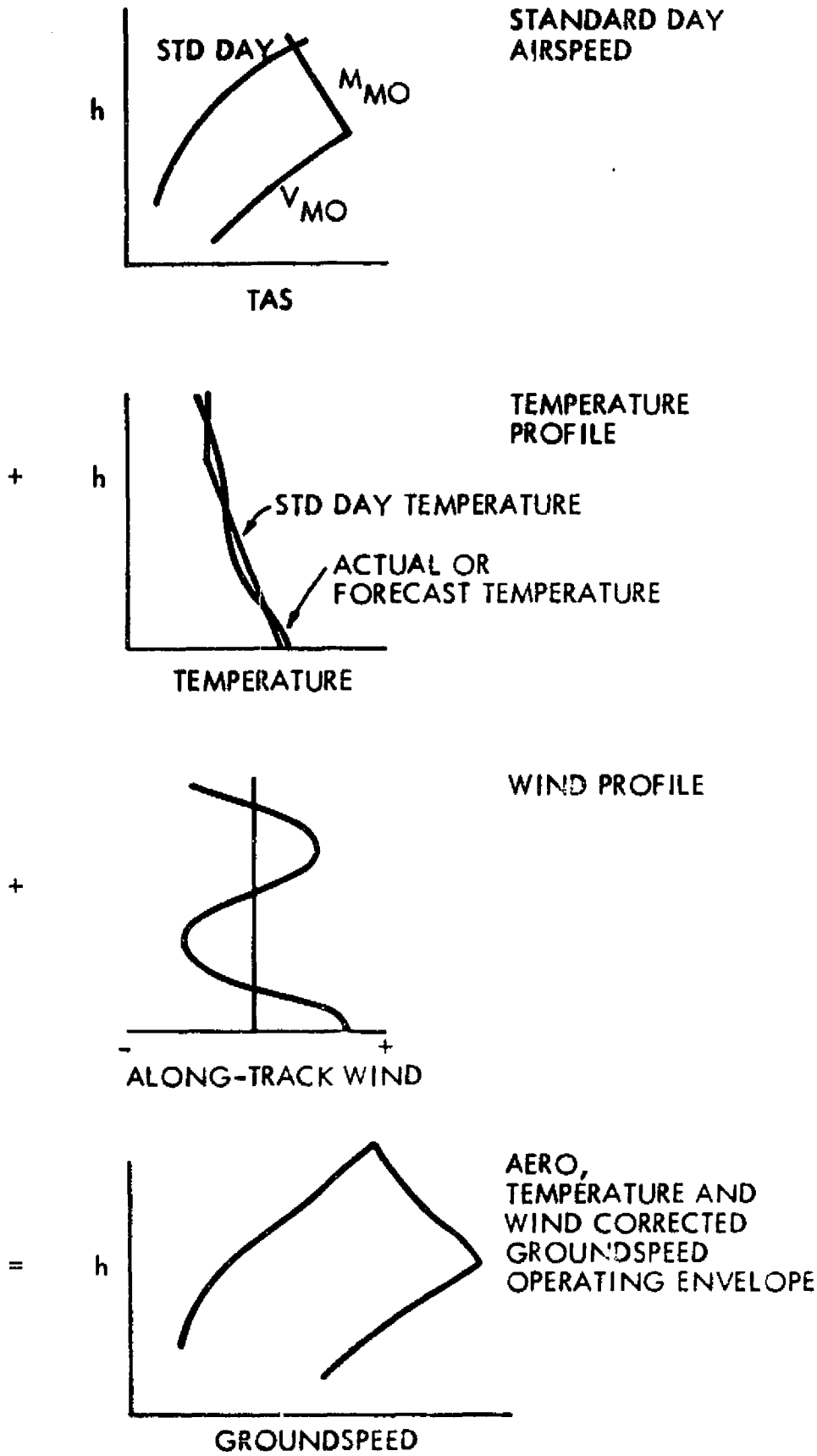

Fig. 2-4 General Construction of Groundspeed Operating Envelope

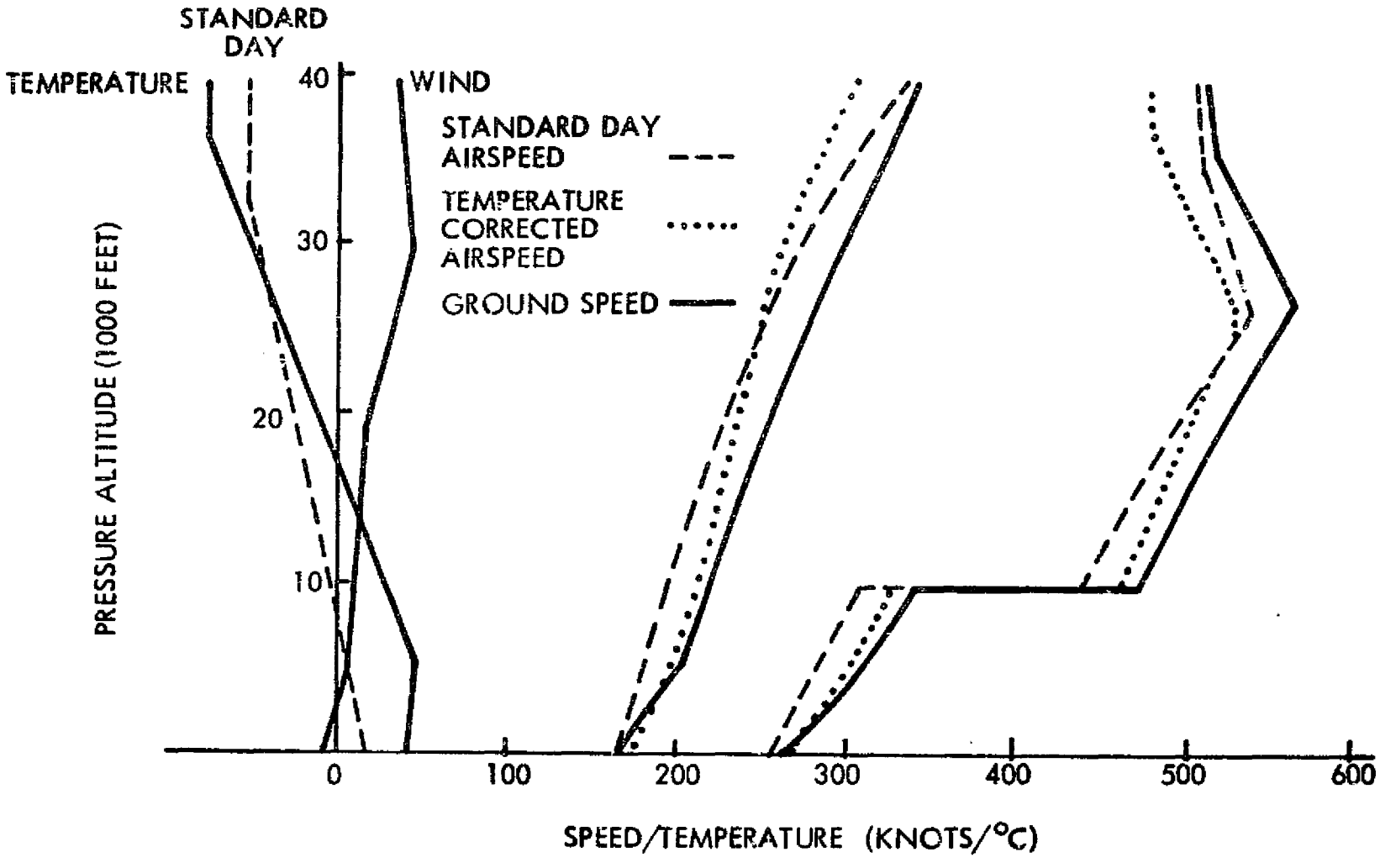

Fig. 2-5 Typical Groundspeed Operating Envelope

The aircraft reaches the initial approach fix altitude at the final descent velocity (FDV). At this altitude, another acceleration or deceleration in level flight is performed to the desired final velocity at the IAF. The initial and final descent speeds are groundspeeds but are converted to Mach number or IAS for use in the route-time profile.

Associated with every possible arrival time at the IAF is a route-time profile consisting of a set of velocity-position-time points that satisfy the boundary conditions at the entry fix and the initial approach fix [5]. The velocities specified in the route-time profile are indicated airspeeds or Mach numbers which are those airspeeds that are indicated in the cockpit and by which the pilot is accustomed to flying. Since the route-time profile is derived using the aircraft's operating envelope, the groundspeeds which must be flown along the descent path must be converted to Mach number or indicated airspeed using altitude and environmental information. The vertical speeds required to maintain the fixed descent path is a simple calculation given the groundspeed curve associated with a particular ATA.

The route-time profile generation strategy is characterized by two basic aspects: 1) the determination of the IDV, the corresponding FDV, and the Mach/IAS profile used in transitioning between these velocities during letdown, and 2) the procedure for acceleration or deceleration in the level flight

segments at the entry fix and initial approach fix altitudes.

In order to describe the Mach/IAS letdown strategy, it is convenient to create certain waypoints along the descent path. These intermediate waypoints between the EF and the IAF as shown in Figure 2-1 are described as follows:

1. WAYPOINT #1 (WP1). At the point where the initial descent from the EF altitude begins.

2. WAYPOINT #2 (WP2). At the point where the descent path passes through the critical (transition) altitude.

3. WAYPOINT #3 (WP3). At the point where the descent path intersects the IAF altitude.

As previously described, the groundspeed operating envelope is defined by the gross weight of the aircraft, forecasted winds, and temperatures along the known strategic control descent profile. In this study, the temperatures are assumed to be standard day temperatures and the forecasted winds are considered variable. The procedure for generating Mach/IAS profiles can best be explained at this point by means of actual examples.

Consider the velocity profile in Figure 2-6 for the Boeing 707-320B aircraft used in this study. The heavy lines indicate a velocity profile for an aircraft gross weight of 225,000 pounds. These lines limit the range of permissible velocities and provide a buffer region for pilot error. It can be seen that the maximum operating velocity is achievable at the critical altitude. The high speed boundary of the velocity

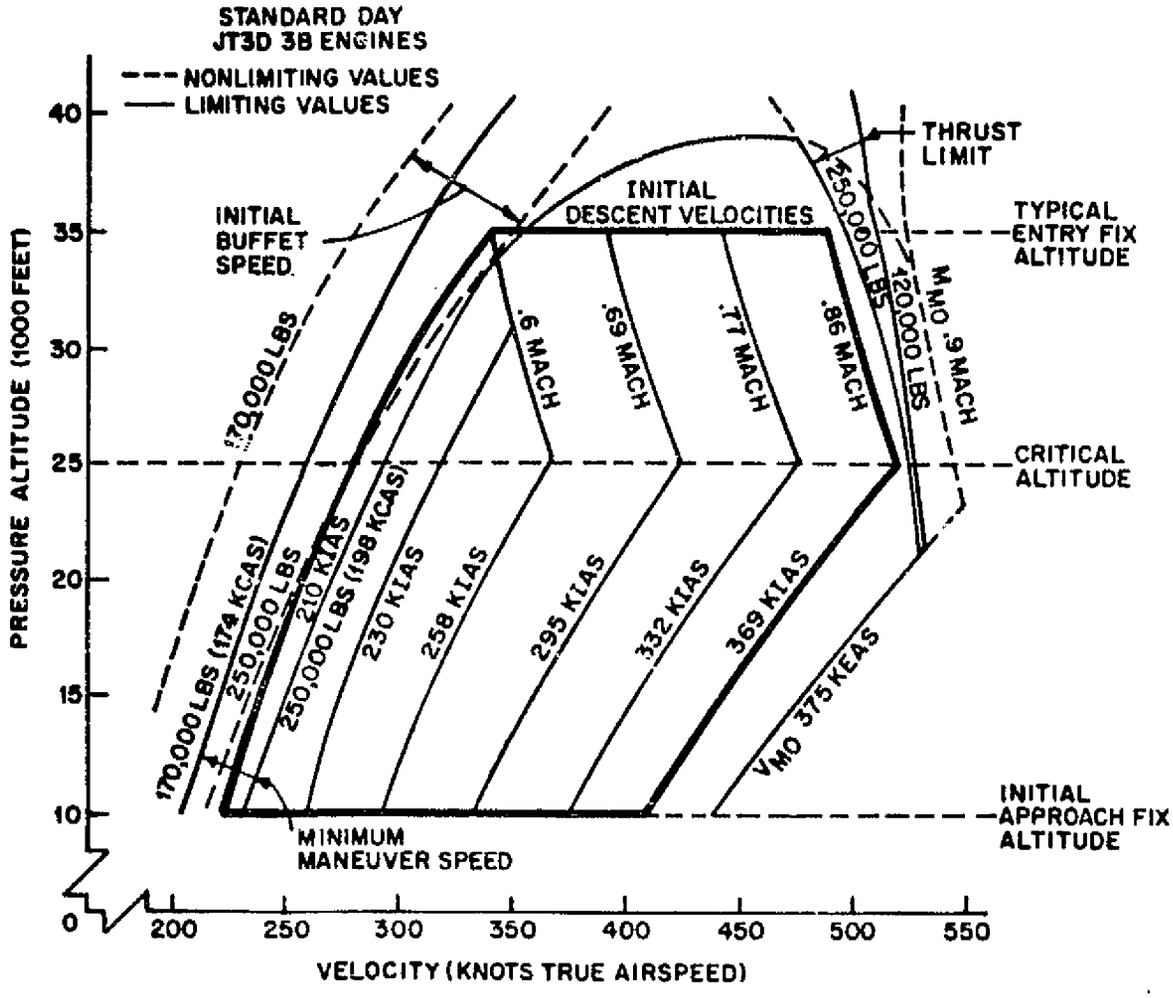

Fig. 2-6 Velocity Profile - Boeing 707-320B

envelope above the critical altitude is constrained by thrust and is closely approximated by a constant Mach number. The high speed boundary below the critical altitude is constrained by the maximum operating velocity and is closely related to a constant equivalent airspeed (EAS). The low speed boundary of the aircraft velocity envelope, which is defined by the airspeed at which the aircraft can perform a 1.3g maneuver without buffeting, is also approximated by a constant EAS. EAS is related to calibrated airspeed (CAS) by a compressibility factor and CAS is related to IAS by the instrument and position errors in the actual airspeed indicator of the aircraft [15]. For purposes of this study and in the real-time simulation of the aircraft, indicated airspeeds are equal to calibrated airspeeds and the compressibility factor can be neglected so that the EAS boundaries of the performance envelope can be approximated by indicated airspeeds.

For a particular initial descent velocity, the route-time profile generation strategy determines a constant Mach number for letdown between the entry fix altitude (at WP1) and the transition altitude (at WP2), and a constant IAS for letdown between the transition altitude and the initial approach fix altitude (at WP3). Thus, the transition altitude is defined as that altitude where transition from a constant Mach airspeed schedule to a constant IAS schedule occurs. For any initial descent velocity within the boundary speeds at the entry fix

altitude, the transition altitude is the same as the critical altitude as defined by the aircraft's velocity envelope. When the initial descent velocity is equal the minimum allowable velocity at the entry fix altitude, the transition altitude can be varied between the critical altitude and the entry fix altitude in order to utilize the entire aeroperformance envelope. Several Mach/IAS letdown profiles are indicated in Figure 2-6.

The Mach/IAS letdown strategy ensures that the resulting rate of change of velocity with respect to altitude (dV/dh) is within the gradient capability of the aircraft [5]. In addition the entire aeroperformance envelope is utilized, thus maximizing the resulting time controllability over the range of possible times of arrival. Although the gradient capability of the aircraft is not exceeded using this strategy, the reserve gradient capability, which is a function of the descent track slope as well as the aircraft performance capabilities, is not optimized. Thus the aircraft has less potential control to adapt to environmental disturbances. At the expense of reducing total time controllability, the reserve gradient capability could be optimized using a letdown strategy based on constant IAS or by using variable slope descent tracks. Such alternative strategies will not be considered here.

The second important aspect of the route-time profile generation strategy is the method of acceleration or deceleration between the boundary speed velocities at the entry fix and initial approach fix, and the initial and final descent velocities respectively. For any possible IDV, the transition between the initial velocity at the entry fix and the IDV is linear with respect to time during the period of level flight at the entry fix altitude. This results in a constant acceleration or deceleration along the entire level flight segment. Likewise, the transition between the FDV and the required final velocity at the IAF is also assumed to be linear with respect to time. Similarly, this results in a constant acceleration or deceleration rate over the 15 nautical mile level flight segment at the initial approach fix altitude.

For the case when the initial descent velocity is at its maximum allowable value, the fastest Mach/IAS profile is flown during letdown. Additional time controllability can be achieved in order to arrive earlier by first varying the rate of acceleration from the initial EF velocity to the IDV and then flying at the IDV for the remaining level flight segment until the descent path is intercepted. The maximum acceleration rate achievable by the aircraft at the EF altitude limits the amount of additional time controllability attainable at that altitude. Then additional time controllability can be

achieved at the IAF altitude by flying level at the FDV and varying the deceleration to the desired final velocity at the IAF. Again, the additional time controllability attainable at this altitude is limited by the aircraft's maximum deceleration rate. In a similar manner, for the case when the slowest Mach/IAS profile is flown during letdown, additional time controllability can be achieved in order to arrive later by varying the deceleration rate at the EF altitude and the acceleration rate at the IAF altitude. The scheduler could also assign a final velocity at the IAF that is less than 250 KIAS in order for the aircraft to be able to arrive even later.

Therefore, the complete route-time profile can be generated using the strategic control strategy described in this section. Summarizing, the aircraft adheres to a specific linear altitude-ground track descent profile, thus any initial descent velocity implies a particular Mach/IAS for letdown. The choice of the initial descent velocity is the primary variable in determining a route-time profile that satisfies the boundary conditions at the entry fix and initial approach fix. In addition, when the initial descent velocity is at its minimum value, the choice of the transition altitude between the critical altitude and the entry fix altitude is an additional variable in determining the route-time profile. For different Mach/IAS letdown profiles, an integration of the

corresponding wind and temperature corrected groundspeed profiles over the fixed descent route results in a range of achievable arrival times at the IAF for the given boundary conditions.

2.2.4 ROUTE-TIME PROFILE BOUNDARY CONDITIONS USED IN THIS STUDY

In this study, the strategic control descent profile between the entry fix and initial approach fix, with dimensions exactly as depicted in Figure 2-1, is applied to the descent phase of flight for airline transports from cruise altitudes down the boundary of the Terminal Control Area of Logan International Airport. The descent route profile lies in a single vertical plane at an orientation of 53.07° from magnetic north. The aircraft enters the strategic control system at a cruise altitude of 35,000 feet with a true airspeed of 475 knots at the entry fix which is located approximately 155.4 natuical miles from the airport and 125.4 nautical miles from the Providence VOR (very high frequency omni-range) station along its 233.07° radial. The IAF is located directly over the Providence VOR at an altitude of 10,000 feet. Imposing the constraint of an assigned time of arrival at the IAF, the aircraft must reach this waypoint with a final indicated airspeed not exceeding 250 KIAS by controlling its airspeed along the route profile.

The aircraft's initial position at the entry fix, its terminal position at the initial approach fix, and the aircraft's ground track in transversing from the EF to the IAF are illustrated in Figure 2-7 with respect to an arbitrarily chosen earth coordinate system. The earth coordinate system has its origin located approximately at 71° 11' W, 42° 12' N, corresponding to a point 1,050 feet past the threshold of runway 4R (approximately at the aircraft touchdown point) at Logan International Airport, Boston, Massachusetts. The positive earth X-axis is coincident with runway 4R at a magnetic heading of 35°. The positive Y-axis is at a magnetic heading of 125°. The positive Z-axis is perpendicular to the earth's surface and points upward; this axis measures altitude (h).

2.3 CALCULATION OF ARRIVAL TIMES AND ROUTE-TIME PROFILES

Applying the route-time generation strategy described previously to the descent profile depicted in Figure 2-1 along with the aircraft's boundary conditions and specific ground track shown in Figure 2-7, the possible times of arrival at the IAF corresponding to various initial descent velocities and transition altitudes are presented in Table 2-1 for the Boeing 707-320B aircraft. These times are based on standard day conditions without wind as described by the aircraft's velocity profile in Figure 2-6. For each initial descent velocity and transition altitude, the times of arrival at the

Fig. 2-7 Earth Coordinate System Map and Aircraft Ground Track

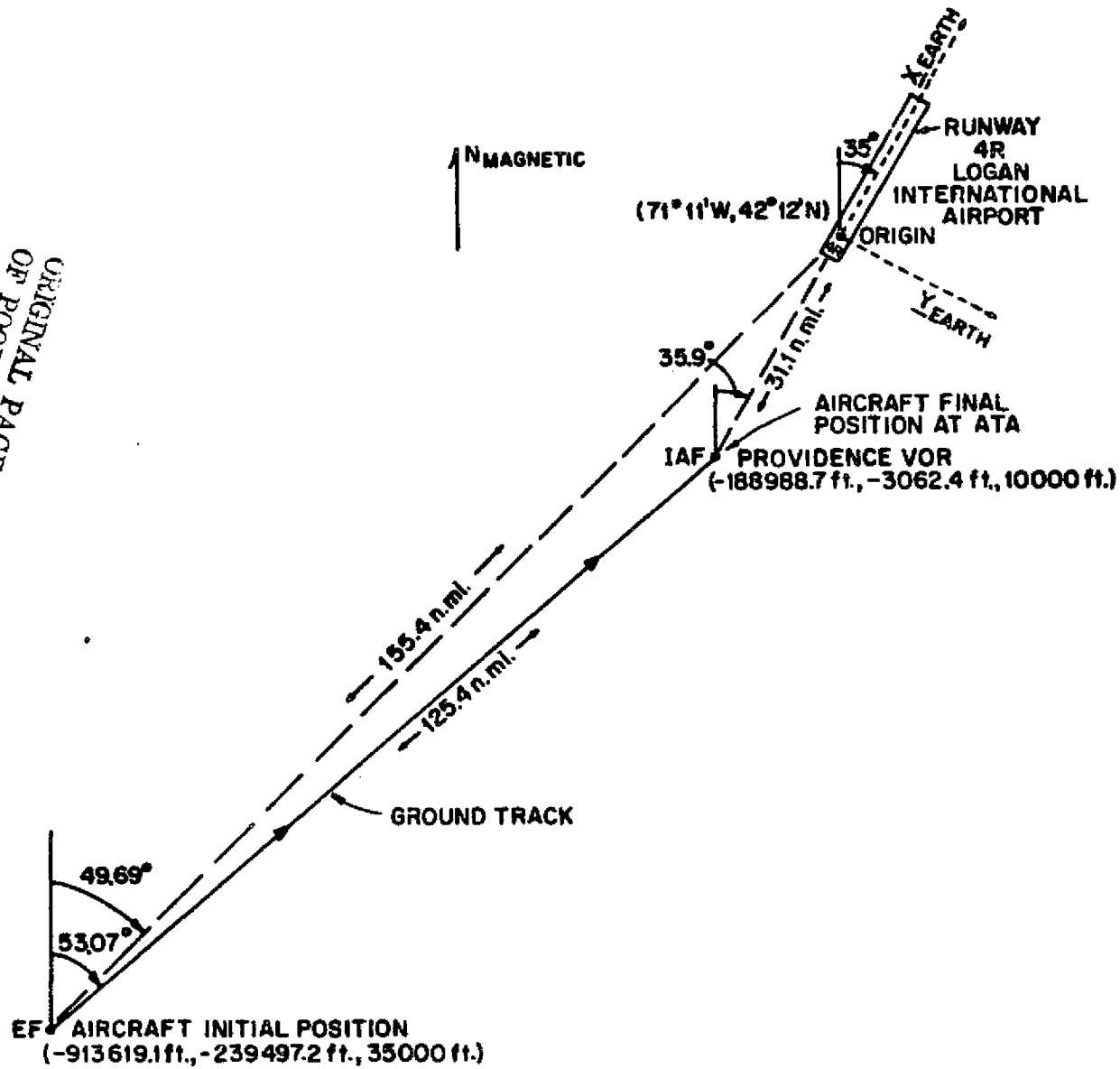

ORIGINAL PAGE IS
OF POOR QUALITY

TABLE 2-1

POSSIBLE TIMES OF ARRIVAL AT IAF FOR BOEING 707-320B

Initial Descent Velocity (KTAS)	Transition Altitude (Ft.)	Acceleration at 35,000 Ft. (Ft./Sec.^{2})	Acceleration at 10,000 Ft. (Ft./Sec.^{2})	Time at WP1 T1 (Min.)	Time at WP2 T2 (Min.)	Time at WP3 T3 (Min.)	Time at IAF ATA (Min.)
496	25000	0.14	-1.47	3.92	7.70	13.82	16.41
491	25000	0.10	-1.41	3.94	7.72	13.96	16.56
486	25000	0.07	-1.37	3.96	7.80	14.04	16.66
481	25000	0.03	-1.31	3.98	7.88	14.18	16.82
476	25000	0.00	-1.26	4.00	7.90	14.32	16.97
471	25000	-0.03	-1.20	4.02	7.98	14.46	17.13
466	25000	-0.07	-1.15	4.04	8.06	14.60	17.29
461	25000	-0.10	-1.11	4.07	8.09	14.69	17.39
456	25000	-0.13	-1.06	4.09	8.17	14.83	17.55
451	25000	-0.17	-1.01	4.11	8.25	14.97	17.70
446	25000	-0.20	-0.96	4.13	8.33	15.11	17.86
441	25000	-0.23	-0.91	4.15	8.35	15.25	18.02
436	25000	-0.26	-0.85	4.18	8.44	15.46	18.25
431	25000	-0.30	-0.81	4.20	8.52	15.60	18.41
426	25000	-0.33	-0.76	4.22	8.60	15.74	18.57
421	25000	-0.36	-0.72	4.25	8.69	15.89	18.73
416	25000	-0.39	-0.67	4.27	8.77	16.09	18.96
411	25000	-0.42	-0.62	4.29	8.79	16.24	19.12
406	25000	-0.45	-0.58	4.32	8.88	16.38	19.28
401	25000	-0.48	-0.54	4.34	8.96	16.58	19.51
396	25000	-0.51	-0.49	4.37	9.05	16.79	19.73
391	25000	-0.54	-0.45	4.39	9.13	16.93	19.90
386	25000	-0.57	-0.41	4.42	9.22	17.14	20.12
381	25000	-0.60	-0.36	4.45	9.31	17.35	20.35
376	25000	-0.62	-0.32	4.47	9.39	17.55	20.58
371	25000	-0.65	-0.28	4.50	9.54	17.70	20.74
366	25000	-0.68	-0.24	4.52	9.62	17.90	20.97
361	25000	-0.71	-0.20	4.55	9.71	18.17	21.26
356	25000	-0.73	-0.16	4.58	9.80	18.38	21.49
351	25000	-0.76	-0.12	4.61	9.89	18.59	21.72
346	25000	-0.78	-0.09	4.63	10.03	18.79	21.95
346	26000	-0.78	-0.03	4.63	9.49	19.03	22.23
346	27000	-0.78	0.02	4.63	8.95	19.21	22.44
346	28000	-0.78	0.07	4.63	8.41	19.45	22.72
346	29000	-0.78	0.12	4.63	7.87	19.75	23.06
346	30000	-0.78	0.17	4.63	7.33	19.99	23.33
346	31000	-0.78	0.22	4.63	6.85	20.35	23.73
346	32000	-0.78	0.27	4.63	6.31	20.65	24.07
346	33000	-0.78	0.31	4.63	5.77	21.01	24.47
346	34000	-0.78	0.36	4.63	5.23	21.43	24.93
346	35000	-0.78	0.41	4.63	4.63	21.91	25.46

specified waypoints along the descent profile are based on: 1) linear groundspeed transitions with respect to time at the entry fix and initial approach fix altitudes, and 2) groundspeeds which are piecewise linear approximations to the constant Mach/IAS profile during letdown between the EF and IAF altitudes, where the groundspeeds reflect approximate wind and temperature corrections [5].

The particular route-time profile used in this study corresponding to an ATA of 19.73 minutes at the IAF is shown in Table 2-2.

The actual equations used in calculating the possible times of arrival at the IAF and the corresponding route-time profiles are included in the computer programs "ATA" and "RTP" which are listed in Appendix B.

TABLE 2-2

ROUTE-TIME PROFILE--ATA = 19.73 MINUTES

Time (Min.)	Altitude (Ft.)	RANGE (N.Mi.)	TAS (Knots)	IAS (Knots)	MACH	dh/dt (Ft./Min.)
0.00	35000	125.4	476.0	279.0	0.827	0
0.60	35000	120.6	465.0	272.5	0.808	0
1.20	35000	116.1	454.0	266.1	0.789	0
1.80	35000	111.6	443.0	259.7	0.769	0
2.40	35000	107.2	432.1	253.2	0.750	0
3.00	35000	102.9	421.1	246.8	0.731	0
3.60	35000	98.8	410.1	240.4	0.712	0
4.20	35000	94.7	399.1	233.9	0.693	0
4.97	33738	89.6	397.9	239.8	0.687	-1632
5.57	32469	85.6	400.0	247.8	0.687	-2114
6.17	31193	81.6	402.1	255.7	0.687	-2125
6.77	29911	77.6	404.3	263.8	0.687	-2137
7.37	28622	73.5	406.4	271.8	0.687	-2148
7.97	27326	69.4	408.6	279.9	0.687	-2159
8.57	26023	65.3	410.8	288.1	0.687	-2171
9.65	23700	58.0	404.6	295.3	0.671	-2151
10.25	22426	54.0	396.2	295.2	0.653	-2122
10.85	21179	50.1	388.4	295.2	0.637	-2079
11.45	19955	46.3	381.1	295.2	0.622	-2039
12.05	18754	42.5	374.3	295.2	0.608	-2001
12.65	17574	38.8	367.8	295.1	0.595	-1966
13.25	16414	35.1	361.8	295.1	0.583	-1933
13.85	15273	31.5	356.1	295.1	0.571	-1902
14.45	14149	28.0	350.7	295.1	0.560	-1873
15.05	13042	24.5	345.6	295.1	0.549	-1845
15.65	11951	21.1	340.7	295.1	0.539	-1818
16.25	10874	17.7	336.1	295.0	0.530	-1793
16.79	10000	15.0	331.7	294.4	0.521	-1620
17.39	10000	11.7	321.1	285.0	0.504	0
17.99	10000	8.5	310.6	275.6	0.488	0
18.59	10000	5.2	300.0	266.3	0.471	0
19.19	10000	2.5	289.5	256.9	0.455	0
19.73	10000	0.0	280.0	250.0	0.440	0

CHAPTER III

THE AIRCRAFT MODEL

Airspeed flexibility is a fundamental requirement for all aircraft operating in a strategic air traffic control environment utilizing a time-controlled navigation system. The similarity in operating airspeeds and cruising altitudes for modern jet transport aircraft is apparent from the aeroperformance data contained in Table 3-1. The conclusion to be drawn from this data is that typical modern jet transport aircraft possess the airspeed flexibility required for an effective time-controlled navigation system. Thus a wide variety of jet transport aircraft would be acceptable for use in a strategic four-dimensional aircraft navigation study.

The Boeing 707-320B aircraft was selected for use in this study primarily due to the availability of a precise and accurate mathematical model [6]. The derivation of the equations of motion using Newtonian mechanics is standard and is available from numerous references [9,10,11]. While the aerodynamic forces and moments are based on a standard derivation, the physical parameters and aerodynamic coefficients are characteristic of the Boeing 707-320B. The equations governing aircraft motion relative to certain reference frames are presented in this chapter, but an evaluation of the aerodynamic coefficients and justification for the assumptions and linearizations used

TABLE 3-1

AIRCRAFT AEROPERFORMANCE DATA[1]

Altitudes (feet)	Minimum Speed at Minimum Wt. (KTAS)	Maximum Speed at Minimum Wt. (KTAS)	Minimum Speed at Maximum Wt. (KTAS)	Maximum Speed at Maximum Wt. (KTAS)
Aircraft - 707	Minimum Weight - 170,000 pounds Maximum Weight - 247,000 pounds			
10,000	202	435	229	435
21,600	243	530	275	527
32,000	288	515	325	505
39,000	330	498	415	470
Aircraft - 727	Minimum Weight - 125,000 pounds Maximum Weight - 160,000 pounds			
10,000	231	452	231	452
20,000	270	535	277	530
31,000	325	510	365	500
36,000	360	490	447	447
Aircraft - 737	Minimum Weight - 80,000 pounds Maximum Weight - 104,000 pounds			
10,000	243	407	243	407
22,500	295	500	295	495
31,000	340	480	353	465
35,000	364	465	395	445
Aircraft - 747	Minimum Weight - 400,000 pounds Maximum Weight - 565,000 pounds			
10,000	230	436	255	436
22,000	276	534	315	532
32,0-0	328	523	385	515
39,000	375	510	468	468
Aircraft - DC-10	Minimum Weight - 270,000 pounds Maximum Weight - 370,000 pounds			
10,000	226	430	262	430
25,000	290	528	330	526
35,000	338	506	388	497
38,000	355	501	417	448
Aircraft - 720B	Minimum Weight - 145,000 pounds Maximum Weight - 175,000 pounds			
10,000	160	420	200	420
22,000	205	530	240	530
35,000	265	525	305	514
40,000	320	505	365	480

[1]Source: [4: pp. 212-213]

in the development of the model are discussed in detail in Corley's study [6].

3.1 REFERENCE FRAMES

The equations of motion of the aircraft are described conveniently by using a relative-coordinate system that has its origin at the aircraft's center of gravity. Within the relative-coordinate system are three reference frames using the aircraft's center of gravity as their common origin. These reference frames--wind axes, body axes, vehicle axes--are related by the aerodynamic and Euler angles. Each reference frame is used for a specific purpose. The aerodynamic forces acting on the aircraft are most easily computed in the wind axis system, although the total aircraft forces and moments are most naturally represented in the body axis system of the aircraft. The orientation of the aircraft with respect to magnetic north and the "flat" earth is described in the vehicle axis system, also known as the Eulerian axis system.

The relative-coordinate system, or more specifically the Eulerian axis system, moves with the linear velocity of the center of gravity of the aircraft and can be referenced to an inertial-coordinate system described by the earth reference frame. The earth axis system has been arbitrarily positioned for purposes of this simulation study and describes the position of the aircraft with respect to its origin located on the

earth's surface. This earth coordinate system, as depicted in Figure 2-7, is convenient for purposes of horizontal and vertical aircraft navigation.

The reference frames are well-defined under the following assumptions [6,10,11]:

1. The aircraft is regarded as a rigid body. This is not strictly true, but for practical purposes, it is valid to consider the aeroelastic effects as negligible for the purposes of this study.

2. The aircraft velocity is below Mach 3.0. This is true of all modern jet transports.

3. The earth's rotation is small compared with the rotation of the aircraft vehicle. This certainly is valid since the rotation of the earth, $w_e = 7 \times 10^{-5}$ rad./sec., is much smaller than any significant aircraft rotation.

4. The earth is fixed in space and the earth's atmosphere is fixed with respect to the earth. In effect, the curvature of the earth's surface in space is neglected and the earth reference is regarded as a plane fixed in inertial space with the gravity vector perpendicular to this plane.

5. The mass, moments of inertia, and products of inertia of the aircraft are time-invariant. In addition, the center of gravity of the aircraft is fixed.

6. The aircraft is symmetrical about the plane defined by the X- and Z- body axes. Therefore, $I_{xy}=I_{yz}=0$.

The wind, body, and vehicle coordinate systems are each a set of right-handed, orthogonal axes with the origin at the aircraft's center of gravity. In the wind axis system, the positive X- axis is coincident with the total aircraft velocity vector which is opposite the "relative wind." The wind axes

are used to compute the aerodynamic forces, lift, drag, and side force, that act on the aircraft.

The body axis system has its positive X-axis coincident with the longitudinal axis of the aircraft. The positive Z-axis is perpendicular to the "belly" of the aircraft and points downward. The X-Z plane is considered the plane of symmetry for the aircraft body. The aerodynamic forces are rotated from the wind axes into the body axes. The body axes are then used to compute the total aircraft forces and moments. The total force components, F_x, F_y, F_z, are determined by the aerodynamic forces, engine thrust, and gravity.

The positive vehicle X-axis is coincident with the gravity vector. The X-Y plane is "parallel" to the earth's surface.

3.2 EULER AND AERODYNAMIC ANGLES

The Euler angles describe the rotation of the body axis system into the vehicle axis system by the following sequence of rotations:

1. A rotation ψ about the vehicle Z-axis is the "azimuth" angle.

2. A rotation θ about the vehicle Y-Axis is the "elevation" angle.

3. A rotation ϕ about the vehicle X-axis is the "bank" angle.

The aerodynamic angles rotate the wind axis system into the body axis system and are used in calculating the resultant

aerodynamic forces acting on the aircraft. The aerodynamic angles of interest are alpha (α), the fuselage angle of attack of the aircraft and beta (β), the sideslip angle. A second angle of attack (α_b), which is used in the lift calculations, differs from the fuselage angle of attack by an additional 2°, the aircraft angle of incidence. A third aerodynamic angle, gamma (γ), is the flight path angle of the aircraft with respect to the ground.

The wind and body axis systems are illustrated in Figure 3-1 along with the aerodynamic angles. The rotation of the body axis system with respect to the vehicle axis system as described by the Euler angles is depicted in the master diagram of the axis systems shown in Figure 3-2 [10].

3.3 EQUATIONS OF MOTION

The aircraft equations of motion are characterized by force and moment equations that are most naturally expressed in several reference frames along with transformation equations relating them to each other. Subject to the previously stated assumptions, these equations are applicable to any aircraft with six degrees of freedom. The linear velocity components (u,v,w) with respect to the body axes are expressed as:

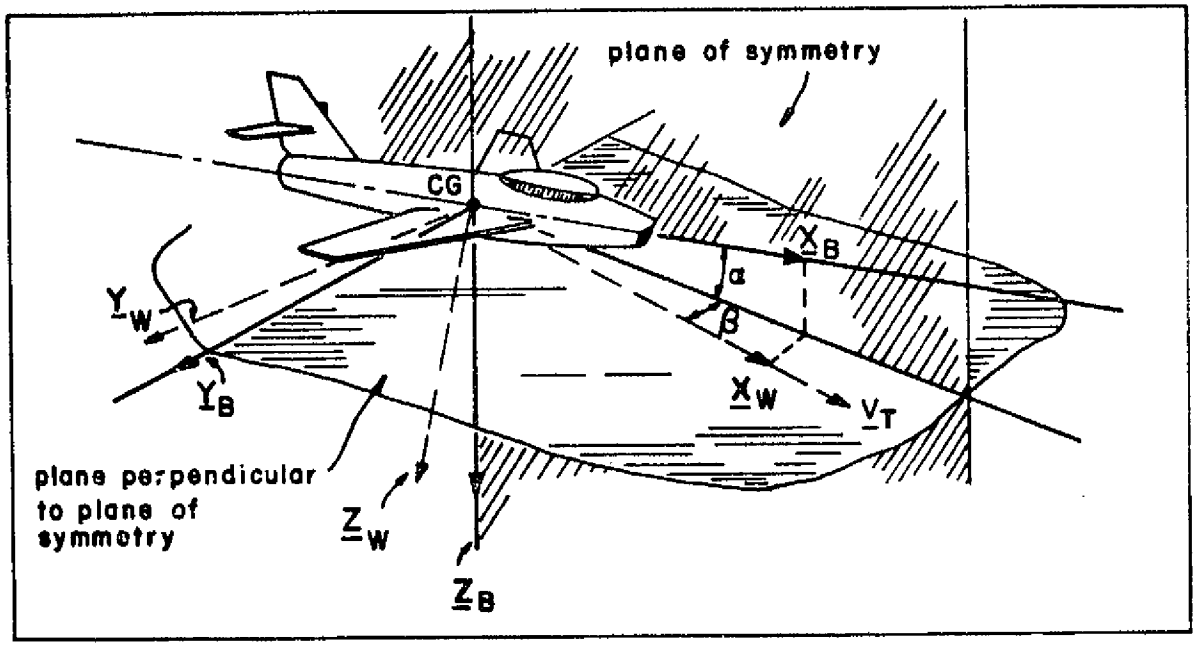

Fig. 3-1 Wind and Body Axes and Aerodynamic Angles

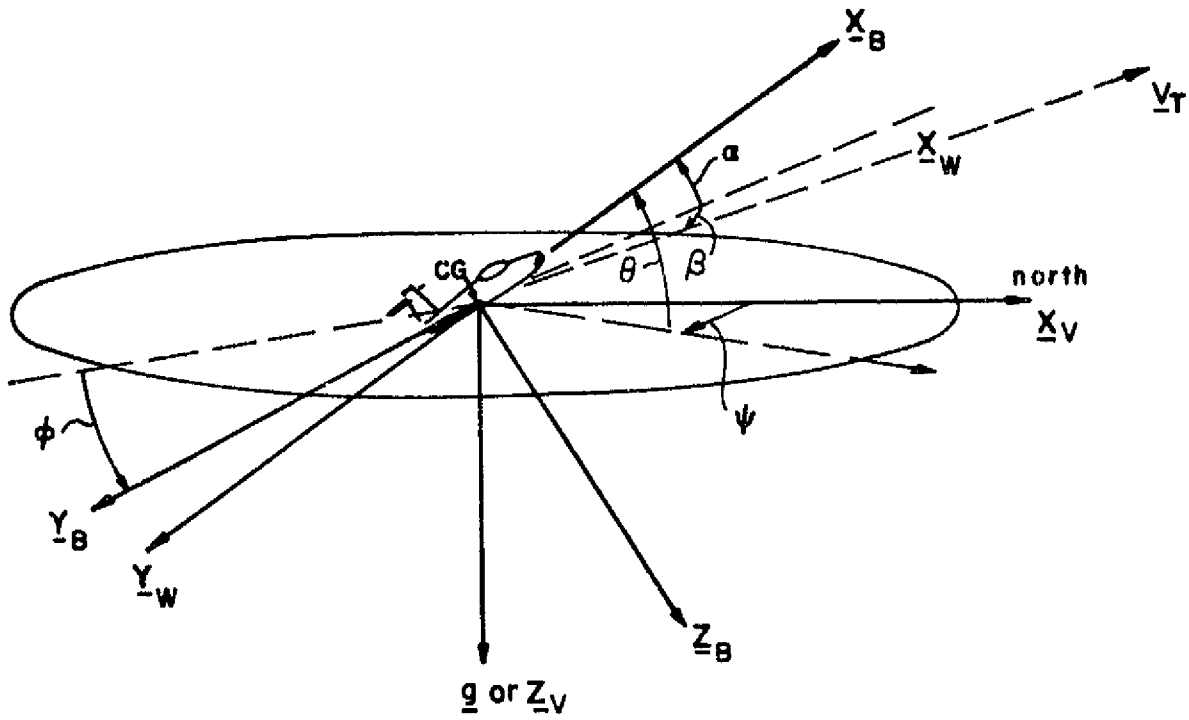

Fig. 3-2 Master Diagram of Axis Systems and Euler Angles

$$\begin{bmatrix} \dot{u} \\ \dot{v} \\ \dot{w} \end{bmatrix} = \frac{1}{\text{Mass}} \begin{bmatrix} F_x \\ F_y \\ F_z \end{bmatrix} + \begin{bmatrix} 0 & r & -q \\ -r & 0 & p \\ q & -p & 0 \end{bmatrix} \begin{bmatrix} u \\ v \\ w \end{bmatrix} \qquad 3\text{-}1$$

where F_x, F_y, and F_z are the force components determined by engine thrust, gravity, and the resultant aerodynamic forces after rotation into the body frame. These force components along the body axes are expressed as:

$$\begin{bmatrix} F_x \\ F_y \\ F_z \end{bmatrix} = \begin{bmatrix} \cos\alpha & 0 & -\sin\alpha \\ 0 & 1 & 0 \\ \sin\alpha & 0 & \cos\alpha \end{bmatrix} \begin{bmatrix} \cos\beta & -\sin\beta & 0 \\ \sin\beta & \cos\beta & 0 \\ 0 & 0 & 1 \end{bmatrix} \begin{bmatrix} \text{-DRAG} \\ \text{SIDE FORCE} \\ \text{-LIFT} \end{bmatrix}$$

$$+ \text{ Weight} \begin{bmatrix} -\sin\theta \\ \cos\theta \sin\phi \\ \cos\theta \cos\phi \end{bmatrix} + \begin{bmatrix} \text{THRUST} \\ 0 \\ 0 \end{bmatrix} \qquad 3\text{-}2$$

The sines and cosines of the aerodynamic angles, which are functions of various airspeeds, are computed using the following approximations:

$$\sin\alpha = \frac{w}{V_T} \approx \alpha \qquad 3\text{-}3$$

$$\cos\alpha = \frac{u}{V_T} \qquad 3\text{-}4$$

$$\sin\beta = \frac{v}{V_T} \approx \beta \qquad 3\text{-}5$$

$$\cos\beta \approx 1 - \frac{\beta^2}{2!} \qquad 3\text{-}6$$

where

$$V_T = \text{total velocity} = \sqrt{u^2 + v^2 + w^2} \qquad 3\text{-}7$$

The angular velocity components (p,q,r) written in the body axes are expressed as:

$$\begin{bmatrix} \dot{p} \\ \dot{q} \\ \dot{r} \end{bmatrix} = \begin{bmatrix} I_{xx} & 0 & -I_{xz} \\ 0 & I_{yy} & 0 \\ -I_{xz} & 0 & I_{zz} \end{bmatrix}^{-1} \left\{ \begin{bmatrix} L \\ M \\ N \end{bmatrix} + \begin{bmatrix} 0 & r & -q \\ -r & 0 & p \\ q & -p & 0 \end{bmatrix} \times \begin{bmatrix} I_{xx} & 0 & -I_{xz} \\ 0 & I_{yy} & 0 \\ -I_{xz} & 0 & I_{zz} \end{bmatrix} \begin{bmatrix} p \\ q \\ r \end{bmatrix} \right\} \qquad 3\text{-}8$$

The linear and angular velocity components along with the total force and moment components are depicted in the body axis system as shown in Figure 3-3. [9]

The Euler angles (ϕ,θ,ψ) are computed from the body axes angular velocities and are expressed as:

$$\begin{bmatrix} \dot{\phi} \\ \dot{\theta} \\ \dot{\psi} \end{bmatrix} = \frac{1}{\cos\theta} \begin{bmatrix} \cos\theta & \sin\phi\sin\theta & \cos\phi\sin\theta \\ 0 & \cos\phi\cos\theta & -\sin\phi\cos\theta \\ 0 & \sin\phi & \cos\phi \end{bmatrix} \begin{bmatrix} p \\ q \\ r \end{bmatrix} \qquad 3\text{-}9$$

The earth frame position is obtained by integrating the sum of the earth frame true airspeed components of the aircraft and the earth frame wind components. The wind velocity components are represented by a horizontal wind component (w_h) from a specific magnetic direction (ψ_w) and a vertical wind component (w_v) with positive direction downward. The earth

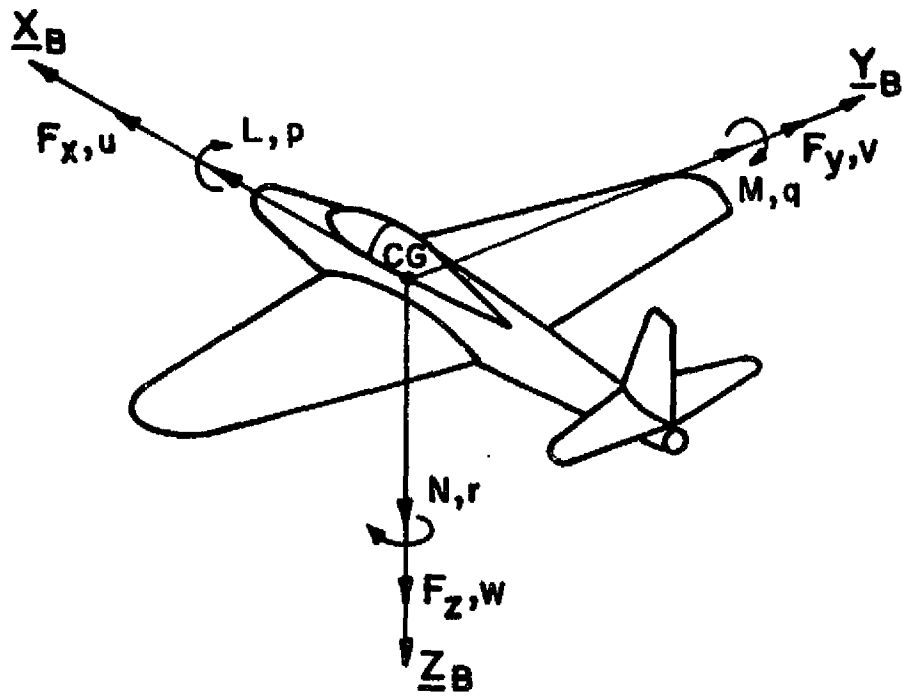

u	= FORWARD VELOCITY	p	= ROLLING VELOCITY
v	= SIDE VELOCITY	q	= PITCHING VELOCITY
w	= DOWNWARD VELOCITY	r	= YAWING VELOCITY
F_x	= TOTAL FORWARD FORCE	L	= ROLLING MOMENT
F_y	= TOTAL SIDE FORCE	M	= PITCHING MOMENT
F_z	= TOTAL DOWNWARD FORCE	N	= YAWING MOMENT

Fig. 3-3 Notation in Body Axes

frame wind components are expressed as:

$$\begin{aligned} \dot{x}_w &= - w_h \cdot \cos\ (\psi_w - 35°) \\ \dot{y}_w &= - w_h \cdot \sin\ (\psi_w - 35°) \\ \dot{h}_w &= - w_v \end{aligned} \qquad 3\text{-}10$$

The earth frame aircraft velocity components are computed by first performing an axis rotation of the body axes velocity components into the vehicle frame system using the Euler angles and then another rotation into the earth frame system. The complete earth frame velocity components are:

$$\begin{bmatrix} \dot{x} \\ \dot{y} \\ \dot{h} \end{bmatrix} = \begin{bmatrix} \cos 35° & \sin 35° & 0 \\ -\sin 35° & \cos 35° & 0 \\ 0 & 0 & -1 \end{bmatrix} \begin{bmatrix} \cos\psi & -\sin\psi & 0 \\ \sin\psi & \cos\psi & 0 \\ 0 & 0 & 1 \end{bmatrix} \begin{bmatrix} \cos\theta & 0 & \sin\theta \\ 0 & 1 & 0 \\ -\sin\theta & 0 & \cos\theta \end{bmatrix} \times$$

$$\begin{bmatrix} 1 & 0 & 0 \\ 0 & \cos\phi & -\sin\phi \\ 0 & \sin\phi & \cos\phi \end{bmatrix} \begin{bmatrix} u \\ v \\ w \end{bmatrix} - \begin{bmatrix} w_h \cdot \cos\ (\psi_w - 35°) \\ w_h \cdot \sin\ (\psi_w - 35°) \\ w_v \end{bmatrix} \qquad 3\text{-}11$$

Alternatively, the earth frame position could be obtained by integrating the polar representation of the aircraft along its magnetic course as described by the following set of equations:

$$\begin{aligned} \dot{r}_e &= [\dot{x}_e \cdot \cos\ (\psi_o - 35°) + \dot{y}_e \cdot \sin\ (\psi_o - 35°)] \angle \psi_e \\ \dot{\psi}_e &= \frac{\dot{y}_e \cdot x_e - y_e \cdot \dot{x}_e}{x_e^{\ 2} + y_e^{\ 2}} \\ \dot{h} &= u \cdot \sin\theta - v \cdot \sin\phi \cos\theta - w \cdot \cos\phi \cos\theta - w_v \end{aligned} \qquad 3\text{-}12$$

where ψ_o is the magnetic direction of the aircraft from the

earth frame origin and ψ is the actual magnetic course of the aircraft as described by equation 3-9.

3.4 AIRCRAFT PHYSICAL PARAMETERS

The aircraft physical parameters which are used in the force and moment equations are characteristic of the Boeing 707-320B aircraft. These parameters are listed in Table 3-2.

A complete diagram of the Boeing 707 aircraft's flight control surfaces is shown in Figure 3-4. However, only certain flight controls are available in the aircraft model used in this study. The allowable control deflections for these controls are summarized in Table 3-3.

TABLE 3-2

BOEING 707-320B PHYSICAL PARAMETERS[1]

Parameter	Value	Units
wing area = S	3010.0	ft.^{2}
wing span = b	145.75	ft.
mean chord = c	22.69	ft.
weight	225000.0	lbs.
mass	6988.0	slugs
I_{xx}	3.82×10^6	lbs.-sec.^{2}-ft.
I_{yy}	4.85×10^6	lbs.-sec.^{2}-ft.
I_{zz}	8.12×10^6	lbs.-sec.^{2}-ft.
I_{xz}	0.372×10^6	lbs.-sec.^{2}-ft.

[1]Source [6]

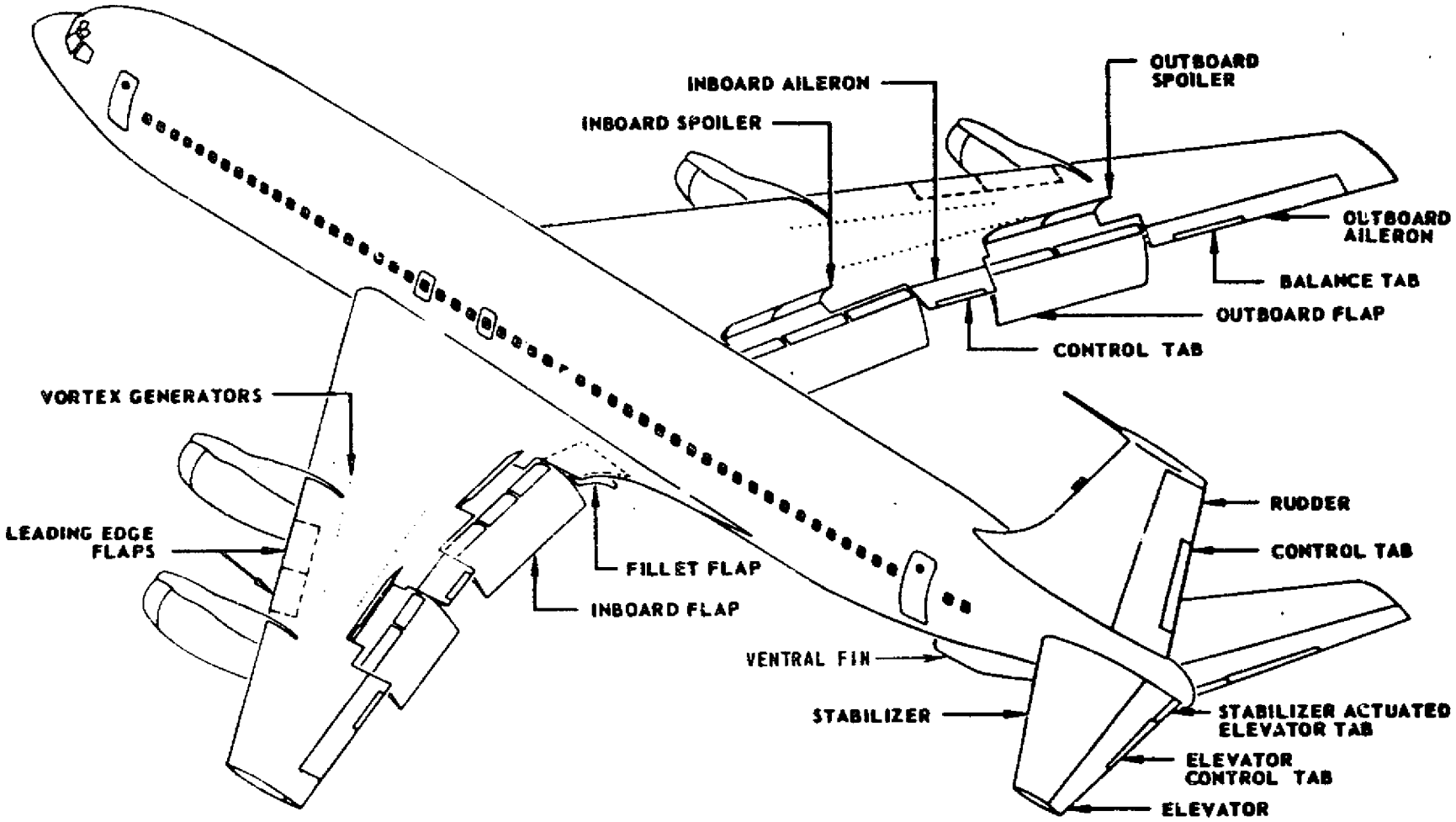

Fig. 3-4 Flight Control Surfaces - Boeing 707 [15]

TABLE 3-3

AIRCRAFT MANEUVERING CONTROL LIMITS

Control	Positive Sign Convention	Maximum	Minimum
Elevator (δ_E)	Trailing edge up	+20°	-20°
Rudder (δ_R)	Trailing edge right	+26.5°	-26.5°
Inboard Ailerons (δ_A)	Right trailing edge up	+18.5°	-18.5°
Spoilers (δ_B)	Positive deployment	60°[1]	0°
Flaps (δ_F)	Positive deployment	50°[2]	0°

[1] $\delta_{B_{max}} = 60° - .283 \cdot \max[0., KIAS - 188.]$

[2] flaps deploy fully in 30 seconds

3.5 ATMOSPHERE MODEL

Variations in atmospheric temperature and pressure are fundamental to the determination of the aerodynamic forces and moments. These equations depend upon the atmospheric density of the air surrounding the aircraft. The local atmospheric density of the air is approximated† by:

†These approximations are based on the U.S. standard atmosphere [16] which is approved for international standardization by the International Civil Aviation Organization (ICAO) and which is used by most nations and major airlines in the world. A standard day at sea level:

temperature - 15° Celsius
barometric pressure - 2116 lb./ft.^{2} = 29.92 inches mercury
atmospheric density - .002378 slugs/ft.^{3}

$$\rho = [1 - 1.835 \cdot (h/65536 + (h/65536)^2]\rho_o \text{ slugs/ft.}^3 \quad 3\text{-}13$$

where

h = altitude in ft.

ρ_o = sea level density = .002378 slugs/ft.^{3}

Mach number, defined as the ratio of the aircraft's true airspeed to the local speed of sound, is also essential to the equations of motion and can be approximated† by:

$$M = \begin{matrix}\text{Mach} \\ \text{Number}\end{matrix} = \frac{V_T}{(1.69) \cdot 661 \left(\frac{a}{a_o}\right)} \quad 3\text{-}14$$

where

$$\frac{a}{a_o} = \frac{\text{local speed of sound}}{\text{Sea level speed of sound}} = 1 - (3.683\text{x}10^{-6}) \cdot h \quad 3\text{-}15$$

a_o = 1116.4 ft./sec.

V_T = total true airspeed of the aircraft in ft./sec.

---

†See footnote on preceding page.

3.6 AERODYNAMIC FORCES

The aircraft aerodynamic force and moment equations are based on dynamic pressure, aircraft physical parameters, and dimensionless aerodynamic coefficients. The aerodynamic coefficients for the Boeing 707-320B aircraft have been determinuted [6] and are presented here for completeness. The aerodynamic force equations are:

$$\text{LIFT} = \frac{1}{2}\rho V_T^{\,2} S\left[C_{L_{\alpha_o}}(M)\cdot\alpha_o + C_{L_{\delta_E}}\cdot\delta_E + C_{L_{\delta_F}}\cdot(\delta_F - 6°) + C_{L_{\delta_F-\alpha_o}}\cdot\alpha_o\right] \qquad 3\text{-}16$$

$$C_{L_{\alpha_o}}(M) = (4.584 - 2.22(\text{Mach}) + 5.387(\text{Mach})^2/\text{radian}$$

$$C_{L_{\delta_E}} = -\ .0055/\text{degree}$$

$$C_{L_{\delta_F}} = \begin{cases} 0 & \delta_F \le 6° \\ .01432/\text{degree} & \delta_F > 6° \end{cases}$$

$$C_{L_{\delta_F-\alpha_o}} = \begin{cases} 0 & \delta_F \le 6° \\ 1.0811/\text{radian} & \delta_F > 6° \end{cases}$$

$$\text{DRAG} = \frac{1}{2}\rho\ V_T^{\,2} S\left[C_{D_{min}}(M) + k(M)\ C_L^{\,2} + C_{D_{gear}} + C_{D_{\delta F}}\cdot(\delta_F - 6°) + C_{D_{\delta_B}}\cdot\delta_B\right] \qquad 3\text{-}17$$

$$C_{D_{min}}(M) = \begin{cases} .012 & \text{Mach} \le .7 \\ .01233 + .0033(\text{Mach}-.8) & .7 < \text{Mach} \le .8 \\ .014 + .0371(\text{Mach}-.845) & .8 < \text{Mach} \le .845 \\ .014 + .1455(\text{Mach}-.845) & .845 < \text{Mach} \end{cases}$$

$$k(M) = \begin{cases} .0524 & \text{Mach} \le .8 \\ .063 + .2356(\text{Mach}-.845) & .8 < \text{Mach} \le .845 \\ .063 + .8333(\text{Mach}-.845) & .845 < \text{Mach} \end{cases}$$

C_L = total lift coefficient in brackets in eqn. 3-16

$C_{D_{gear}}$ = .0105 (when gear is down)

$$C_{D_{\delta_F}} = \begin{cases} 0 & \delta_F \leq 6° \\ .0018/\text{degree} & \delta_F > 6° \end{cases}$$

$C_{D_{\delta_B}}$ = .000833/degree

$$\text{SIDE FORCE} = \frac{1}{2}\rho V_T^2 S\left[C_{y_\beta}\cdot\beta + C_{y_{\delta_R}}\cdot\delta_R\right] \qquad 3\text{-}18$$

C_{y_β} = -.917/radian

$C_{y_{\delta_R}}$ = -.004/degree

3.7 AERODYNAMIC MOMENTS

The aerodynamic moment equations, which determine the roll, pitch, and yaw characteristics of the aircraft are:

$$L = \begin{matrix}\text{ROLLING}\\ \text{MOMENT}\end{matrix} = \frac{1}{2}\rho\ V_T^2\ Sb\left[C_{l_\beta}\cdot\beta + C_{l_{\delta_A}}\cdot\delta_A + C_{l_{\delta_R}}\cdot\delta_R\right] + \frac{1}{4}\rho\ V_T\ Sb^2\ C_{l_p}\cdot p \qquad 3\text{-}19$$

C_{l_β} = -.1719/radian

$C_{l_{\delta_A}}$ = .00113/degree

$C_{l_{\delta_R}}$ = -.0002/degree

C_{l_p} = -.38/radian

$$M = \begin{matrix}\text{PITCHING}\\ \text{MOMENT}\end{matrix} = \frac{1}{2}\rho\ V_T^2\ Sc\left[C_{m_o} + C_{m_\alpha}\cdot\alpha + C_{m_{\delta_E}}\cdot\delta_E + C_{m_{\delta_F}}\cdot(\delta_F - 14°)\right] + \frac{1}{4}\rho\ V_T\ Sc^2\left[C_{m_q} + C_{m_{\dot\alpha}}\right]q \qquad 3\text{-}20$$

C_{m_o} = .048

C_{m_α} = -.955/radian

$$C_{m_{\delta_E}} = .009/\text{degree}$$

$$C_{m_{\delta_F}} = \begin{cases} 0 & \delta_F < 14° \\ -.0033/\text{degree} & \delta_F < 14° \end{cases}$$

$$C_{m_q} = -29/\text{degree}$$

$$C_{m_{\dot{\alpha}}} = -3.7/\text{degree}$$

$$N = \begin{matrix}\text{YAWING}\\ \text{MOMENT}\end{matrix} = \frac{1}{2}\rho V_T^2 \, Sb\left[C_{n_\beta}\cdot\beta + C_{n_{\delta_R}}\cdot\delta_R\right] + \frac{1}{4}\rho \, V_T \, Sb^2 \, C_{n_r}\cdot r \qquad 3\text{-}21$$

$$C_{n_\beta} = .115/\text{radian}$$

$$C_{n_{\delta_R}} = .0011/\text{degree}$$

$$C_{n_r} = -.15/\text{radian}$$

The components of velocity, position, force, and moment are presented notationally in Table 3-4. The rotation is consistent with the reference frames depicted in Figures 3-1, 3-2, and 3-3, and note should be taken that a right-hand sign convention is observed throughout.

3.8 THE ENGINE MODEL

The variation of thrust with altitude and Mach number is considered important in time-controlled navigation. The most significant engine parameters [6] are maximum and minimum thrust. These parameters limit the flexibility in speed control of the aircraft which is necessary to ensure precise four-dimensional navigation.

TABLE 3-4

NOTATION USED IN EQUATIONS OF MOTION

Components	Axis			Units
	X	Y	Z	
Linear Velocity Along Body Axis	y	w	v	ft./sec.
Angular Velocity Along Body Axis	p	q	r	rad./sec.
Angular Displacements About Vehicle Axis	ϕ	θ	ψ	rad.
Earth Frame Position	x	y	h	ft.
Aerodynamic Forces Along Wind Axis	-DRAG	SIDE FORCE	-LIFT	lbs.
Total Force Components Along Body Axis	F_x	F_y	F_z	lbs.
Aerodynamic Moments Along Body Axis	L	M	N	ft.-lbs.
Moment of Inertia About Body Axis	I_{XX}	I_{yy}	I_{zz}	lbs.-sec.^{2}-ft.

The range of achievable thrust for the turbofan engine modeled in this study was determined [6] from the engine manufacturer's performance data over the range of altitudes and Mach numbers flown by the Boeing 707-320B. One such performance graph for the Pratt and Whitney JT3D-1 Turbofan Engine at sea level is shown in Figure 3-5. The normal operating Mach speeds for the Boeing 707 aircraft are listed in Table 3-5 for various altitudes.

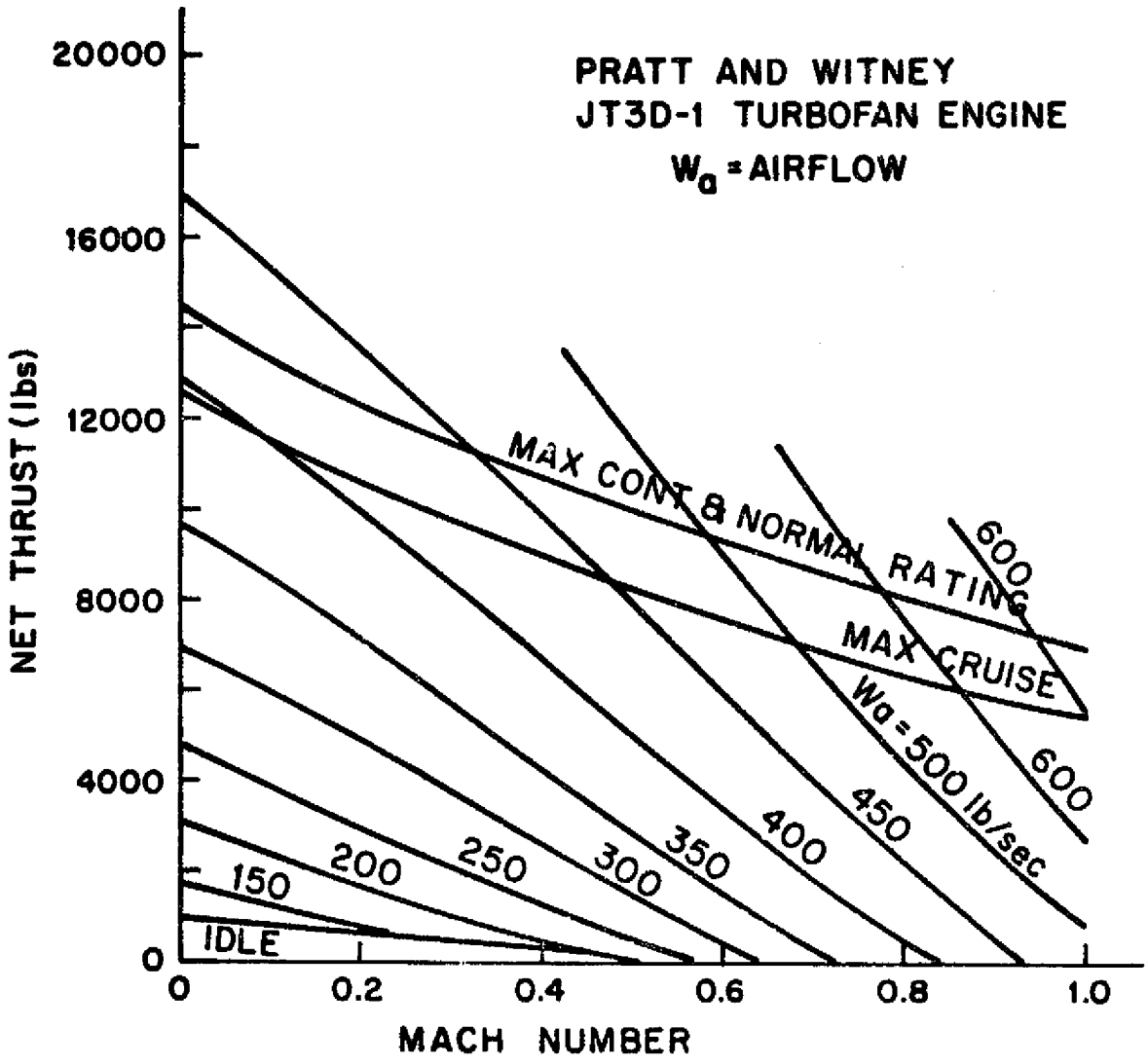

Fig. 3-5 Sea Level Thrust for P&W JT3D-1 Turbofan Engine

TABLE 3-5

BOEING 707 NORMAL OPERATING RANGE[1]

ALTITUDE	MINIMUM MACH[2]	MAXIMUM MACH[3]
Sea Level	.17	.51
5000	.17	.57
10000	.33	.63
15000	.37	.71
20000	.42	.79
25000	.47	.88
30000	.53	.88
35000	.61	.88
40000	.75	.88

[1]Source: [6: p. 53]

[2]V_{ref} or initial buffet for 1.3g maneuver

[3]Indicated airspeed structural limit converted to Mach below 25000 ft. Mach limit above 25000.

Using the engine performance charts along with the aircraft's Mach ranges for each altitude, the following equation was derived [6] for approximating the aircraft's thrust variation with altitude and Mach:

$$T(h,M) = T(h_o,0) + \frac{\partial T}{\partial h}\bigg|_{M=0} \dot{h} + \frac{\partial T}{\partial M}\bigg|_{h=h_o} \dot{M} + \frac{\partial^2 T}{\partial h \partial M}\bigg|_{\substack{M=0 \\ h=h_o}} (h-h_o)\cdot M \qquad 3\text{-}22$$

For calculating maximum thrust, let

$$\text{Maximum Thrust} = T(h,M) \qquad 3\text{-}23$$

using the following values:

$$h_o = \begin{cases} 0 & 0 \le h \le 15{,}000 \text{ ft.} \\ 15{,}000 & h > 15{,}000 \text{ ft.} \end{cases}$$

$$T(h,0) = 13{,}800 \text{ lbs.} \qquad \text{all } h_o$$

$$\left.\frac{\partial T}{\partial h}\right|_{M=0} = -.28125 \text{ lbs./ft.} \qquad \text{all } h_o$$

$$\left.\frac{\partial T}{\partial M}\right|_{h=h_o} = \begin{cases} -7800 \text{ lbs./Mach} & h_o = 0 \\ -3125 \text{ lbs./Mach} & h_o = 15{,}000 \end{cases}$$

$$\left.\frac{\partial^2 T}{\partial h \partial M}\right|_{\substack{M=0 \\ h=h_o}} = \begin{cases} +.3117 \text{ lbs./Mach-ft.} & h_o = 0 \\ +.185 \text{ lbs./Mach-ft.} & h_o = 15{,}000 \end{cases}$$

For idle thrust, let

$$\text{Idle Thrust} = \text{Max}[T(h,M),0] \qquad 3\text{-}24$$

using the following values:

$$h_o = \begin{cases} 0 & 0 \le h \le 15{,}000 \text{ ft.} \\ 15{,}000 & h > 15{,}000 \text{ ft.} \end{cases}$$

$$T(h,0) = 1{,}000 \text{ lbs.} \qquad \text{all } h_o$$

$$\left.\frac{\partial T}{\partial h}\right|_{M=0} = 0 \qquad \text{all } h_o$$

$$\left.\frac{\partial T}{\partial M}\right|_{h=h_o} = -2{,}000 \text{ lbs./Mach} \qquad \text{all } h_o$$

$$\left.\frac{\partial^2 T}{\partial h \partial M}\right|_{\substack{M=0 \\ h=h_o}} = \begin{cases} 0 & h_o = 0 \\ +.07 \text{ lbs./Mach-ft.} & h_o = 15{,}000 \end{cases}$$

The maximum and minimum thrust variation per aircraft engine using the derived approximation is compared to the manufacturer's thrust values in Figures 3-6 and 3-7. [6]

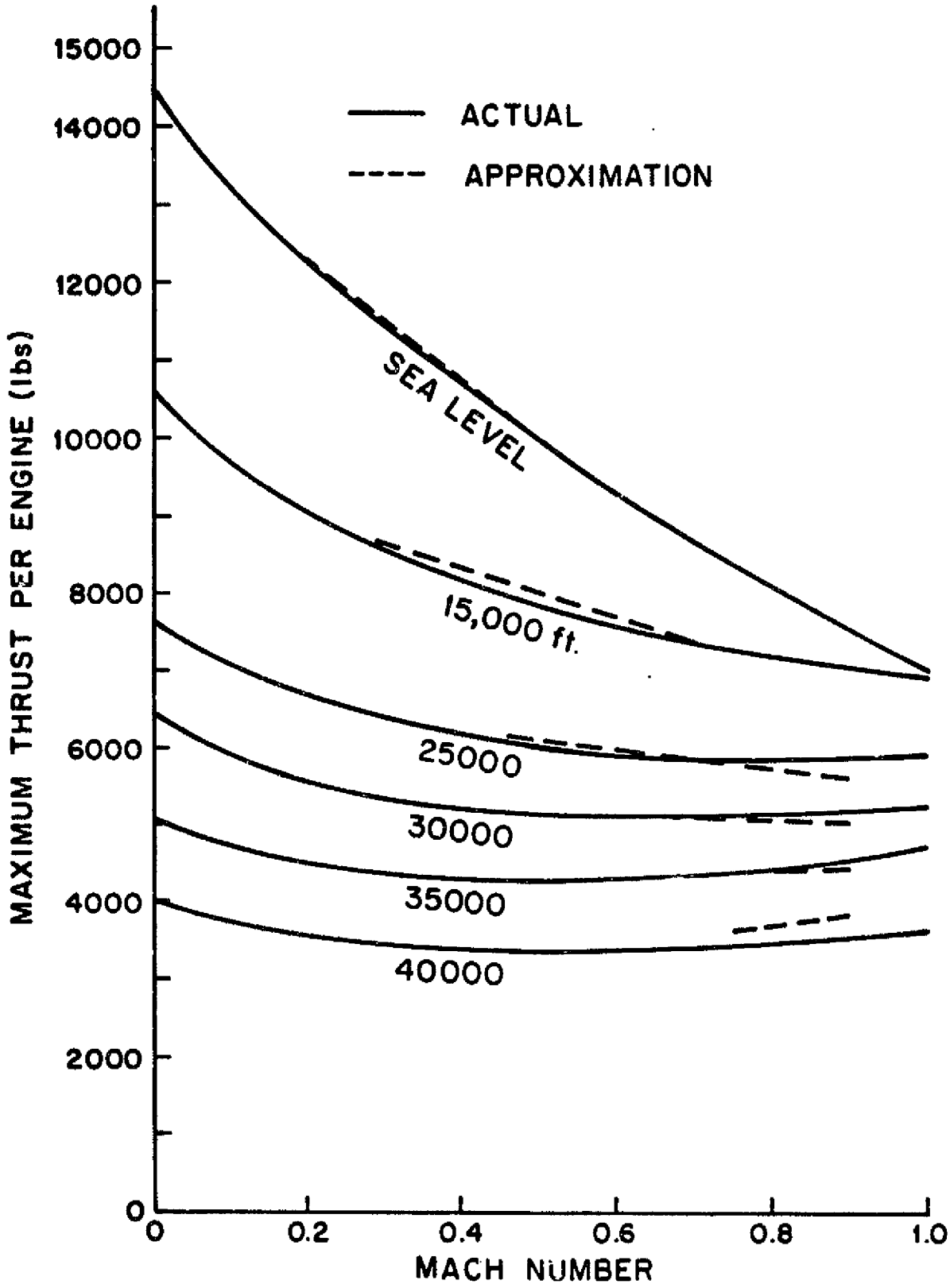

Fig. 3-6 Maximum Thrust Variation

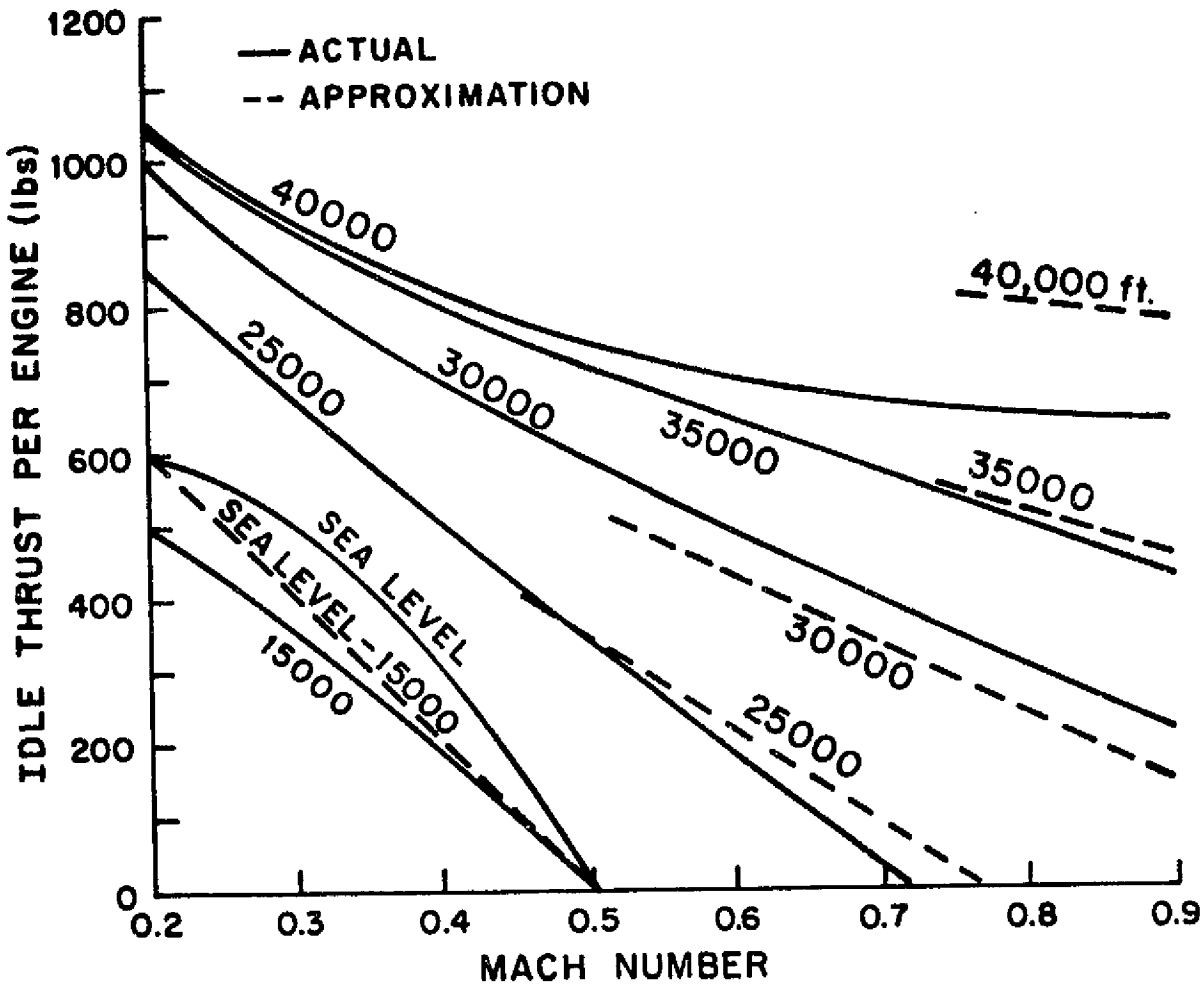

Fig. 3-7 Idle Thrust Variation

The dotted lines represent data obtained from the actual simulation as contained in Corley's study [6] using the thrust approximation equation over the airspeed ranges of interest for each altitude.

It is ultimately desirable to relate aircraft throttle position (T_p) to thrust variation. In general, the throttle controls engine speed by regulating fuel flow. [12,13] Engine speed and thrust are not linearly related, but the air flow (W_a) through the engine may be considered proportional to engine speed. [14] Therefore, throttle position can be related to thrust by normlizing the airflow for a given altitude and Mach number. The following relationship between thrust and throttle position was derived by Corley:

$$\frac{\text{Net Thrust}}{\text{Engine}} = \begin{matrix}\text{Idle}\\ \text{Thrust}\end{matrix} + \left(\begin{matrix}\text{Max}\\ \text{Thrust}\end{matrix} - \begin{matrix}\text{Idle}\\ \text{Thrust}\end{matrix}\right)\left(\begin{matrix}\text{Throttle}\\ \text{Position}\end{matrix}\right)^2 ;$$

$$0 \leq \begin{matrix}\text{Throttle}\\ \text{Position}\end{matrix} (T_p) \leq 1 \qquad 3\text{-}25$$

where maximum thrust and idle thrust are defined by equations 3-23 and 3-24. Using the thrust data depicted in Fig. 3-5, the actual net thrust per engine, based on the assumption that airflow is proportional to engine speed and engine speed is proportional to throttle position, is compared to the above approximation in Fig. 3-8. [6]

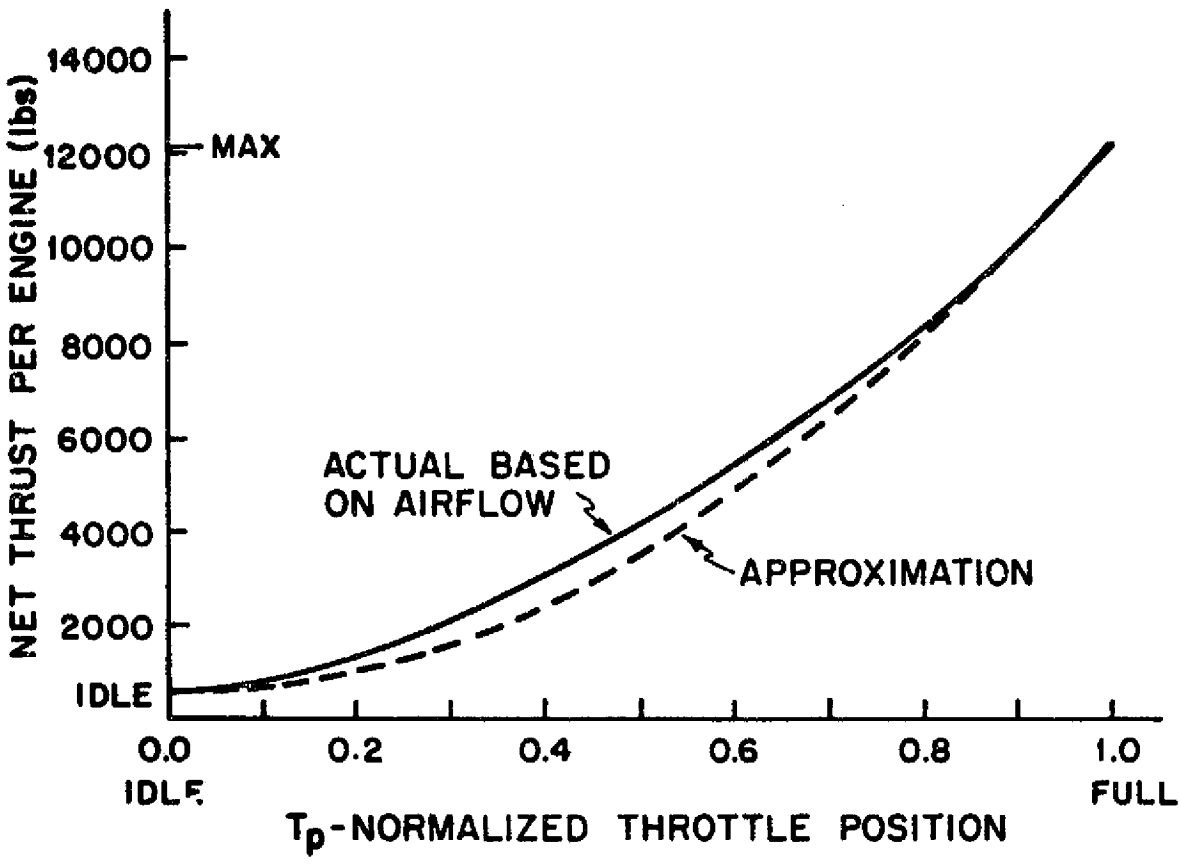

Fig. 3-8 Thrust Related to Throttle Position

3.9 REAL-TIME SIMULATION OF NONLINEAR AIRCRAFT MODEL

The complete Boeing 707-320B aircraft aerodynamics are represented by the equations of motion that have been presented in this chapter. Using the simulation facilities mentioned herein, these equations have been programmed to provide a real-time simulation of the aircraft's aerodynamics.

In the aircraft simulation program, the aircraft dynamics are straight-forward solutions to the equations presented in this chapter. The linear and angular accelerations (eqns. 3-1 and 3-8) and the Euler angle velocities (eqn. 3-9) are integrated using the trapezoidal rule:

$$V_n = V_{n-1} + \Delta t \cdot (3\dot{V}_n - \dot{V}_{n-1})/2 \qquad 3\text{-}26$$

The earth frame position is obtained by rectangular integration of the earth frame velocities (eqn. 3-11):

$$X_n = X_{n-1} + \Delta t \; V_n \qquad 3\text{-}27$$

The real-time simulation computer program is included in Appendix B. The program is documented throughout in order to provide its user with a basic outline of its organizational structure.

CHAPTER IV

DESIGN OF A 4-D NAVIGATION CONTROLLER

Using the aircraft model previously described and the associated atmosphere model, a 4-D strategic navigation control regulator has been designed. This controller incorporates two parts: a geographical navigation controller and a time navigation controller. Aircraft position, measured airspeed, and a route-time profile are the primary inputs for a 4-D navigation control system. Only navigation in the vertical plane is considered in this study. Vertical and time navigation are accomplished by controlling aircraft airspeed and descent rate.

In this chapter, a linear discrete-time system describing the aircraft's longitudinal aerodynamics is formulated from the complete nonlinear continuous-time system. Considerable care was exercised to make the aircraft linearization faithful to the basic aircraft physics while at the same time to make the controller compatible with the simulation: dynamic linearization requires fore knowledge of the nominal trajectories whereas the real-time simulation uses step-by-step integration of the aerodynamic equations. Using optimal linear quadratic control techniques, as available from numerous references [see for example 19, 20, 21], a cost function is formulated and an optimal linear feedback control solution is derived for application to time-controlled navigation.

4.1 LINEARIZATION

The equations of motion as expressed by equations 3-1, 3-8, 3-9, and 3-11 are nonlinear in that they contain products of the dependent variables as well as dependent variables that appear as transcendental functions. These nonlinear equations of motion can be expressed in the following form:

$$\dot{\underline{X}}(t) = \underline{F}\left(X(t),\ \underline{U}(t),\ \underline{W}(t)\right) \qquad 4\text{-}1$$

where the state vector is

$$\underline{X}(t) = \begin{bmatrix} u \\ v \\ w \\ p \\ q \\ r \\ \theta \\ \phi \\ \psi \\ x \\ y \\ h \end{bmatrix} = \begin{bmatrix} \text{forward body velocity} \\ \text{side body velocity} \\ \text{downward body velocity} \\ \text{roll angular velocity} \\ \text{pitch angular velocity} \\ \text{yaw angular velocity} \\ \text{pitch angle} \\ \text{bank angle} \\ \text{heading angle} \\ \text{X-axis earth position} \\ \text{Y-axis earth position} \\ \text{altitude} \end{bmatrix}$$

the control vector is

$$\underline{U}(t) = \begin{bmatrix} T \\ \delta_E \\ \delta_A \\ \delta_R \\ \delta_B \\ \delta_F \end{bmatrix} = \begin{bmatrix} \text{thrust} \\ \text{elevator deflection} \\ \text{aileron deflection} \\ \text{rudder deflection} \\ \text{spoiler deployment} \\ \text{flap deployment} \end{bmatrix}$$

and the exogenous wind vector is

$$\underline{W}(t) = \begin{bmatrix} w_v \\ w_h \end{bmatrix} = \begin{bmatrix} \text{vertical wind} \\ \text{horizontal wind from } \psi_w \end{bmatrix}$$

The states, controls, and exogenous variables are functions of time although this is not explicitly indicated.

The particular design problem of this study concerns 4-D navigation in the vertical plane from cruise altitudes to 10,000 feet above sea level. For the design applicable to these flight conditions, the following assumptions are made:

1. Since navigation is in the vertical plane, the following states can be considered constant:

   $v = p = r = \phi = 0.$
   ψ = initial aircraft magnetic course

2. The following controls can be considered constant for the flight conditions considered in this design:

   $\delta_A = \delta_R = \delta_B = \delta_F = 0.$

   The use of spoiler deployment, δ_B, is acceptable, but it is considered as an inactive control in this design as its application is usually limited to special flight conditions.

3. The drag coefficients $C_{D_{min}}$ and k vary with u, w, and h, but their variation is small enough so that it may be neglected:

   $0.012 \leq C_{D_{min}} \leq 0.014;\ 0.0524 \leq k \leq 0.063;\ \text{Mach} \leq .845$

4. The slope of the lift coefficient curve, $C_{L_{\alpha_o}}$, varies significantly with u, w, and h, and this variation may not be neglected:

   $3.925 \leq C_{L_{\alpha_o}} \leq 6.584;\ 0.2 \leq \text{Mach} \leq .845$

It is essential to include states in the system that describe aircraft position since the primary objective of time-

controlled navigation is to place the aircraft at specified 3-D geographical locations at specified times. The x and y earth frame coordinates can be combined to create a range state $r = r_e$ (as described by equation 3-12). In addition the earth frame origin can be translated to the initial approach fix so that the range reflects the horizontal distance of the aircraft from the IAF. For navigation in the vertical plane, both the range and altitude states can completely describe the aircraft position from the IAF along the constant magnetic course of the aircraft.

Therefore, for application to the particular navigation situation considered in this study, the nonlinear system can be reduced and written in the following form:

$$\dot{\underline{x}}(t) = \underline{f}\left(\underline{x}(t),\ \underline{u}(t),\ \underline{w}(t)\right) \qquad 4\text{-}2$$

where

$$\underline{x}(t) = \begin{bmatrix} u \\ w \\ q \\ \theta \\ h \\ r \end{bmatrix} \qquad \underline{u}(t) = \begin{bmatrix} T \\ \delta_E \end{bmatrix} \qquad \underline{w}(t) = \begin{bmatrix} w_v \\ w_h \end{bmatrix}$$

Let the following notation be used throughout this study:

$\underline{x}^o = \underline{x}^o(t)$ = nominal state vector

$\underline{u}^o = \underline{u}^o(t)$ = nominal control vector

$\underline{w}^o = \underline{w}^o(t)$ = predicted or nominal wind vector

$\delta\underline{x} = \underline{x}(t) - \underline{x}^{o}(t)$ = the incremental difference between the actual and nominal states; the state perturbation vector

$\delta\underline{u} = \underline{u}(t) - \underline{u}^{o}(t)$ = the incremental difference between the actual and nominal controls; the control correction vector

$\delta\underline{w} = \underline{w}(t) - \underline{w}^{o}(t)$ = the difference between the measured and predicted winds

Using a Taylor series expansion, we linearize as follows:

$$\dot{\underline{x}}^{o} + \delta\dot{\underline{x}} = \underline{f}(\underline{x}^{o} + \delta\underline{x},\ \underline{u}^{o} + \delta\underline{u},\ \underline{w}^{o} + \delta\underline{w}) \qquad 4\text{-}3$$

$$= \underline{f}(\underline{x}^{o},\underline{u}^{o},\underline{w}^{o}) + \left.\frac{\partial\underline{f}}{\partial\underline{x}}\right|_{\substack{\underline{x}=x^{o}\\ \underline{u}=\underline{u}^{o}\\ \underline{w}=\underline{w}^{o}}} \cdot \delta\underline{x} + \left.\frac{\partial\underline{f}}{\partial\underline{u}}\right|_{\substack{\underline{x}=\underline{x}^{o}\\ \underline{u}=\underline{u}^{o}\\ \underline{w}=\underline{w}^{o}}} \cdot \delta\underline{u} + \left.\frac{\partial\underline{f}}{\partial\underline{w}}\right|_{\substack{\underline{x}=\underline{x}^{o}\\ \underline{u}=\underline{u}^{o}\\ \underline{w}=\underline{w}^{o}}} \cdot \delta\underline{w}$$

+ higher order terms

Neglecting the higher order terms,

$$\delta\dot{\underline{x}} = \left.\frac{\partial\underline{f}}{\partial\underline{x}}\right|_{o} \cdot \delta\underline{x} + \left.\frac{\partial\underline{f}}{\partial\underline{u}}\right|_{o} \cdot \delta\underline{u} + \left.\frac{\partial\underline{f}}{\partial\underline{w}}\right|_{o} \cdot \delta\underline{w} \qquad 4\text{-}4$$

$$= \underline{A} \cdot \delta\underline{x} + \underline{B} \cdot \delta\underline{u} + \underline{D} \cdot \delta\underline{w} \qquad 4\text{-}5$$

where

$$\underline{A} = \left.\frac{\partial\underline{f}}{\partial\underline{x}}\right|_{o} \qquad \underline{B} = \left.\frac{\partial\underline{f}}{\partial\underline{u}}\right|_{o} \qquad \underline{D} = \left.\frac{\partial\underline{f}}{\partial\underline{w}}\right|_{o} \qquad 4\text{-}6$$

are in general time-varying matrices.

Expanding equation 4-4, we have:

$$
\begin{bmatrix} \delta\dot{u} \\ \delta\dot{w} \\ \delta\dot{q} \\ \delta\dot{\theta} \\ \delta\dot{h} \\ \delta\dot{r} \end{bmatrix}
=
\begin{bmatrix}
\left.\frac{\partial\dot{u}}{\partial u}\right|_o & \left.\frac{\partial\dot{u}}{\partial w}\right|_o & \left.\frac{\partial\dot{u}}{\partial q}\right|_o & \left.\frac{\partial\dot{u}}{\partial\theta}\right|_o & \left.\frac{\partial\dot{u}}{\partial h}\right|_o & \left.\frac{\partial\dot{u}}{\partial r}\right|_o \\
\left.\frac{\partial\dot{w}}{\partial u}\right|_o & \left.\frac{\partial\dot{w}}{\partial w}\right|_o & \left.\frac{\partial\dot{w}}{\partial q}\right|_o & \left.\frac{\partial\dot{w}}{\partial\theta}\right|_o & \left.\frac{\partial\dot{w}}{\partial h}\right|_o & \left.\frac{\partial\dot{w}}{\partial r}\right|_o \\
\left.\frac{\partial\dot{q}}{\partial u}\right|_o & \left.\frac{\partial\dot{q}}{\partial w}\right|_o & \left.\frac{\partial\dot{q}}{\partial q}\right|_o & \left.\frac{\partial\dot{q}}{\partial\theta}\right|_o & \left.\frac{\partial\dot{q}}{\partial h}\right|_o & \left.\frac{\partial\dot{q}}{\partial r}\right|_o \\
\left.\frac{\partial\dot{\theta}}{\partial u}\right|_o & \left.\frac{\partial\dot{\theta}}{\partial w}\right|_o & \left.\frac{\partial\dot{\theta}}{\partial q}\right|_o & \left.\frac{\partial\dot{\theta}}{\partial\theta}\right|_o & \left.\frac{\partial\dot{\theta}}{\partial h}\right|_o & \left.\frac{\partial\dot{\theta}}{\partial r}\right|_o \\
\left.\frac{\partial\dot{h}}{\partial u}\right|_o & \left.\frac{\partial\dot{h}}{\partial w}\right|_o & \left.\frac{\partial\dot{h}}{\partial q}\right|_o & \left.\frac{\partial\dot{h}}{\partial\theta}\right|_o & \left.\frac{\partial\dot{h}}{\partial h}\right|_o & \left.\frac{\partial\dot{h}}{\partial r}\right|_o \\
\left.\frac{\partial\dot{r}}{\partial u}\right|_o & \left.\frac{\partial\dot{r}}{\partial w}\right|_o & \left.\frac{\partial\dot{r}}{\partial q}\right|_o & \left.\frac{\partial\dot{r}}{\partial\theta}\right|_o & \left.\frac{\partial\dot{r}}{\partial h}\right|_o & \left.\frac{\partial\dot{r}}{\partial r}\right|_o
\end{bmatrix}
\begin{bmatrix} \delta u \\ \delta w \\ \delta q \\ \delta\theta \\ \delta h \\ \delta r \end{bmatrix}
$$

$$
+
\begin{bmatrix}
\left.\frac{\partial\dot{u}}{\partial T}\right|_o & \left.\frac{\partial\dot{u}}{\partial\delta_E}\right|_o \\
\left.\frac{\partial\dot{w}}{\partial T}\right|_o & \left.\frac{\partial\dot{w}}{\partial\delta_E}\right|_o \\
\left.\frac{\partial\dot{q}}{\partial T}\right|_o & \left.\frac{\partial\dot{q}}{\partial\delta_E}\right|_o \\
\left.\frac{\partial\dot{\theta}}{\partial T}\right|_o & \left.\frac{\partial\dot{\theta}}{\partial\delta_E}\right|_o \\
\left.\frac{\partial\dot{h}}{\partial T}\right|_o & \left.\frac{\partial\dot{h}}{\partial\delta_E}\right|_o \\
\left.\frac{\partial\dot{r}}{\partial T}\right|_o & \left.\frac{\partial\dot{r}}{\partial\delta_E}\right|_o
\end{bmatrix}
\begin{bmatrix} \delta T \\ \delta\delta_E \end{bmatrix}
+
\begin{bmatrix}
\left.\frac{\partial\dot{u}}{\partial w_v}\right|_o & \left.\frac{\partial\dot{u}}{\partial w_h}\right|_o \\
\left.\frac{\partial\dot{w}}{\partial w_v}\right|_o & \left.\frac{\partial\dot{w}}{\partial w_h}\right|_o \\
\left.\frac{\partial\dot{q}}{\partial w_v}\right|_o & \left.\frac{\partial\dot{q}}{\partial w_h}\right|_o \\
\left.\frac{\partial\dot{\theta}}{\partial w_v}\right|_o & \left.\frac{\partial\dot{\theta}}{\partial w_h}\right|_o \\
\left.\frac{\partial\dot{h}}{\partial w_v}\right|_o & \left.\frac{\partial\dot{h}}{\partial w_h}\right|_o \\
\left.\frac{\partial\dot{r}}{\partial w_v}\right|_o & \left.\frac{\partial\dot{r}}{\partial w_h}\right|_o
\end{bmatrix}
\begin{bmatrix} \delta w_v \\ \delta w_h \end{bmatrix}
\qquad 4\text{-}7
$$

Using the aircraft's dynamic equations as presented in Chapter III, along with the previous assumptions, the above partial derivatives can be expanded. A discussion pertaining to the derivation of the nominal state and control trajectories as well as the actual values of these trajectories which are to be used to evaluate the above partial derivatives will be presented in Section 5.1. The general expressions for the partial derivatives in equation 4-7 are as follows:

$$A_{11} = \frac{\partial \dot{u}}{\partial u} = \frac{1}{\text{Mass}} \Bigg\{ (\tfrac{1}{2}\rho\ V_T{}^2 S)\left(C_{D_{min}} + kC_L{}^2\right)\left(\frac{u^2}{V_T{}^3} - \frac{1}{V_T}\right)$$

$$- \left(\tfrac{1}{2}\ V_T{}^2 S\right)\left[C_{L_{\alpha_o}}(M)\left(\frac{w}{V_T} + .0331\right) + C_{L_{\delta_E}} \cdot \delta_E \frac{wu}{V_T{}^3}\right.$$

$$\left. - \frac{u}{V_T}(\tfrac{1}{2}\rho S)\left(C_{D_{min}} + kC_L{}^2\right)(2u)\right] + \frac{w}{V_T}(\tfrac{1}{2}\rho S)\left[C_{L_{\delta_E}}\delta_E(2u)\right.$$

$$\left. + C_{L_{\alpha_o}}(M)\left(\frac{wu}{V_T} + 0.0331(2u)\right)\right] + \frac{w}{V_T}\left(\tfrac{1}{2}\rho\ V_T{}^2 S\right)\left(\frac{w}{V_T} + .0331\right) \times$$

$$\left[\frac{-2.22u}{(1.69)(661.-.002434h)V_T} + \frac{5.387(2u)}{(1.69)^2(661.-.002434h)^2}\right]$$

$$+ \frac{\partial\ \text{Thrust}}{\partial u}\Bigg\} \qquad 4\text{-}8$$

$$A_{12} = \frac{\partial \dot{u}}{\partial w} = \frac{1}{\text{Mass}} \Bigg\{ (\tfrac{1}{2}\rho\ V_T{}^2 S)\left(C_{D_{min}} + kC_L{}^2\right)\left(\frac{uw}{V_T{}^3}\right) + \left(\tfrac{1}{2}\ V_T{}^2 S\right) \times$$

$$\left[C_{L_{\alpha_o}}(M)\left(\frac{w}{V_T} + .0331\right) + C_{L_{\delta_E}} \cdot \delta_E\right]\left(\frac{1}{V_T} - \frac{w^2}{V_T{}^3}\right) - \left(\frac{u}{V_T}\right)(\tfrac{1}{2}\rho S) \times$$

$$\left(C_{D_{min}} + kC_L{}^2\right)(2w) + \left(\frac{w}{V_T}\right)(\tfrac{1}{2}\rho S)\left[C_{L_{\delta_E}} \cdot \delta_E(2w) + C_{L_{\alpha_o}}(M) \times\right.$$

$$\left.\left(V_T + \frac{w^2}{V_T} + .0331(2w)\right)\right] + \frac{w}{V_T}\left(\tfrac{1}{2}\rho\ V_T{}^2 S\right)\left(\frac{w}{V_T} + .0331\right) \times$$

$$\left[\frac{-2.22w}{(1.69)(661.-.002434h)V_T} + \frac{5.387(2w)}{(1.69)^2(661.-.002434h)^2}\right]$$

$$+ \frac{\partial\ \text{Thrust}}{\partial w}\Bigg\} - q \qquad 4\text{-}9$$

$$A_{13} = \frac{\partial \dot{u}}{\partial q} = -w \qquad 4\text{-}10$$

$$A_{14} = \frac{\partial \dot{u}}{\partial \theta} = -g \cos \theta \qquad 4\text{-}11$$

$$A_{15} = \frac{\dot{u}}{h} = \frac{1}{\text{Mass}}\Bigg\{\Bigg[-\frac{u}{V_T}\left(\tfrac{1}{2} V_T{}^2 S\right)\left(C_{D_{min}} + kC_L{}^2\right) + \frac{w}{V_T}\left(\tfrac{1}{2} V_T{}^2 S\right) \times$$

$$\left(C_{L_{\alpha_o}}(M)\left(\frac{w}{V_T} + .0331\right) + C_{L_{\delta_E}}\delta_E\right)\Bigg]\left[\frac{-1.835}{65536} + \frac{2h}{(65536)^2}\right] \times$$

$$(.002378) + \frac{\partial\ \text{Thrust}}{\partial h} + \frac{w}{V_T}\left(\tfrac{1}{2}\rho\ V_T{}^2 S\right) \quad \frac{w}{V_T} + .0331 \quad \times$$

$$\left[\frac{2.22V_T(-.002434)}{1.69(661.-.002434h)^2} + \frac{5.387\ V_T^2(-2)(-.002434)}{(1.69)^2(661.-.002434h)^3}\right]\Bigg\} \qquad 4\text{-}12$$

$$A_{16} = \frac{\partial \dot{u}}{\partial r} = 0 \qquad 4\text{-}13$$

$$A_{21} = \frac{\partial \dot{w}}{\partial u} = \frac{1}{\text{Mass}}\Bigg\{\left(\tfrac{1}{2}\rho\ V_T{}^2 S\right)\left(C_{D_{min}} + kC_L{}^2\right)\left(\frac{uw}{V_T{}^3}\right) - \left(\tfrac{1}{2}\rho\ V_T{}^2 S\right) \times$$

$$\left(\frac{1}{V_T} - \frac{u^2}{V_T{}^3}\right)\left[C_{L_{\alpha_o}}(M)\left(\frac{w}{V_T} + .0331\right) + C_{L_{\delta_E}} \cdot \delta_E\right]$$

$$- \frac{w}{V_T}(\tfrac{1}{2}\rho S)\left(C_{D_{min}} + kC_L{}^2\right) \quad (2u) - \frac{u}{V_T}(\tfrac{1}{2}\rho S) \quad C_{L_{\delta_E}} \cdot \delta_E(2u)$$

$$+ C_{L_{\alpha_o}}(M)\left(\frac{wu}{V_T} + .0331(2u)\right) - \frac{u}{V_T}\left(\tfrac{1}{2}\rho\ V_T{}^2 S\right)\left(\frac{w}{V_T} + .0331\right) \times$$

$$\Bigg[\frac{-.22u}{1.69(661.-.002434h)V_T}$$

$$+ \frac{5.387(2u)}{(1.69)^2(661.-.002434h)^2}\Bigg]\Bigg\} + q \qquad 4\text{-}14$$

$$A_{22} = \frac{\partial \dot{w}}{\partial w} = \frac{1}{\text{Mass}}\left\{\left(\tfrac{1}{2}\rho\, V_T{}^2 S\right)\left(C_{D_{min}} + kC_L{}^2\right)\left(-\frac{1}{V_T} + \frac{w^2}{V_T{}^3}\right)\right.$$

$$+ \left(\tfrac{1}{2}\rho\, V_T{}^2 S\right)\left[C_{L_{\alpha_o}}(M)\left(\frac{w}{V_T} + .0331\right) + C_{L_{\delta_E}}\delta_E\right]\left(\frac{uw}{V_T{}^3}\right)$$

$$- \left(\frac{w}{V_T}\right)(\tfrac{1}{2}\rho S)\left(C_{D_{min}} + kC_L{}^2\right)(2w)$$

$$- \frac{u}{V_T}(\tfrac{1}{2}\rho S)\left[C_{L_{\delta_E}}\cdot\delta_E(2w) + C_{L_{\alpha_o}}(M)\left(V_T + \frac{w^2}{V_T} + .0331(2w)\right)\right]$$

$$- \frac{u}{V_T}\left(\tfrac{1}{2}\rho\, V_T{}^2 S\right)\left(\frac{w}{V_T} + .0331\right)\left[\frac{-2.22w}{1.69(661.-.002434h)V_T}\right.$$

$$\left.\left. + \frac{5.387(2w)}{(1.69)^2(661.-.002434h)^2}\right]\right\} \qquad 4\text{-}15$$

$$A_{23} = \frac{\partial \dot{w}}{\partial q} = u \qquad 4\text{-}16$$

$$A_{24} = \frac{\partial \dot{w}}{\partial \theta} = -g\cos\phi\ \sin\theta \qquad 4\text{-}17$$

$$A_{25} = \frac{\partial \dot{w}}{\partial h} = \frac{1}{\text{Mass}}\left\{-\frac{w}{V_T}\left(\tfrac{1}{2}\, V_T{}^2 S\right)\left(C_{D_{min}} + kC_L{}^2\right) - \frac{u}{V_T}\left(\tfrac{1}{2}\, V_T{}^2 S\right)\times\right.$$

$$\left.\left[C_{L_{\alpha_o}}(M)\left(\frac{w}{V_T} + .0331\right) + C_{L_{\delta_E}}\cdot\delta_E\right]\right\}\left[-\frac{1.835}{65536} + \frac{2h}{(65536)^2}\right]\times$$

$$(.002378) - \frac{1}{\text{Mass}}\left(\frac{u}{V_T}\right)\left(\tfrac{1}{2}\rho\, V_T{}^2 S\right)\left(\frac{w}{V_T} + .0331\right)\times$$

$$\left[\frac{2.22\, V_T(-.002434)}{1.69(661.-.002434h)^2} + \frac{5.387\, V_T{}^2(-2)(-.002434)}{(1.69)^2(661.-.002434h)^3}\right]$$

4-18

$$A_{26} = \frac{\partial \dot{w}}{\partial r} = 0 \ . \qquad 4\text{-}19$$

$$A_{31} = \frac{\partial \dot{q}}{\partial u} = \frac{1}{I_{yy}} \left\{ \tfrac{1}{2}\rho Sc\left[\left(C_{m_o} + C_{m_{\delta_E}} \cdot \delta_E\right)(2u) + C_{m_\alpha} \frac{uw}{V_T}\right] \times \right.$$

$$\left. + \tfrac{1}{4}\rho Sc^2 \left[C_{m_q} + C_{m_{\dot{\alpha}}}\right] q \frac{u}{V_T} \right\} \qquad 4\text{-}20$$

$$A_{32} = \frac{\partial \dot{q}}{\partial w} = \frac{1}{I_{yy}} \left\{ \tfrac{1}{2}\rho Sc\left[\left(C_{m_o} + C_{m_{\delta_E}} \cdot \delta_E\right)(2w) + C_{m_\alpha}\left(V_T + \frac{w^2}{V_T}\right)\right] \right.$$

$$\left. + \tfrac{1}{4}\rho Sc^2 \left[C_{m_q} + C_{m_{\dot{\alpha}}}\right] q \frac{w}{V_T} \right\} \qquad 4\text{-}21$$

$$A_{33} = \frac{\partial \dot{q}}{\partial q} = \frac{1}{I_{yy}} \left[\tfrac{1}{4}\rho\, V_T\, Sc^2 \left(C_{m_q} + C_{m_{\dot{\alpha}}}\right)\right] \qquad 4\text{-}22$$

$$A_{34} = \frac{\partial \dot{q}}{\partial \theta} = 0 \ . \qquad 4\text{-}23$$

$$A_{35} = \frac{\partial \dot{q}}{\partial h} = \frac{1}{I_{yy}} \left\{ \left(\tfrac{1}{2}\, V_T{}^2 Sc\right)\left[C_{m_o} + C_{m_\alpha} \frac{w}{V_T} + C_{m_{\delta_E}} \cdot \delta_E\right] \right.$$

$$\left. + \tfrac{1}{4}\, V_T\, Sc^2 \left[C_{m_q} + C_{m_{\dot{\alpha}}}\right] q \right\} \left[- \frac{1.835}{65536} \right.$$

$$\left. + \frac{2h}{(65536)^2} \right] (.002378) \qquad 4\text{-}24$$

$$A_{36} = \frac{\partial \dot{q}}{\partial r} = 0 \ . \qquad 4\text{-}25$$

$$A_{41} = \frac{\partial \dot{\theta}}{\partial u} = 0 \ . \qquad 4\text{-}26$$

$$A_{42} = \frac{\partial \dot{\theta}}{\partial w} = 0 \ . \qquad 4\text{-}27$$

$$A_{43} = \frac{\partial \dot{\theta}}{\partial q} = \cos \phi = 1 \ . \qquad 4\text{-}28$$

$$A_{44} = \frac{\partial \dot{\theta}}{\partial \theta} = 0 \ . \qquad 4\text{-}29$$

$$A_{45} = \frac{\partial \dot{\theta}}{\partial h} = 0 \ . \qquad 4\text{-}30$$

$$A_{46} = \frac{\partial \dot{\theta}}{\partial r} = 0 \ . \qquad 4\text{-}31$$

$$A_{51} = \frac{\partial \dot{h}}{\partial u} = \sin \theta \qquad 4\text{-}32$$

$$A_{52} = \frac{\partial \dot{h}}{\partial w} = - \cos \phi \cos \theta = - \cos \theta \qquad 4\text{-}33$$

$$A_{53} = \frac{\partial \dot{h}}{\partial q} = 0 \ . \qquad 4\text{-}34$$

$$A_{54} = \frac{\partial \dot{h}}{\partial \theta} = u \cos \theta + w \sin \theta \qquad 4\text{-}35$$

$$A_{55} = \frac{\partial \dot{h}}{\partial h} = 0 \ . \qquad 4\text{-}36$$

$$A_{56} = \frac{\partial \dot{h}}{\partial r} = 0 \ . \qquad 4\text{-}37$$

$$A_{61} = \frac{\partial \dot{r}}{\partial u} = - \cos \theta \qquad 4\text{-}38$$

$$A_{62} = \frac{\partial \dot{r}}{\partial w} = - \sin \theta \qquad 4\text{-}39$$

$$A_{63} = \frac{\partial \dot{r}}{\partial q} = 0 \ . \qquad 4\text{-}40$$

$$A_{64} = \frac{\partial \dot{r}}{\partial \theta} = u \sin \theta - w \cos \theta \qquad 4\text{-}41$$

$$A_{65} = \frac{\partial \dot{r}}{\partial h} = 0 \ . \qquad 4\text{-}42$$

$$A_{66} = \frac{\partial \dot{r}}{\partial r} = 0 \ . \qquad 4\text{-}43$$

where

$$\frac{\partial \text{ Thrust}^{\dagger}}{\partial u} = (4)\left[\frac{u\left(-2000+.05(h-10{,}000)\right)}{(1.69)\ V_T\ (661.-.002434h)}\right]\left(1 - T_p^{\ 2}\right)$$

$$+\left[(4)\ \frac{u\left(-3125+.12(h-10{,}000)\right)}{(1.69)\ V_T\ (661.-.002434h)}\right] T_p^{\ 2} \qquad 4\text{-}44$$

$$h \geq 10{,}000 \text{ ft.}$$

---

†Several coefficients in the maximum and idle thrust approximation equations, as described by equations 3-23 and 3-24 respectively, were slightly modified to ensure a valid linearization for all altitudes of interest above 10,000 feet. For both thrust equations, $h_o = 10{,}000$ for $h \geq 10{,}000$ ft. and

$$\left.\frac{\partial^2 T}{\partial h \partial M}\right|_{\substack{M=0 \\ h=h_o=10{,}000}} = \begin{cases} +.12 \text{ lbs./Mach-ft. for maximum thrust} \\ +.05 \text{ lbs./Mach-ft. for idle thrust} \end{cases}$$

$$\frac{\partial\ \text{Thrust}^{\dagger}}{\partial w} = (4)\left[\frac{w\left(-2000+.05(h-10{,}000)\right)}{(1.69)\ V_T\ (661.-.00243h)}\right]\left(1-T_p^{\,2}\right)$$

$$+\ (4)\left[\frac{w\left(-3125+.12(h-10{,}000)\right)}{(1.69)\ V_T\ (661.-.002434h)}\right]T_p^{\,2} \qquad 4\text{-}45$$

$$h \geq 10{,}000\ \text{ft.}$$

$$\frac{\partial\ \text{Thrust}^{\dagger}}{\partial h} = (4)\left[\frac{(0.002434)\left(-2000+0.05(h-10{,}000)\right)}{(1.69)(661.-0.002434h)^2}\right.$$

$$\left.+\ \frac{0.05}{(1.69)(661.-.002434h)}\right]\left(1-T_p^{\,2}\right)$$

$$+\ (4)\left[-.28125\ +\ \left[\frac{(0.002434)}{(1.69)(661-.002434h)^2}\right]\ \times\right.$$

$$\left.\left[-3125+.12(h-10{,}000)\right]\ +\ \frac{.12}{(1.69)(661-.002434h)}\right]T_p^{\,2}$$

$$h \geq 10{,}000\ \text{ft.} \qquad 4\text{-}46$$

$$V_T = \sqrt{u^2 + w^2} \qquad 4\text{-}47$$

$$B_{11} = \frac{\partial \dot{u}}{\partial T} = \frac{1}{\text{Mass}} \qquad 4\text{-}48$$

$$B_{12} = \frac{\partial \dot{u}}{\partial \delta_E} = \frac{w}{\text{Mass}}\left(\tfrac{1}{2}\rho\ V_T^{\,2}S\right)C_{L_{\delta_E}} \qquad 4\text{-}49$$

$$B_{21} = \frac{\partial \dot{w}}{\partial T} = 0\ . \qquad 4\text{-}50$$

$$B_{22} = \frac{\partial \dot{w}}{\partial \delta_E} = \frac{-u}{\text{Mass}}\left(\tfrac{1}{2}\rho\ V_T^{\,2}S\right)C_{L_{\delta_E}} \qquad 4\text{-}51$$

---

†See footnote on preceding page.

$$B_{31} = \frac{\partial \dot{q}}{\partial T} = 0 \ . \qquad 4\text{-}52$$

$$B_{32} = \frac{\partial \dot{q}}{\partial \delta_E} = \frac{1}{I_{yy}} \left(\tfrac{1}{2}\rho \ V_T{}^2 Sc \right) C_{M_{\delta_E}} \qquad 4\text{-}53$$

$$B_{41} = \frac{\partial \dot{\theta}}{\partial T} = 0 \ . \qquad 4\text{-}54$$

$$B_{42} = \frac{\partial \dot{\theta}}{\partial \delta_E} = 0 \ . \qquad 4\text{-}55$$

$$B_{51} = \frac{\partial \dot{h}}{\partial T} = 0 \ . \qquad 4\text{-}56$$

$$B_{52} = \frac{\partial \dot{h}}{\partial \delta_E} = 0 \ . \qquad 4\text{-}57$$

$$B_{61} = \frac{\partial \dot{r}}{\partial T} = 0 \ . \qquad 4\text{-}58$$

$$B_{62} = \frac{\partial \dot{r}}{\partial \delta_E} = 0 \ . \qquad 4\text{-}59$$

$$D_{11} = \frac{\partial \dot{u}}{\partial w_v} = 0 \ . \qquad 4\text{-}60$$

$$D_{12} = \frac{\partial \dot{u}}{\partial w_h} = 0 \ . \qquad 4\text{-}61$$

$$D_{21} = \frac{\partial \dot{w}}{\partial w_v} = 0 \ . \qquad 4\text{-}62$$

$$D_{22} = \frac{\partial \dot{w}}{\partial w_h} = 0 \ . \qquad 4\text{-}63$$

$$D_{31} = \frac{\partial \dot{q}}{\partial w_v} = 0 \ . \qquad 4\text{-}64$$

$$D_{32} = \frac{\partial \dot{q}}{\partial w_h} = 0 \ . \qquad 4\text{-}65$$

$$D_{41} = \frac{\partial \dot{\theta}}{\partial w_v} = 0 \ . \qquad 4\text{-}66$$

$$D_{42} = \frac{\partial \dot{\theta}}{\partial w_h} = 0 \ . \qquad 4\text{-}67$$

$$D_{51} = \frac{\partial \dot{h}}{\partial w_v} = -1 \ . \qquad 4\text{-}68$$

$$D_{52} = \frac{\partial \dot{h}}{\partial w_h} = 0 \ . \qquad 4\text{-}69$$

$$D_{61} = \frac{\partial \dot{r}}{\partial w_v} = 0 \ . \qquad 4\text{-}70$$

$$D_{62} = \frac{\partial \dot{r}}{\partial w_h} = -1 \ . \qquad 4\text{-}71$$

Given the linearized continuous-time system as described by the equations presented in this section, the equivalent discrete-time version of the system has been formulated for real-time simulation purposes. This formulation and its solution is described in the following section.

4.2 THE DISCRETE-TIME LINEAR MODEL

The discrete-time equivalent to the continuous-time linear system is more practicable than direct integration of the continuous-time system when considering the actual physical implementation of the system. This discrete-time system is the sampled-data version of the continuous-time system.

As derived in the preceding section, the continuous-time linearized system is expressed by:

$$\delta\dot{\underline{x}}(t) = \underline{A}(t)\delta\underline{x}(t) + \underline{B}(t)\delta\underline{u}(t) + \underline{D}(t)\delta\underline{w}(t) \qquad 4\text{-}72$$

C-2

Using the Variation of Constants Formula [22], the solution to the continuous-time linear system is given by:

$$\delta\underline{x}(t) = \underline{\Phi}(t,t_o)\delta\underline{x}(t_o) + \int_0^t \underline{\Phi}(t,\tau)\underline{B}(\tau)\delta\underline{u}(\tau)d\tau$$

$$+ \int_0^t \underline{\Phi}(t,\tau)\underline{D}(\tau)\delta\underline{w}(\tau)d\tau \qquad 4\text{-}73$$

An approximately equivalent discrete-time linear system is:

$$\delta\underline{x}_{k+1} = \underline{F}_k\delta\underline{x}_k + \underline{G}_k\delta u_k + \underline{H}_k\delta\underline{w}_k \qquad 4\text{-}74$$

where

$$\underline{F}_k = \underline{\Phi}(t_{k+1},t_k) = e^{\underline{A}_k(t_{k+1}-t_k)}$$

$$= e^{\underline{A}_k\Delta} = \sum_{n=0}^{\infty} \underline{A}_k^n \frac{\Delta^n}{n!} \qquad 4\text{-}75$$

$$\underline{G}_k = \int_{t_k}^{t_{k+1}} \underline{\Phi}(t_{k+1},\tau)\underline{B}(\tau)d\tau = \int_{t_k}^{t_{k+1}} e^{\underline{A}_k(t_{k+1}-\tau)}d\tau\underline{B}_k$$

$$= \sum_{n=0}^{\infty} \underline{A}_k^n \frac{\Delta^{n+1}}{(n+1)!}\underline{B}_k \qquad 4\text{-}76$$

$$\underline{H}_k = \int_{t_k}^{t_{k+1}} \underline{\Phi}(t_{k+1},\tau)B(\tau)d\tau \simeq \int_{t_k}^{t_{k+1}} e^{\underline{A}_k(t_{k+1}-\tau)} d\tau \underline{B}_k$$

$$= \sum_{n=0}^{\infty} \underline{A}_k^{\,n} \frac{\Delta^{n+1}}{(n+1)!} \underline{B}_k \qquad 4\text{-}77$$

$$\Delta = t_{k+1} - t_k = \text{time interval} \qquad 4\text{-}78$$

and

$$\underline{A}_k = \underline{A}(t_k) \qquad \underline{B}_k = \underline{B}(t_k) \qquad \underline{D}_k = \underline{D}(t_k) = \underline{D} \qquad 4\text{-}79$$

will be considered constant over the time interval from t_k to t_{k+1} since their time-variation is slow relative to the system time-constants.†

The time interval, Δ , was chosen to be 3 seconds. The length of this time interval is very important. If the time interval is too large, this will imply that the control action is "sluggish" and subsequently will not allow the control to respond as quickly to a disturbance. Also, a large time step will tend to degrade the discrete-time system approximation to the continuous-time equations. On the other hand, if the time

---

†The above expressions are function-space approximations to the Peano-Baker series expressions [22] for the transition function and were verified to be quite accurate in the present application.

interval is too small, the system may develop what is known as quantization instabilities -- these can result from consecutive corrective control commands without allowing sufficient time between commands to give the system enough time to respond, thus causing quantization errors to integrate. The 3 second time interval used has shown to be satisfactory in view of the aircraft's time-constants. The nominal state, control, and wind values, along with their corresponding discrete-time linear system matrices are presented in Appendix A for several selected times.

4.3 THE LINEAR FEEDBACK LAW AND RICCATI EQUATION

We desire to obtain a discrete-time linear feedback law whereby the deviations of the control are a function of any deviations in the state as well as a known deterministic disturbance. In particular, we wish to find an optimal feedback law of the form

$$\delta \underline{u}_k^* = \underline{K}_k \delta \underline{x}_k + \underline{f}_k(\delta \underline{w}_k) \qquad 4\text{-}80$$

Consider the linear discrete-time system

$$\delta \underline{x}_{k+1} = \underline{F}_k \delta \underline{x}_k + \underline{G}_k \delta \underline{u}_k + H_k \delta \underline{w}_k \qquad k=0,1,\ldots,T-1 \qquad 4\text{-}81$$

and the quadratic cost functional

$$J(U) = \sum_{k=0}^{T-1} \Big[\delta \underline{x}_k' \underline{Q}_k \delta \underline{x}_k + \delta \underline{x}_k' \underline{S}_k \delta \underline{u}_k + \delta \underline{u}_k' \underline{S}_k' \delta \underline{x}_k$$

$$+ \delta \underline{u}_k' \underline{R}_k \delta \underline{u}\Big] + \delta \underline{x}_T' \underline{Q}_T \delta \underline{x}_T$$

$$= \sum_{k=0}^{T-1} \begin{bmatrix} \delta \underline{x}_k' & \delta \underline{u}_k' \end{bmatrix} \begin{bmatrix} \underline{Q}_k & \underline{S}_k \\ \underline{S}_k & \underline{R}_k \end{bmatrix} \begin{bmatrix} \delta \underline{x}_k \\ \delta \underline{u}_k \end{bmatrix} + \delta \underline{x}_T' \underline{Q}_T \delta \underline{x}_T \qquad 4\text{-}82$$

$$= \sum_{k=0}^{T-1} L(\delta \underline{x}_k, \delta \underline{u}_k) + \psi(\delta \underline{x}_T) \qquad 4\text{-}83$$

where the weighting matrices possess the following properties:

$$\begin{aligned} &\begin{bmatrix} \underline{Q}_k & \underline{S}_k \\ \underline{S}_k' & \underline{R}_k \end{bmatrix} \geq \underline{O} \text{ for all } \quad k=0,1,\ldots,T-1 \\ &\underline{R}_k \quad > \underline{O} \text{ for all } \quad k=0,1,\ldots,T-1 \\ &\underline{Q}_T \quad \geq \underline{O} \end{aligned} \qquad 4\text{-}84$$

In equation 4-81, $\delta \underline{w}_k$ is viewed as a known deterministic disturbance. In order to derive the discrete-time linear feedback law, state augmentation is used to yield the following system:

$$\begin{bmatrix} \delta \underline{x}_{k+1} \\ \delta \underline{w}_{k+1} \end{bmatrix} = \begin{bmatrix} \underline{F}_k & \underline{H}_k \\ \underline{O} & \underline{O} \end{bmatrix} \begin{bmatrix} \delta \underline{x}_k \\ \delta \underline{w}_k \end{bmatrix} + \begin{bmatrix} \underline{G}_k & \underline{O} \\ \underline{O} & \underline{I} \end{bmatrix} \begin{bmatrix} \delta u_k \\ \delta \underline{v}_k \end{bmatrix} \qquad 4\text{-}85$$

with cost functional

$$J(U) = \sum_{k=0}^{T-1} \left\{ \begin{bmatrix} \delta \underline{x}_k \\ \delta \underline{w}_k \end{bmatrix}' \begin{bmatrix} \underline{Q}_k & \underline{O} \\ \underline{O} & \underline{O} \end{bmatrix} \begin{bmatrix} \delta \underline{x}_k \\ \delta \underline{w}_k \end{bmatrix} + \begin{bmatrix} \delta \underline{x}_k \\ \delta \underline{w}_k \end{bmatrix}' \begin{bmatrix} \underline{S}_k & \underline{O} \\ \underline{O} & \underline{O} \end{bmatrix} \begin{bmatrix} \delta \underline{u}_k \\ \delta \underline{v}_k \end{bmatrix} \right.$$

$$\left. + \begin{bmatrix} \delta \underline{u}_k \\ \delta \underline{v}_k \end{bmatrix}' \begin{bmatrix} \underline{S}_k & \underline{O} \\ \underline{O} & \underline{O} \end{bmatrix}' \begin{bmatrix} \delta \underline{x}_k \\ \delta \underline{w}_k \end{bmatrix} + \begin{bmatrix} \delta \underline{u}_k \\ \delta \underline{v}_k \end{bmatrix}' \begin{bmatrix} \underline{R}_k & \underline{O} \\ \underline{O} & \underline{O} \end{bmatrix} \begin{bmatrix} \delta \underline{u}_k \\ \delta \underline{v}_k \end{bmatrix} \right\}$$

$$+ \begin{bmatrix} \delta \underline{x}_T \\ \delta \underline{w}_T \end{bmatrix}' \begin{bmatrix} \underline{Q}_T & \underline{O} \\ \underline{O} & \underline{O} \end{bmatrix} \begin{bmatrix} \delta \underline{x}_T \\ \delta \underline{w}_T \end{bmatrix} \qquad 4\text{-}86$$

$$= \sum_{k=0}^{T-1} \begin{bmatrix} \delta \tilde{\underline{x}}_k \\ \delta \tilde{\underline{u}}_k \end{bmatrix}' \begin{bmatrix} \tilde{\underline{Q}}_k & \tilde{\underline{S}}_k \\ \tilde{\underline{S}}_k & \tilde{\underline{R}}_k \end{bmatrix} \begin{bmatrix} \delta \tilde{\underline{x}}_k \\ \delta \tilde{\underline{u}}_k \end{bmatrix} + \tilde{\underline{x}}_T' \tilde{\underline{Q}}_T \tilde{\underline{x}}_T \qquad 4\text{-}87$$

$$= \sum_{k=0}^{T-1} L(\delta \tilde{\underline{x}}_k, \delta \tilde{\underline{u}}_k) + \psi(\delta \tilde{\underline{x}}_T) \qquad 4\text{-}88$$

where

$$\delta \tilde{\underline{x}}_{k+1} = \tilde{\underline{F}}_k \delta \tilde{\underline{x}}_k + \tilde{\underline{G}}_k \delta \tilde{\underline{u}}_k \qquad 4\text{-}89$$

with

$$\delta \tilde{\underline{x}}_k = \begin{bmatrix} \delta \underline{x}_k \\ \delta \underline{w}_k \end{bmatrix} \qquad \delta \tilde{\underline{u}}_k = \begin{bmatrix} \delta \underline{u}_k \\ \delta \underline{v}_k \end{bmatrix} \qquad \tilde{\underline{F}}_k = \begin{bmatrix} \underline{F}_k & \underline{H}_k \\ \underline{O} & \underline{O} \end{bmatrix}$$

$$\tilde{\underline{G}}_k = \begin{bmatrix} \underline{G}_k & \underline{O} \\ \underline{O} & \underline{I} \end{bmatrix} \qquad \tilde{\underline{Q}}_k = \begin{bmatrix} \underline{Q}_k & \underline{O} \\ \underline{O} & \underline{O} \end{bmatrix} \qquad 4\text{-}90$$

$$\tilde{\underline{R}}_k = \begin{bmatrix} \underline{R}_k & \underline{O} \\ \underline{O} & \underline{O} \end{bmatrix} \qquad \tilde{\underline{S}}_k = \begin{bmatrix} \underline{S}_k & \underline{O} \\ \underline{O} & \underline{O} \end{bmatrix}$$

and

$$L(\delta\tilde{\underline{x}}_k, \delta\tilde{\underline{u}}_k) = \delta\tilde{\underline{x}}_k'\tilde{\underline{Q}}_k\delta\tilde{\underline{x}}_k + \delta\tilde{\underline{x}}_k'\tilde{\underline{S}}_k\delta\tilde{\underline{u}}_k + \delta\tilde{\underline{u}}_k'\tilde{\underline{S}}_k'\delta\tilde{\underline{x}}_k + \delta\tilde{\underline{u}}_k'\tilde{\underline{R}}_k\delta\tilde{\underline{u}}_k \qquad 4\text{-}91$$

Using the Dynamic Programming algorithm [19,20], we proceed to derive the discrete-time linear feedback law. At time k, define the optimal cost-to-go as:

$$V^*(\delta\tilde{\underline{x}}_k) = \min_{\delta\underline{u}_k \cdots \delta\underline{u}_{T-1}} \left[L(\delta\tilde{\underline{x}}_k, \delta\tilde{\underline{u}}_k) + \sum_{t=k+1}^{T-1} L(\delta\tilde{\underline{x}}_t, \delta\tilde{\underline{u}}_t) + \psi(\delta\tilde{\underline{x}}_T) \right] \qquad 4\text{-}92$$

$$= \min_{\delta\underline{u}_k} \left[L(\delta\tilde{\underline{x}}_k, \delta\tilde{\underline{u}}_k) + V^*(\delta\tilde{\underline{x}}_{k+1}) \right] \qquad 4\text{-}93$$

with boundary condition

$$V^*(\delta\tilde{\underline{x}}_T) = \psi(\delta\tilde{\underline{x}}_T) = \text{the terminal cost} \qquad 4\text{-}94$$

We guess that the optimal cost-to-go at time k is of the form

$$V^*(\delta\tilde{\underline{x}}_k) = \delta\tilde{\underline{x}}_k'\tilde{\underline{P}}_k\delta\tilde{\underline{x}}_k + p_k \qquad 4\text{-}95$$

with

$$\tilde{\underline{P}}_k = \tilde{\underline{P}}_k' = \begin{bmatrix} \underline{P}_k & \underline{N}_k \\ \underline{N}_k' & \underline{M}_k \end{bmatrix}$$

At k=T ,

$$V^*(\delta\tilde{\underline{x}}_T) = (\delta\tilde{\underline{x}}_T) = \delta\tilde{\underline{x}}_T'\tilde{\underline{Q}}_T\delta\tilde{\underline{x}}_T \qquad 4\text{-}96$$

so

$$\tilde{\underline{P}}_T = \tilde{\underline{Q}}_T \qquad \text{and} \qquad p_T = 0 \qquad 4\text{-}97$$

Now, assume that the optimal cost-to-go at time k+1 is

$$V^*(\delta\tilde{\underline{x}}_{k+1}) = \delta\tilde{\underline{x}}_{k+1}'\tilde{\underline{P}}_{k+1}\delta\tilde{\underline{x}}_{k+1} + p_{k+1} \qquad 4\text{-}98$$

Equation 4-95 will be proved by induction.

Substituting equations 4-89, 4-91, and 4-98 into equation 4-93 we have the following expression:

$$V^*(\delta\tilde{\underline{x}}_k) = \min_{\delta\underline{u}_k}\Bigg\{\Bigg[\delta\tilde{\underline{x}}_k'\tilde{\underline{Q}}_k\delta\tilde{\underline{x}}_k + \delta\tilde{\underline{x}}_k'\tilde{\underline{S}}_k\delta\tilde{\underline{u}}_k + \delta\tilde{\underline{u}}_k'\tilde{\underline{S}}_k'\delta\tilde{\underline{x}}_k + \delta\tilde{\underline{u}}_k'\tilde{\underline{R}}_k\delta\tilde{\underline{u}}_k\Bigg] + \Bigg[\delta\tilde{\underline{x}}_k'\tilde{\underline{F}}_k' + \delta\tilde{\underline{u}}_k'\tilde{G}_k'\Bigg] \times \tilde{\underline{P}}_{k+1}\Bigg[\tilde{\underline{F}}_k\delta\tilde{\underline{x}}_k + \tilde{\underline{G}}_k\delta\tilde{\underline{u}}_k\Bigg] + p_{k+1}\Bigg\} \qquad 4\text{-}99$$

Minimizing the cost-to-go at time k by setting the partial derivative of $V(\delta\tilde{\underline{x}}_k)$ with respect to $\delta\underline{u}_k$ equal to zero yields:

$$\frac{\partial V(\delta\tilde{\underline{x}}_k)}{\partial\underline{u}_k} = 2\Bigg[\delta\tilde{\underline{x}}_k'\tilde{\underline{S}}_k + \delta\tilde{\underline{u}}_k'\tilde{\underline{R}}_k + \delta\tilde{\underline{x}}_k'\tilde{\underline{F}}_k'\tilde{\underline{P}}_{k+1}\tilde{\underline{G}}_k + \delta\tilde{\underline{u}}_k'\tilde{\underline{G}}_k'\tilde{\underline{P}}_{k+1}\tilde{\underline{G}}_k\Bigg]\begin{bmatrix}\underline{I}\\ \underline{O}\end{bmatrix} \qquad 4\text{-}100$$

$$\frac{\partial V(\delta \underline{x}_k)}{\partial \underline{u}_k} = \delta \underline{x}_k' \underline{S}_k + \delta \underline{u}_k'^{*} \underline{R}_k + (\delta \underline{x}_k' \underline{F}_k' + \delta \underline{w}_k \underline{H}_k') \underline{P}_{k+1} \underline{G}_k$$

$$+ (\delta \underline{u}_k'^{*} \underline{G}_k \underline{P}_{k+1} + \delta \underline{v}_k' \underline{N}_{k+1}') \underline{G}_k$$

$$\begin{aligned} = \; & \underline{x}_k' (\underline{S}_k + \underline{F}_k' \underline{P}_{k+1} \underline{G}_k) \\ & + \delta \underline{w}_k' (\underline{H}_k' \underline{P}_{k+1} \underline{G}_k) \\ & + \delta \underline{v}_k' (\underline{N}_{k+1}' \underline{G}_k) \\ & + \delta \underline{u}_k'^{*} (R_k + \underline{G}_k' \underline{P}_{k+1} \underline{G}_k) \end{aligned} \qquad 4\text{-}101$$

$$= \underline{0}$$

Since $\underline{R}_k$ is positive definite and $\underline{G}_k' \underline{P}_{k+1} \underline{G}_k$ is at least positive semi-definite, then $(\underline{R}_k + \underline{G}_k' \underline{P}_{k+1} \underline{G}_k)$ is invertible† and we can solve for $\delta \underline{u}_k^*$ to obtain the optimal linear feedback control law:

$$\delta \underline{u}_k^* = - \left[\underline{R}_k + \underline{G}_k' \underline{P}_{k+1} \underline{G}_k \right]^{-1} \left\{ \left[\underline{S}_k' + \underline{G}_k' \underline{P}_{k+1} \underline{F}_k \right] \delta \underline{x}_k + \underline{G}_k' \left[\underline{P}_{k+1} \underline{H}_k \delta \underline{w}_k + \underline{N}_{k+1} \delta \underline{v}_k \right] \right\} \qquad 4\text{-}102$$

which is precisely in the desired form $\delta \underline{u}_k^* = \underline{K}_k \delta \underline{x}_k + \underline{f}_k (\delta \underline{w}_k)$ where

$$\underline{K}_k = - \left[\underline{R}_k + \underline{G}_k' \underline{P}_{k+1} \underline{G}_k \right]^{-1} \left[\underline{S}_k' + \underline{G}_k' \underline{P}_{k+1} \underline{F}_k \right] \qquad 4\text{-}103$$

$$\underline{f}_k (\delta \underline{w}_k) = - \left[\underline{R}_k + \underline{G}_k' \underline{P}_{k+1} \underline{G}_k \right]^{-1} \underline{G}_k' \left[\underline{P}_{k+1} \underline{H}_k \delta \underline{w}_k + \underline{N}_{k+1} \delta \underline{v}_k \right] \qquad 4\text{-}104$$

---

†Second order conditions show this to be a minimum. Uniqueness can be proved by completion of squares.

Substituting equations 4-90 and 4-102 into equation 4-99 gives the optimal cost-to-go at time k:

$$
\begin{aligned}
V^*(\delta \underline{x}_k) = {} & \delta \underline{x}_k' \Big[\underline{Q}_k + \underline{F}_k' \underline{P}_{k+1} \underline{F}_k - (\underline{S}_k + \underline{F}_k' \underline{P}_{k+1} \underline{G}_k) \times \\
& (\underline{R}_k + \underline{G}_k' \underline{P}_{k+1} \underline{G}_k)^{-1} (\underline{S}_k' + \underline{G}_k' \underline{P}_{k+1} \underline{F}_k) \Big] \delta \underline{x}_k \\
& + \delta \underline{x}_k' \Big[\underline{F}_k' - (\underline{S}_k + \underline{F}_k' \underline{P}_{k+1} \underline{G}_k)(\underline{R}_k + \underline{G}_k' \underline{P}_{k+1} \underline{G}_k)^{-1} \underline{G}_k' \Big] \times \\
& \Big[\underline{P}_{k+1} \underline{H}_k \delta \underline{w}_k + \underline{N}_{k+1} \delta \underline{v}_k \Big] + \Big[\delta \underline{w}_k' \underline{H}_k' \underline{P}_{k+1} + \delta \underline{v}_k' \underline{N}_{k+1}' \Big] \times \\
& \Big[\underline{F}_k - \underline{G}_k (\underline{R}_k + \underline{G}_k' \underline{P}_{k+1} \underline{G}_k)^{-1} (\underline{S}_k' + \underline{G}_k' \underline{P}_{k+1} \underline{F}_k) \Big] \delta \underline{x}_k \\
& + \begin{bmatrix} \underline{H}_k \delta \underline{w}_k \\ \delta \underline{v}_k \end{bmatrix}' \begin{bmatrix} \underline{P}_{k+1} & \underline{N}_{k+1} \\ \underline{N}_{k+1}' & \underline{M}_{k+1} \end{bmatrix} \begin{bmatrix} \underline{H}_k \delta \underline{w}_k \\ \delta \underline{v}_k \end{bmatrix} \\
& - \Big[\delta \underline{w}_k' \underline{H}_k' \underline{P}_{k+1} + \delta \underline{v}_k' \underline{N}_{k+1}' \Big] \underline{G}_k \Big[\underline{R}_k + \underline{G}_k' \underline{P}_{k+1} \underline{G}_k \Big]^{-1} \times \\
& \underline{G}_k' \Big[\underline{P}_{k+1} \underline{H}_k \delta \underline{w}_k + \underline{N}_{k+1} \delta \underline{v}_k \Big] + p_{k+1}
\end{aligned}
\qquad 4\text{-}105
$$

which is precisely of the form

$$
V^*(\delta \tilde{\underline{x}}_k) = \delta \tilde{\underline{x}}_k' \tilde{\underline{P}}_k \delta \tilde{\underline{x}}_k + p_k \qquad 4\text{-}106
$$

$$
\begin{aligned}
= {} & \delta \underline{x}_k' \underline{P}_k \delta \underline{x}_k \\
& + \delta \underline{x}_k' [\underline{N}_k \delta \underline{w}_k] \\
& + [\delta \underline{w}_k' \underline{N}_k'] \delta \underline{x}_k \\
& + [\delta \underline{w}_k' \underline{M}_k \delta \underline{w}_k] + p_k
\end{aligned}
\qquad 4\text{-}107
$$

which we originally assumed. Therefore,

$$
p_k = p_{k+1} = 0 \quad \text{since} \quad p_T = 0 \qquad 4\text{-}108
$$

and by equating equations 4-105 and 4-107, we obtain the following relationships:

1. The Discrete-Time Matrix Riccati Equation.

$$\underline{P}_k = \underline{Q}_k + \underline{F}_k'\underline{P}_{k+1}\underline{F}_k - [\underline{S}_k + \underline{F}_k'\underline{P}_{k+1}\underline{G}_k] \times$$

$$[\underline{R}_k + \underline{G}_k'\underline{P}_{k+1}\underline{G}_k]^{-1} \; [\underline{S}_k' + \underline{G}_k'\underline{P}_{k+1}\underline{F}_k] \qquad 4\text{-}109$$

with $\underline{P}_T = \underline{Q}_T$

2. The Driving Function.

$$\underline{N}_k \delta\underline{w}_k = \underline{N}_k \delta\underline{v}_{k-1}$$

$$= [\underline{F}_k' - (\underline{S}_k + \underline{F}_k'\underline{P}_{k+1}\underline{G}_k)(\underline{R}_k + \underline{G}_k'\underline{P}_{k+1}\underline{G}\;)^{-1} \; \underline{G}_k'] \times$$

$$[\underline{P}_{k+1}\underline{H}_k \delta\underline{w}_k + \underline{N}_{k+1}\delta\underline{v}_k] \qquad 4\text{-}110$$

with $\underline{N}_T = \underline{0}$

3. The Scalar Term.

$$\delta\underline{w}_k'\underline{M}_k\delta\underline{w}_k = \begin{bmatrix} \underline{H}_k\delta\underline{w}_k \\ \delta\underline{v}_k \end{bmatrix}' \begin{bmatrix} \underline{P}_{k+1} & \underline{N}_{k+1} \\ \underline{N}_{k+1}' & \underline{M}_{k+1} \end{bmatrix} \begin{bmatrix} \underline{H}_k\delta\underline{w}_k \\ \delta\underline{v}_k \end{bmatrix}$$

$$-[\delta\underline{w}_k'\underline{H}_k'\underline{P}_{k+1} + \delta\underline{v}_k'\underline{N}_{k+1}']\underline{G}_k[\underline{R}_k + \underline{G}_k'\underline{P}_{k+1}\underline{G}_k]^{-1} \times$$

$$\underline{G}_k'[\underline{P}_{k+1}\underline{H}_k\delta\underline{w}_k + \underline{N}_{k+1}\delta\underline{v}_k] \qquad 4\text{-}111$$

with $\underline{M}_T = \underline{0}$

Summarizing the results of this section, the discrete-time linear feedback law and the appropriate matrix Riccati equation and driving function have been derived. These are the necessary tools for designing the four-dimensional control regulator.

4.4 OUTLINE OF ALGORITHM FOR COMPUTING OPTIMAL FEEDBACK LAW

Combining the results of each section in this chapter, the following outline is a step-by-step procedure to determine the optimal feedback law to be implemented in the 4-D navigation system:

1. Derive the nominal state and control trajectories.

2. Evaluate the continuous-time $\underline{A}$, $\underline{B}$, and $\underline{D}$ linear system matrices along the nominal trajectories for each time interval.

3. Compute the discrete-time $\underline{F}_k$, $\underline{G}_k$, and $\underline{H}_k$ linear system matrices which are the sampled-data version of the continuous-time linear system.

4. With knowledge of the weighting matrices and wind components, iterate the discrete-time matrix Riccati equation (eqn. 4-109), the driving function (eqn. 4-110), and the scalar term (eqn. 4-111) backwards in time.

5. Compute the feedback gains (eqn. 4-103) and the feedback exogenous components (eqn. 4-104) to be used in the optimal feedback law (eqn. 4-102) during each time interval.

CHAPTER V

EXPERIMENTAL RESULTS

The simulation facilities utilizing the Adage digital computer as described in Chapter I were used to compute and test the linear feedback solution on the complete nonlinear aircraft model. The Boeing 707 cockpit simulator provided ideal conditions for observing the response of the aircraft in a real-time simulation. The displayed aircraft instruments indicated the response of the aircraft to the action of the control regulator in the presence of winds.

The computer programs used in each step of the design process are included in Appendix B, along with appropriate documentation. These programs are included primarily for the purpose of aiding successive researchers.

5.1 NOMINAL STATE AND CONTROL TRAJECTORIES

The strategic control descent route profile as described in Chapter II along with the strategy for generating the route-time profile corresponding to a desired time of arrival at the initial approach fix is used in the simulation. The ATA at the IAF was chosen to be 19.73 minutes. The associated route-time profile satisfying the aircraft boundary conditions depicted in Figure 2-7 is shown in Table 2-2. Using the simulation facilities, this route-time profile was "flown" by

a pilot using the complete nonlinear aircraft model along the desired descent path. The nominal state and control trajectories were recorded and are depicted in Figures 5-1 through 5-8. This procedure ensured nominal trajectories which were consistent with the nonlinear simulation, thus improving the accuracy of the linear model.

The route-time profile was designed for the presence of no wind and was "flown" as such. The execution of the route-time profile was not done by an automatic system, but rather by pilot control. The pilot "error" inherent in the nominal state and control trajectories from those ideal trajectories dictated by the route-time profile can be considered negligible since it is the recorded trajectories against which the error signal of the controller is measured.

5.2 WIND DISTURBANCES

The wind disturbance, $\delta \underline{w}_k$, which appears as an exogenous variable in the linear discrete-time system, is treated as a known deterministic disturbance. This wind disturbance is the difference between the nominal wind (that wind predicted and used to determine the aircraft's route-time profile) and the actual or measured wind. In reality, winds are not deterministic and must be estimated; this study does not consider this problem but one can view the winds used here as if they were the solution to an estimation problem.

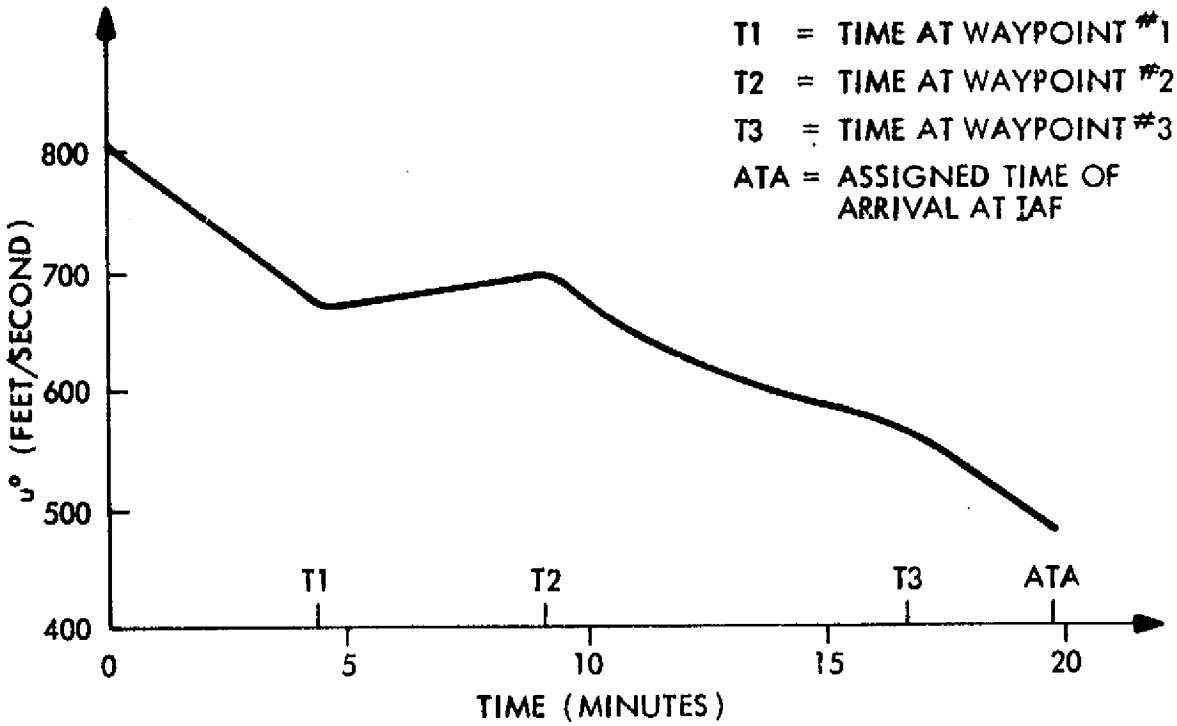

Fig. 5-1 Nominal Forward Body Velocity - State u

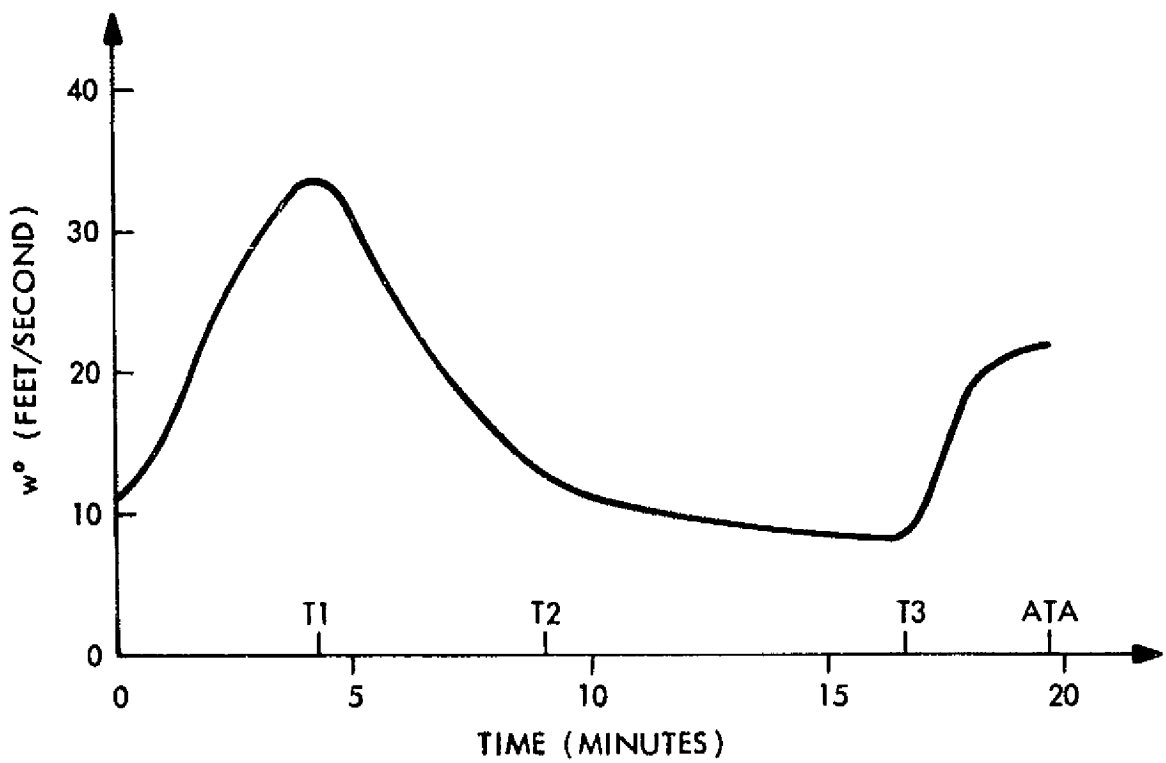

Fig. 5-2 Nominal Downward Body Velocity - State w

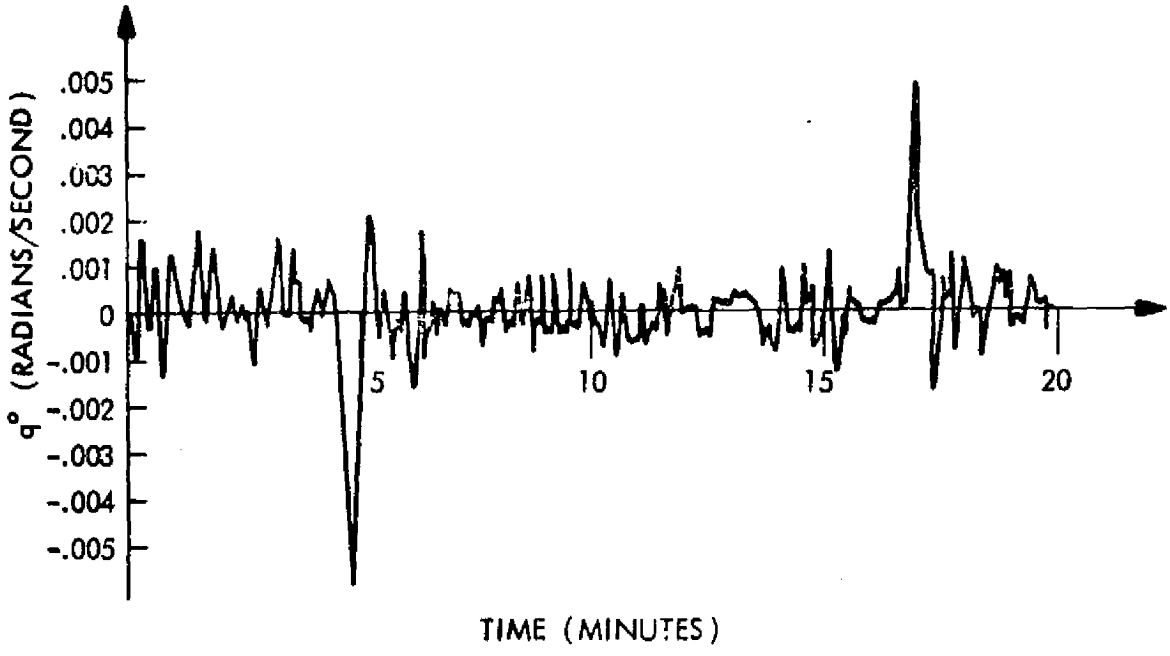

Fig. 5-3 Nominal Pitch Rate - State q

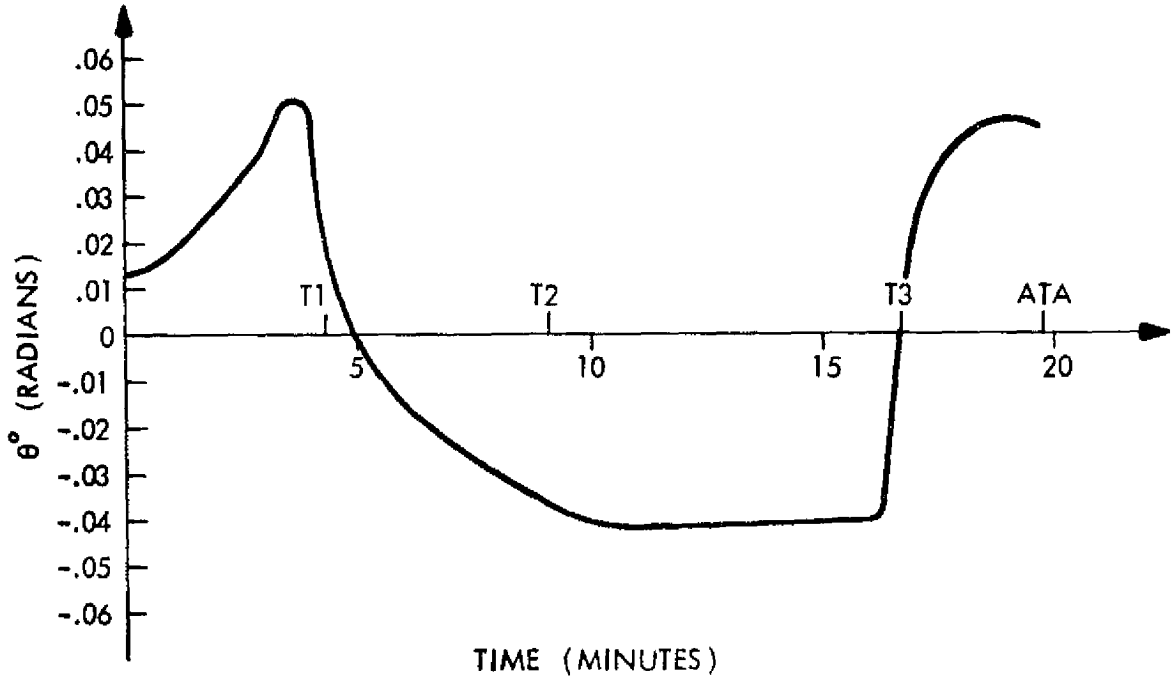

Fig. 5-4 Nominal Pitch Angle - State θ

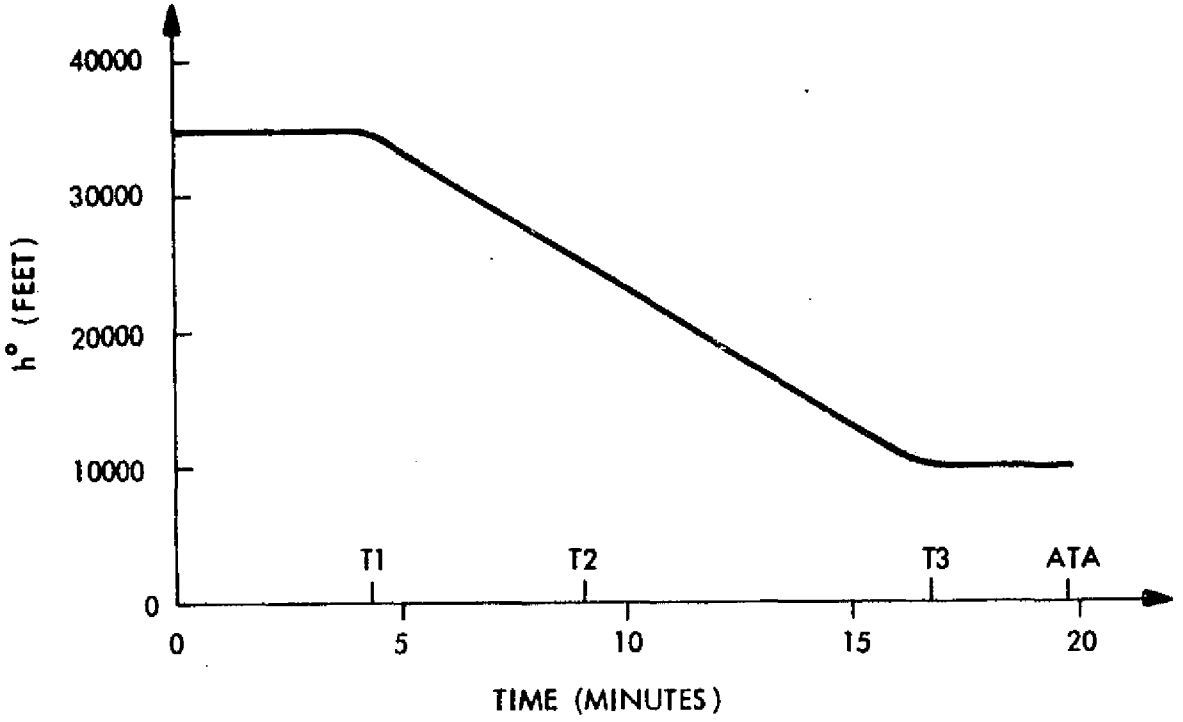

Fig. 5-5 Nominal Altitude - State h

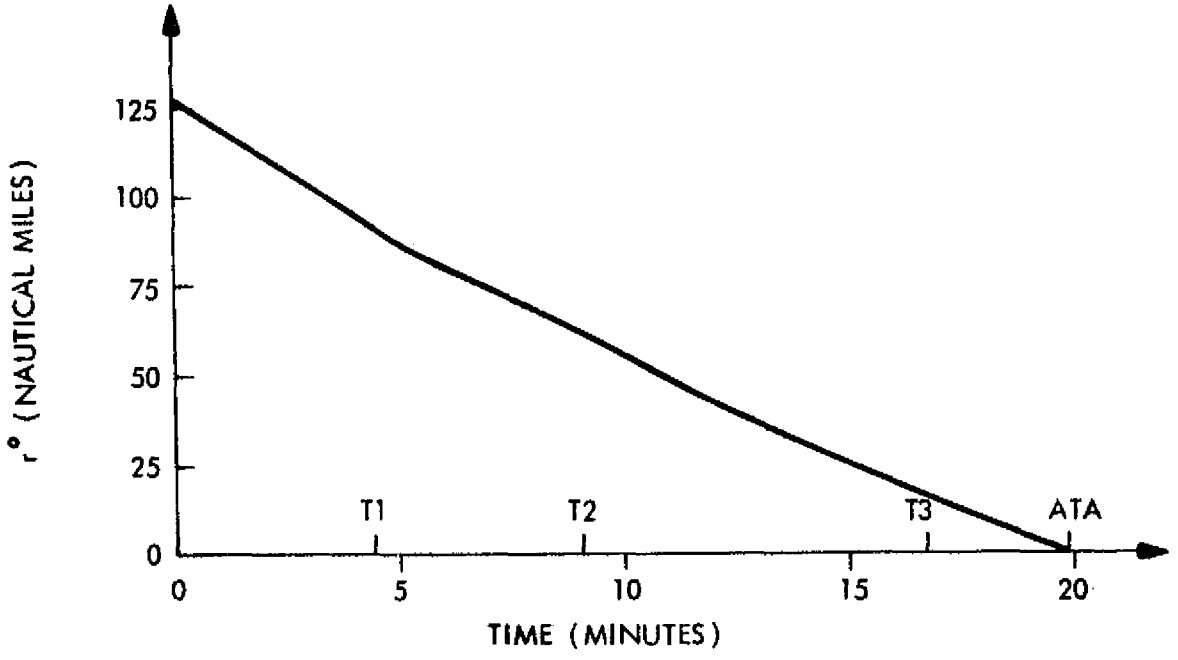

Fig. 5-6 Nominal Range - State r

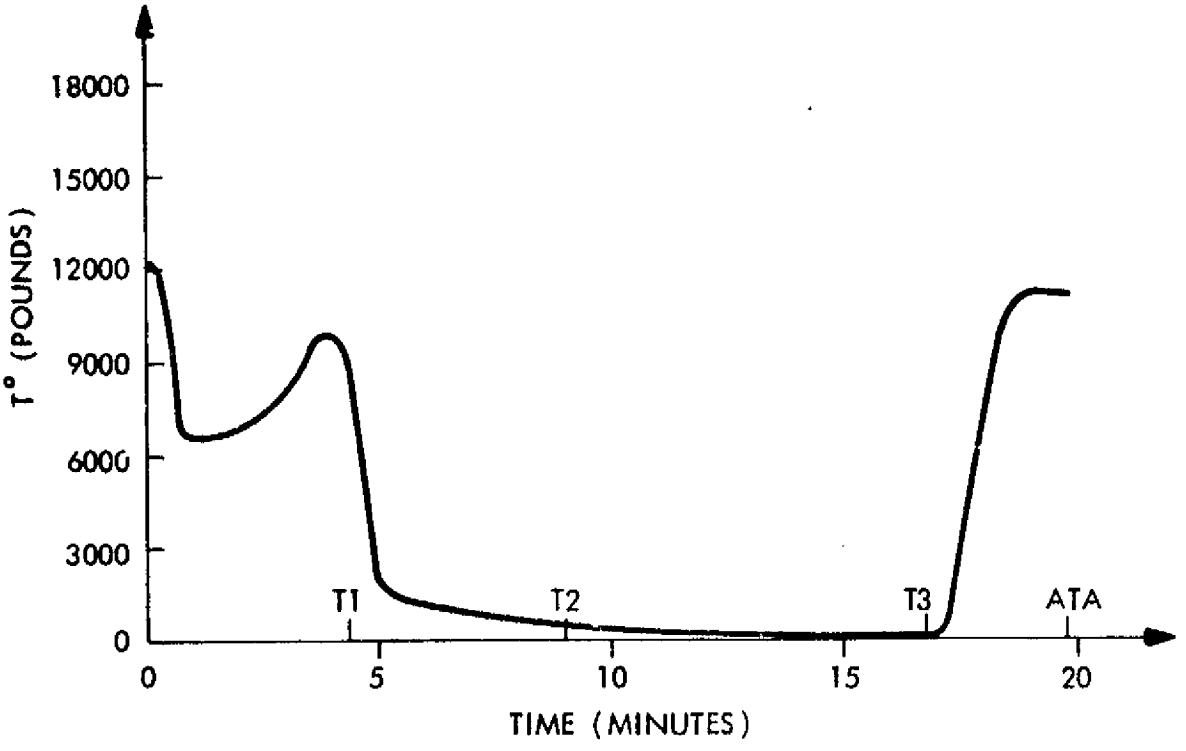

Fig. 5-7 Nominal Thrust - Control T

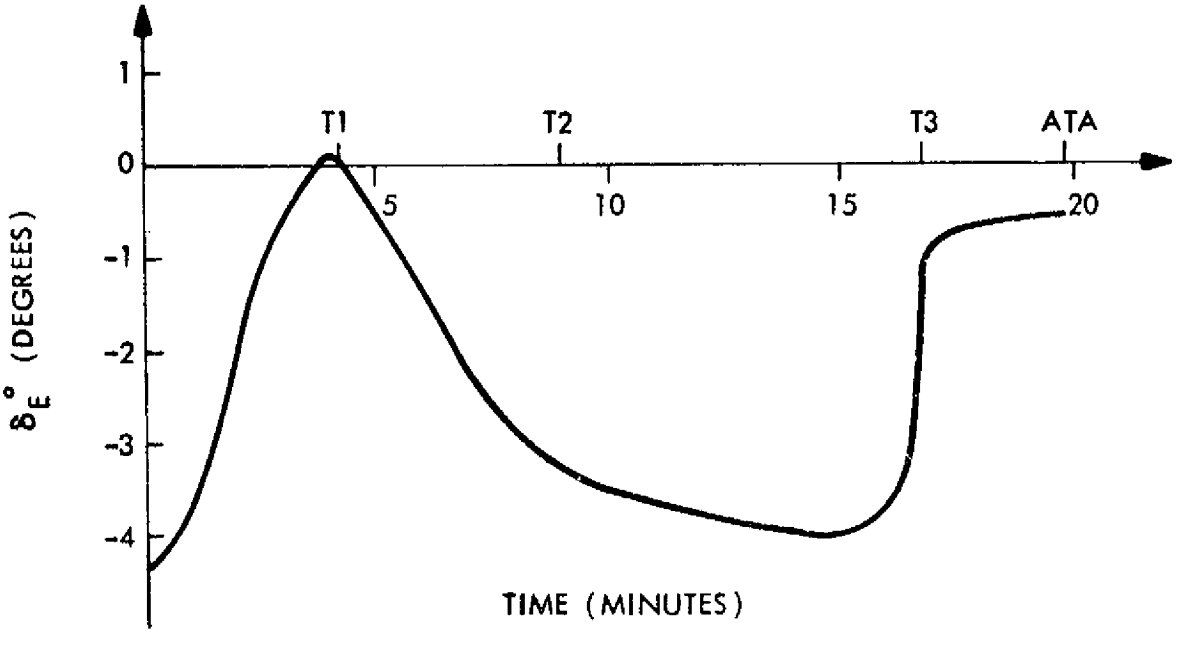

Fig. 5-8 Nominal Elevator Deflection - Control δ_E

In this study, the route-time profile is designed in the presence of no wind. Therefore, $\delta \underline{w}_k$ is the actual wind that the aircraft encounters in flight. Three different actual wind conditions are used in this study. Each wind is a direct head-wind and is constant along the entire descent path. The winds used are 15, 30, and 45 knot head-winds. The system was designed to handle vertical winds also, but these are not considered in this study

Since the route-time profile assigned to the aircraft is based on a groundspeed profile, the effect of the wind disturbance, $\delta \underline{w}_k$, is to alter several of the nominal state trajectories with an additional component, $\Delta \underline{x}_k^o$, in order to maintain the groundspeed profile which is required to achieve accurate 4-D navigation. The nominal attitude and range state trajectories remain unchanged under wind disturbances for a particular route-time profile. The most important change occurs in the aircraft nominal forward velocity state. This change, Δu_k^o, is equal to the horizontal component of the wind $(-w_h)$ along the aircraft's ground track. For example, since a head-wind is assumed to be negative, the change in the nominal forward velocity trajectory is positive in order to compensate for the head-wind and remain on a desired groundspeed profile. The changes in the aircraft's nominal downward velocity, pitch rate, and pitch angle states are a result of the change in the nominal forward velocity state. These changes are small

and neglected in the nominal state trajectories. However, if these nominal state trajectories were adjusted to account for these small changes, the errors sensed by the feedback system would be reduced for these states.

5.3 PERFORMANCE WEIGHTING MATRICES

Perhaps one of the most important aspects of the design is the choice of the weighting matrices $\underline{Q}$, $\underline{R}$, and $\underline{S}$. This choice is initially based on the desired maximum allowable deviation of the states and controls from their nominal values at any instant in time [10,20,21]. The maximum and minimum values of the nominal state and control trajectories, and the desired maximum allowable deviations along these nominal trajectories, are listed in Table 5-1.

TABLE 5-1

ACCEPTABLE STATE AND CONTROL DEVIATIONS

	Maximum Nominal Value	Minimum Nominal Value	Allowable Deviation	Units
States				
u	$804.(+\Delta u^o)$	$480.(+\Delta u^o)$	±10.0	ft./sec.
w	33.5	7.7	±2.0	ft./sec.
q	0.0049	-0.0058	±0.001	rad./sec.
θ	0.051	-0.0425	±0.01	rad.
h	35000.0	10000.0	±200.0	ft.
r	125.4	0.0	±0.1	n. mi.
Controls				
T	12198.0	0.0	±500.0	lbs.
δ_E	0.127	-4.32	±2.0	deg.

The selection of the weighting matrices in the quadratic performance function is by no means a simple task. Usually, they are selected by the designer on the basis of experience and readjusted accordingly based on the results of simulation runs [19]. For most practical applications, $\underline{Q}$ and $\underline{R}$ are selected to be diagonal as they have been in this study. This allows specific components of the state perterbation vector $\delta\underline{x}_k$ to be penalized individually. This is a common rule of thumb applicable to aerospace systems that have a "physical" set of state variables and control variables [19].

The particular design considered here is particularly applicable to passenger-carrying airline transports. Therefore, from a practical viewpoint, the levels of acceleration or deceleration produced by any maneuvers must be acceptable to avoid discomfort in the passenger cabin. This leads to a high penalty on pitch rate. In order to preserve the accuracy desired in 4-D navigation, high penalties on altitude, range, and particularly on forward airspeed are imposed. In addition, in order to regulate these states about the nominal trajectory, it is desirable to use elevator deflection rather than thrust in order to minimize the cycling up and down of the engines, thus minimizing fuel consumption. Therefore, thrust is penalized more heavily than elevator deflection. The cross-term weighting matrix $\underline{S}$ is used to smooth the performance of the control regulator.

Using the simulation facilities, the linear feedback control system's response to various wind conditions imposed upon the nonlinear aircraft model was evaluated in a real-time simulation. After much frustration and "juggling" of the weighting matrices, it was found that the following matrices produced acceptable responses to wind disturbances:

$$\underline{Q}_k = \begin{matrix}\text{state}\\ \text{weighting}\\ \text{matrix}\end{matrix} = \begin{bmatrix} .72 & 0 & 0 & 0 & 0 & 0 \\ 0 & .5 & 0 & 0 & 0 & 0 \\ 0 & 0 & .8E+3 & 0 & 0 & 0 \\ 0 & 0 & 0 & .75E+2 & 0 & 0 \\ 0 & 0 & 0 & 0 & .88E-2 & 0 \\ 0 & 0 & 0 & 0 & 0 & .55E-5 \end{bmatrix} \qquad 5\text{-}1$$

$$\underline{R}_k = \begin{matrix}\text{control}\\ \text{weighting}\\ \text{matrix}\end{matrix} = \begin{bmatrix} .39E-4 & 0 \\ 0 & .11 \end{bmatrix} \qquad 5\text{-}2$$

$$\underline{S}_k = \begin{matrix}\text{cross-term}\\ \text{weighting}\\ \text{matrix}\end{matrix} = \begin{bmatrix} .53E-2 & 0 \\ .44E-2 & 0 \\ 0 & .94E+1 \\ 0 & .28E+1 \\ 0 & .31E-1 \\ .15E-4 & 0 \end{bmatrix} \qquad 5\text{-}3$$

$$\underline{Q}_T = \begin{matrix}\text{terminal}\\ \text{state}\\ \text{weighting}\\ \text{matrix}\end{matrix} = \begin{bmatrix} .1E+1 & 0 & 0 & 0 & 0 & 0 \\ 0 & .5 & 0 & 0 & 0 & 0 \\ 0 & 0 & .8E+3 & 0 & 0 & 0 \\ 0 & 0 & 0 & .75E+2 & 0 & 0 \\ 0 & 0 & 0 & 0 & .99E-2 & 0 \\ 0 & 0 & 0 & 0 & 0 & .44E-4 \end{bmatrix} \qquad 5\text{-}4$$

Note that higher penalties are placed upon the forward velocity, altitude, and range states at the terminal time in an

attempt to preserve the accuracy and precision inherent in the time-controlled navigation concept.

5.4 THE OPTIMAL FEEDBACK SOLUTION

Using the nominal state and control trajectories along with the weighting matrices described in the previous sections, the optimal discrete-time feedback law with the appropriate Riccati equation and driving function as derived in Chapter IV can now be solved. The discrete-time versions of the Riccati equation and driving function as described by equations 4-109 and 4-110 respectively are solved backward in time. For each time interval of 3 seconds, new solutions to these equations are computed and used to update the feedback gain matrix $\underline{K}_k$ and exogenous component $\underline{f}_k(\delta\underline{w}_k)$. These matrices are used in the linear feedback law $\delta\underline{u}_k^* = \underline{K}_k\ \delta\underline{x}_k + \underline{f}_k(\delta\underline{w}_k)$ and remain constant during the following 3 second interval in the real-time simulation.

The solutions to the Riccati equation and the resulting feedback gain and exogenous component matrices are included in Appendix A for the initial time interval and the time interval immediately preceding the terminal time.

The optimal feedback gains are time-varying, but their values are unaffected by the value of the wind disturbance. However, the values of exogenous feedback terms are directly

proportional† to the magnitude of the wind disturbance at any instant in time. The optimal feedback gains for each control corresponding to the appropriate states are depicted in Figures 5-9 and 5-10 as a function of time. It is important to consider the relative magnitudes of the deviations in the states in order to interpret the relative strengths of the gains required for each control. These deviations in the states will be considered in the following section.

In addition, it is important to notice the change in the feedback gains at certain times in the flight, namely at those times when the initial descent begins (at time T1) and ends (at time T3) as well as at the terminal time (ATA). At times T1 and T3, the most noticeable changes in the feedback gains occur for those gains multiplying the deviations in the downward velocity, pitch rate, and pitch angle states. This is logical since it is at these two particular times that the nominal values of these particular states are changing most rapidly due to the desired change in orientation of the aircraft in order to stay on the descent path. Overall, the most radical changes in the feedback gains are noticeable at the terminal time due to the terminal time penalties on the states. In general, the feedback gains near the terminal time are acceptable. However, the rate of change in magnitude of the

---

† Assuming constant wind, $\delta \underline{w}_k = \delta \underline{v}_k = \delta \underline{v}$.

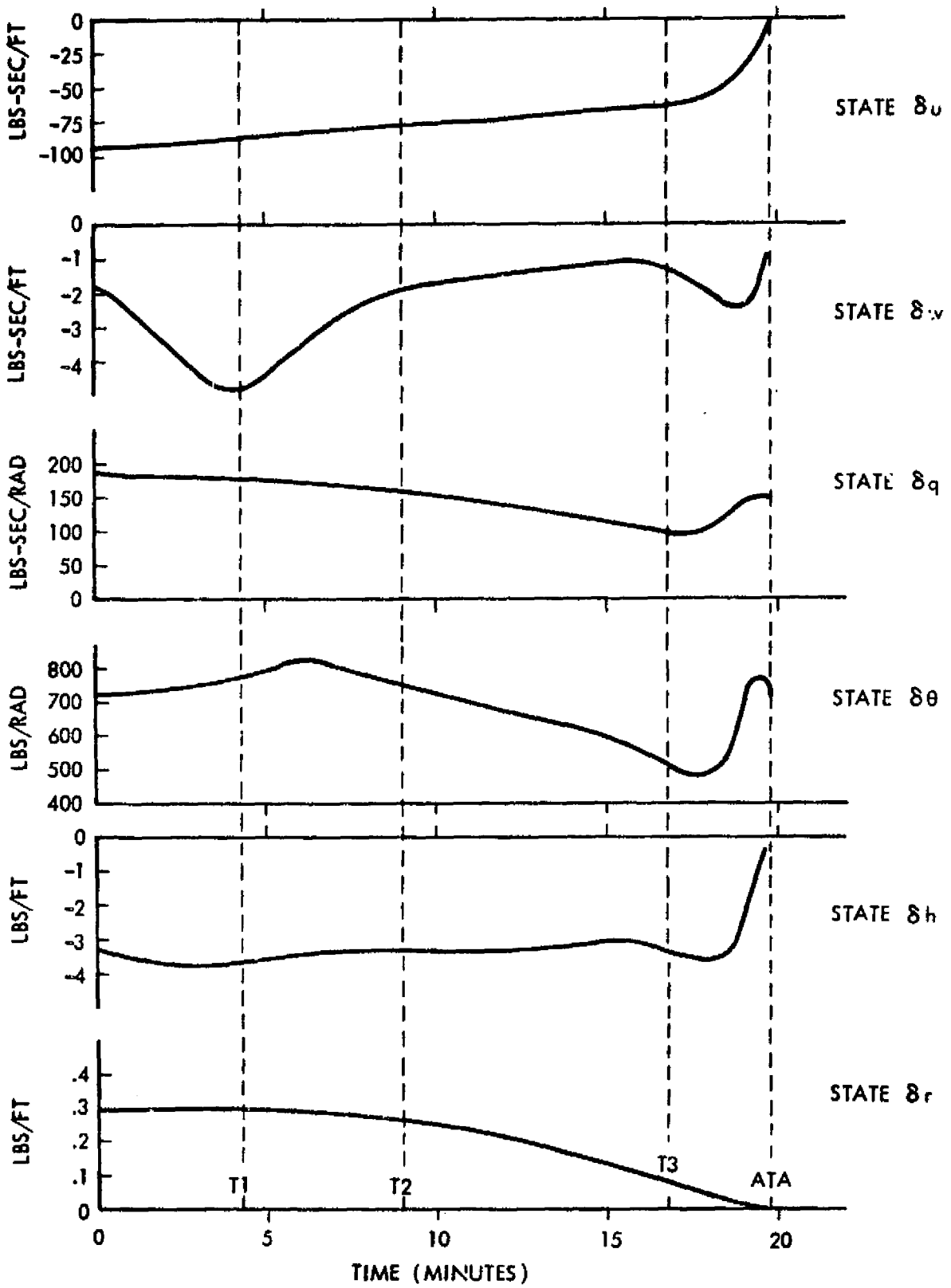

Fig. 5-9 δT* Thrust Control Feedback Gains

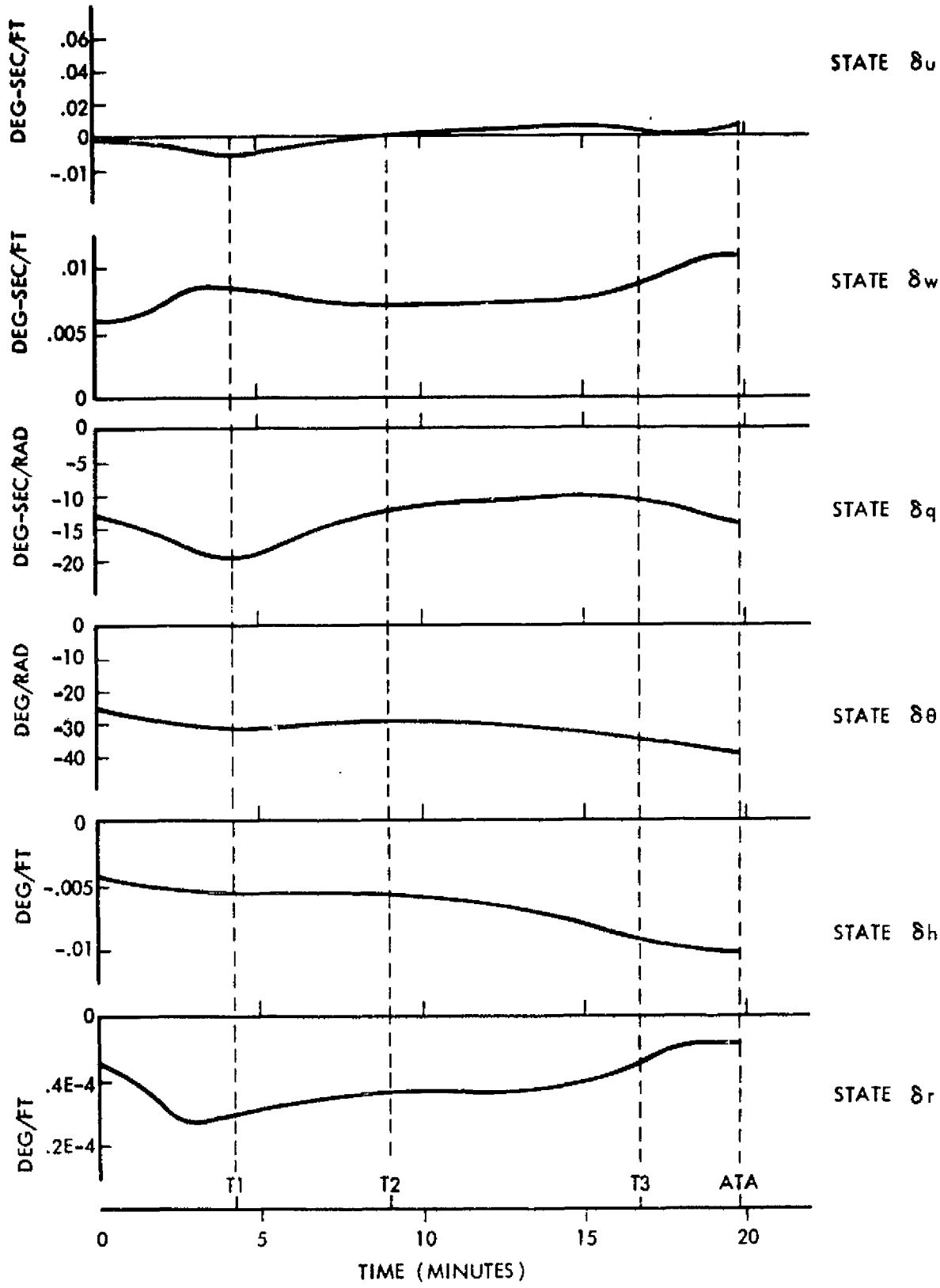

Fig. 5-10 $\delta\delta_E$* Elevator Control Feedback Gains

feedback gains near the terminal time could be reduced by artificially extending the terminal time in order to achieve less change in the gains near the true terminal time. Ultimately, this would be desirable when extending the time-controlled navigation concept completely down to the runway threshold.

The exogenous feedback control components are depicted in Figures 5-11 and 5-12 as functions of time. The exogenous components of the feedback control, which are directly related to the magnitude of the wind disturbance, are designed to compensate for the overall disturbance along the descent route profile. These components tend to decay linearly to zero with respect to time. This is a result of the method of solution chosen to determine the exogenous feedback components. The solution is designed to minimize the total additional control provided by the exogenous components.

As an alternative to this method of solution, the exogenous components could be determined as the additional control, $\Delta \underline{u}_k^o$, needed at each instant of time to keep the states of the system on their adjusted nominal trajectories, $\underline{x}_k^o + \Delta \underline{x}_k^o$, based on the wind disturbance as previously described. Although the second method was not investigated in this study, it is possible to qualitatively compare the two solutions while examining the results of the system's response using the first method of solution. The possible advantages of this second approach were

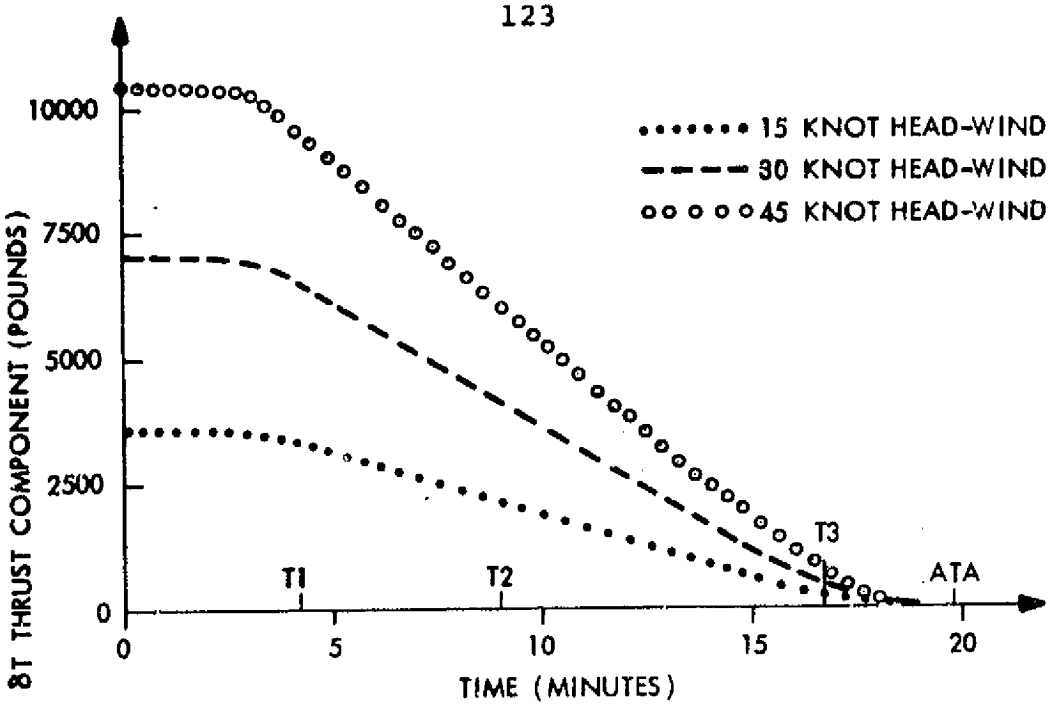

Fig. 5-11 Exogenous Feedback Thrust Component

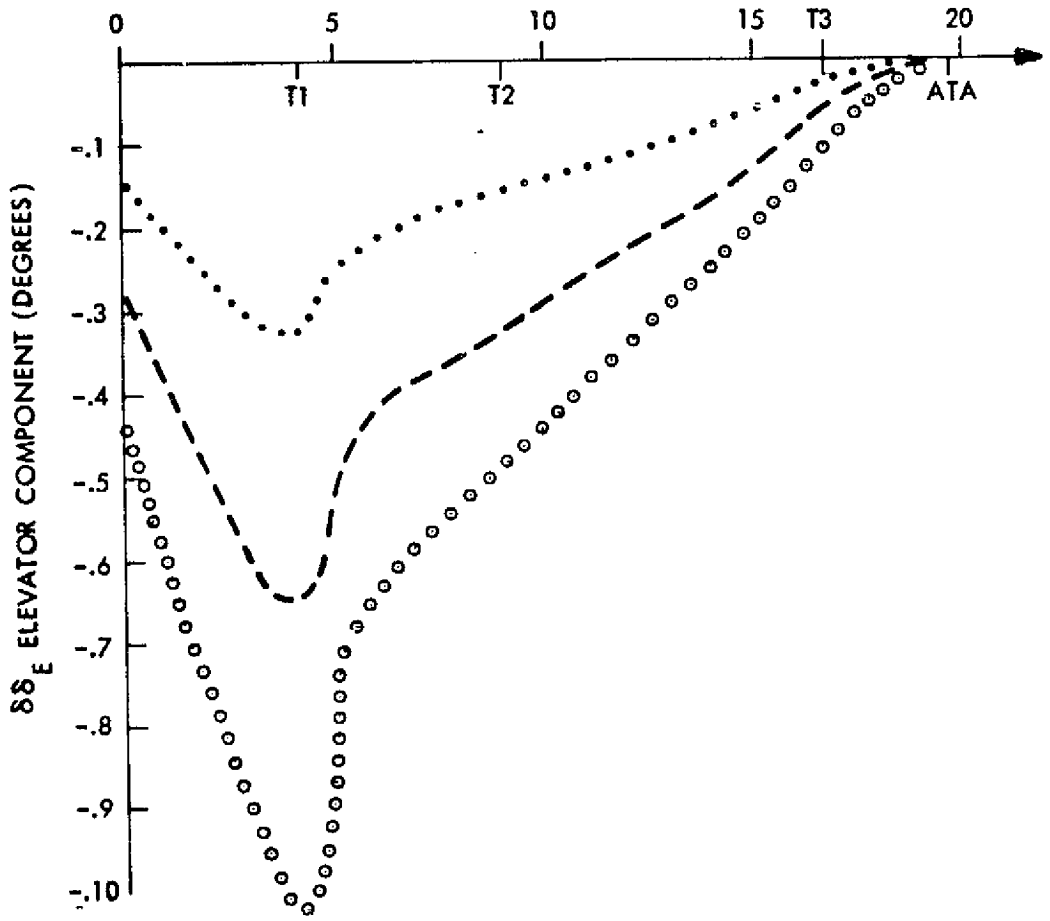

Fig. 5-12 Exogenous Feedback Elevator Component

only apparent in the final simulation results and time was insufficient to permit a full evaluation. The results of the approach taken in this study will be presented in the following section. The feedback gains remain unchanged using either method of solution for the exogenous feedback components.

5.5 TIME-CONTROLLED NAVIGATION EVALUATION

The optimal control solution obtained in the form of a feedback law was evaluated in a real-time simulation by introducing wind disturbances into the state of the system. As previously explained, the linear feedback law is composed of two parts: one part dependent upon deviations in the state and another part dependent upon the exogenous wind variables. Both the complete linear feedback system and one without the exogenous component were analyzed under identical wind disturbances. The important point to note is that the linear feedback law was implemented on the complete nonlinear aircraft model.

The absolute deviations of the states and controls from their nominal values, when the complete linear feedback system with its exogenous components were implemented on the nonlinear aircraft system, are depicted in Figures 5-13 through 5-20 for the various wind disturbances. The deviation in the aircraft forward body velocity, δu, is based on the adjusted nominal trajectory due to the wind disturbance. The deviation

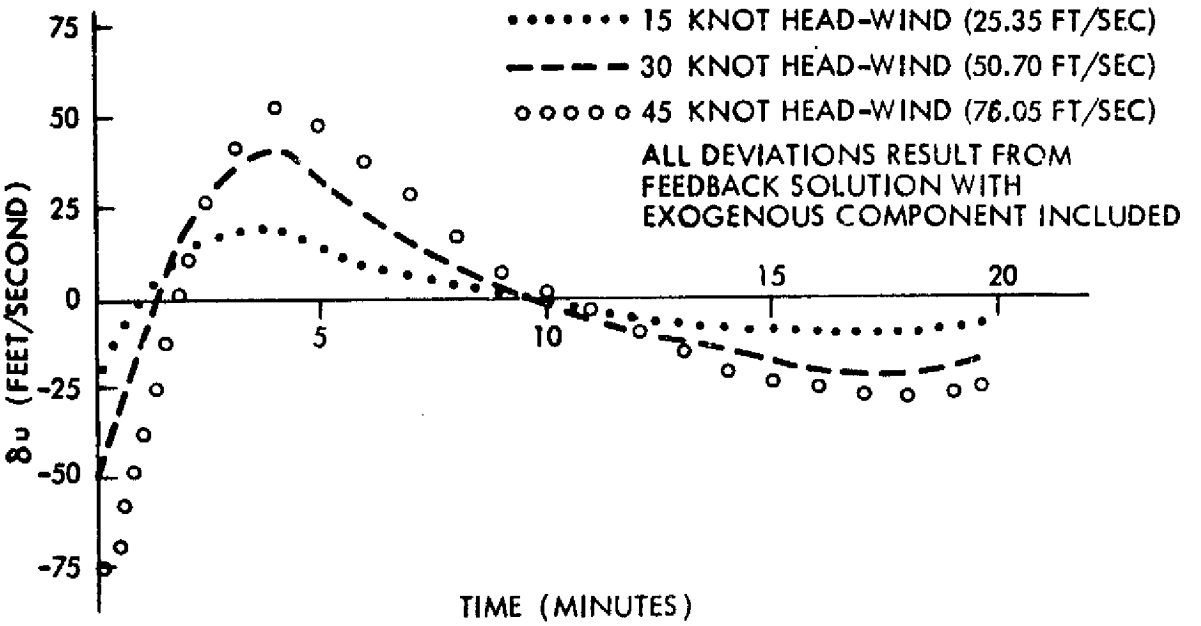

Fig. 5-13 Deviation in Forward Body Velocity - δu

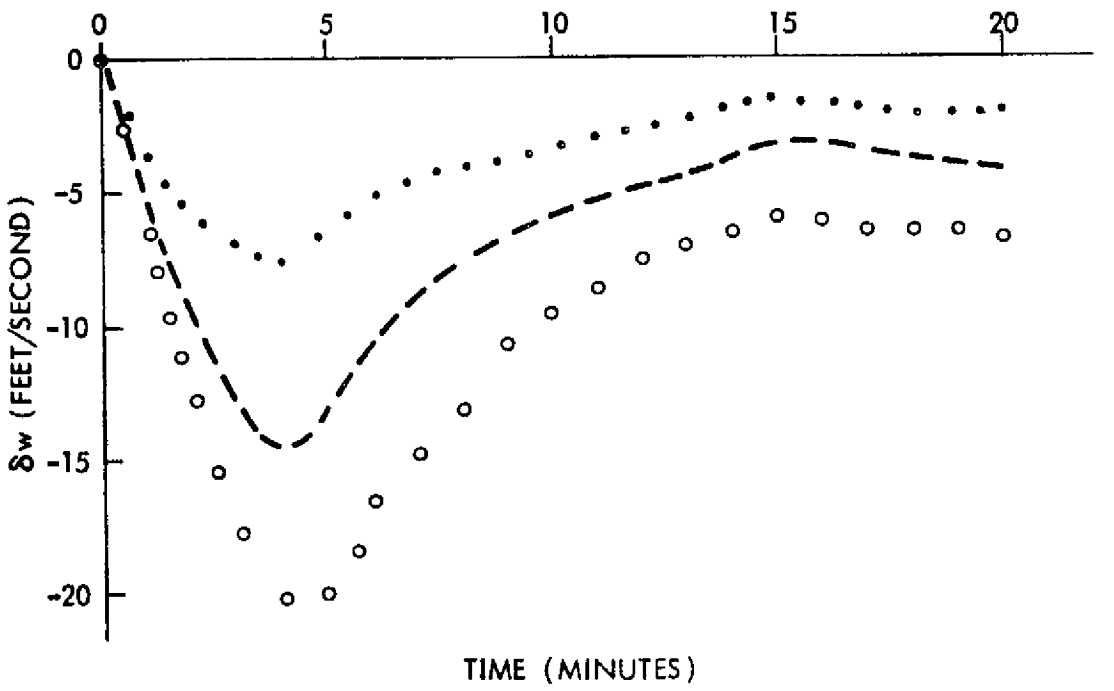

Fig. 5-14 Deviation in Downward Body Velocity - δw

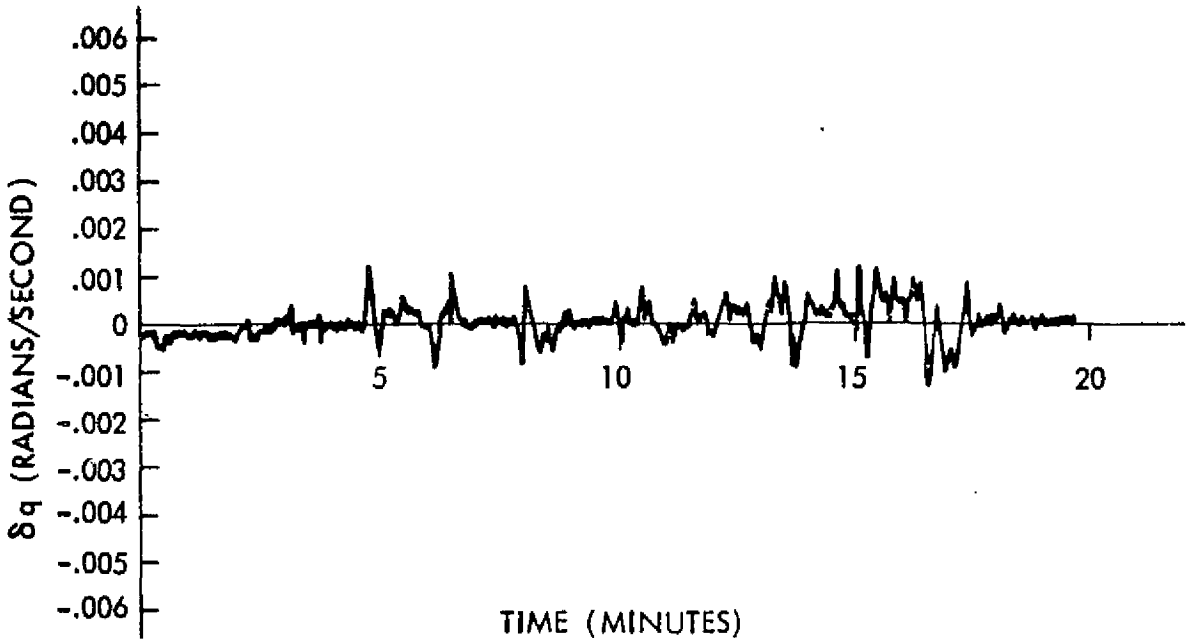

Fig. 5-15 Deviation in Pitch Rate - δq

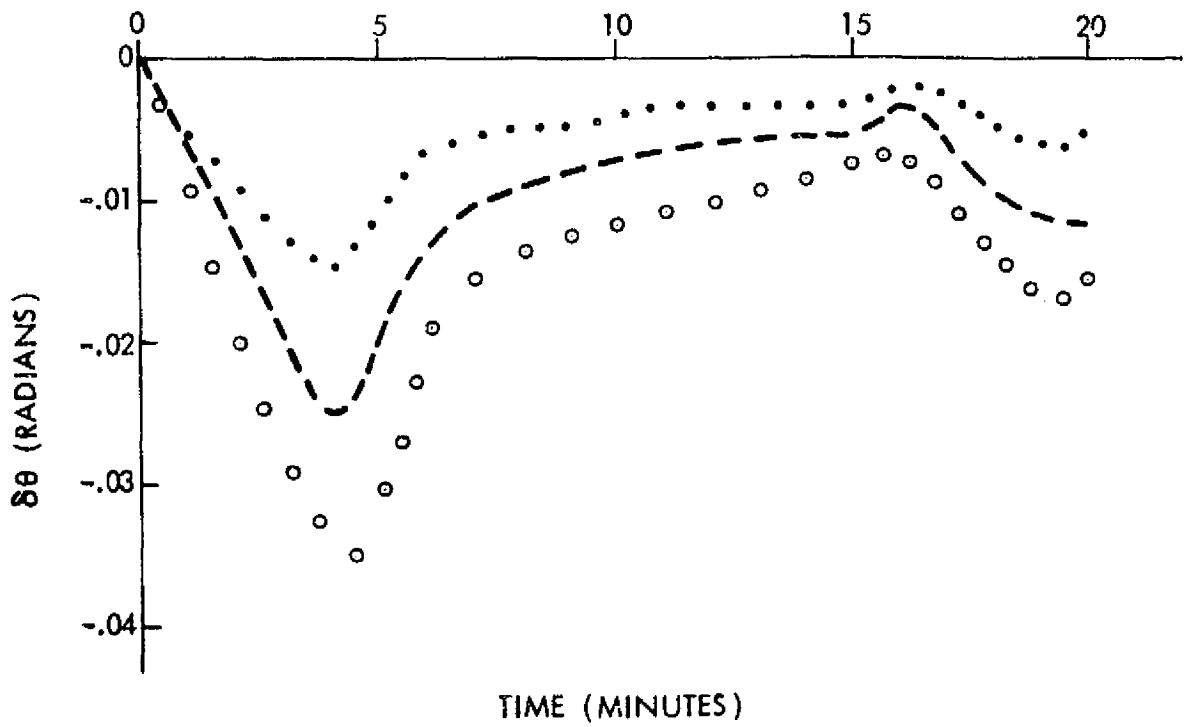

Fig. 5-16 Deviation in Pitch Angle - δθ

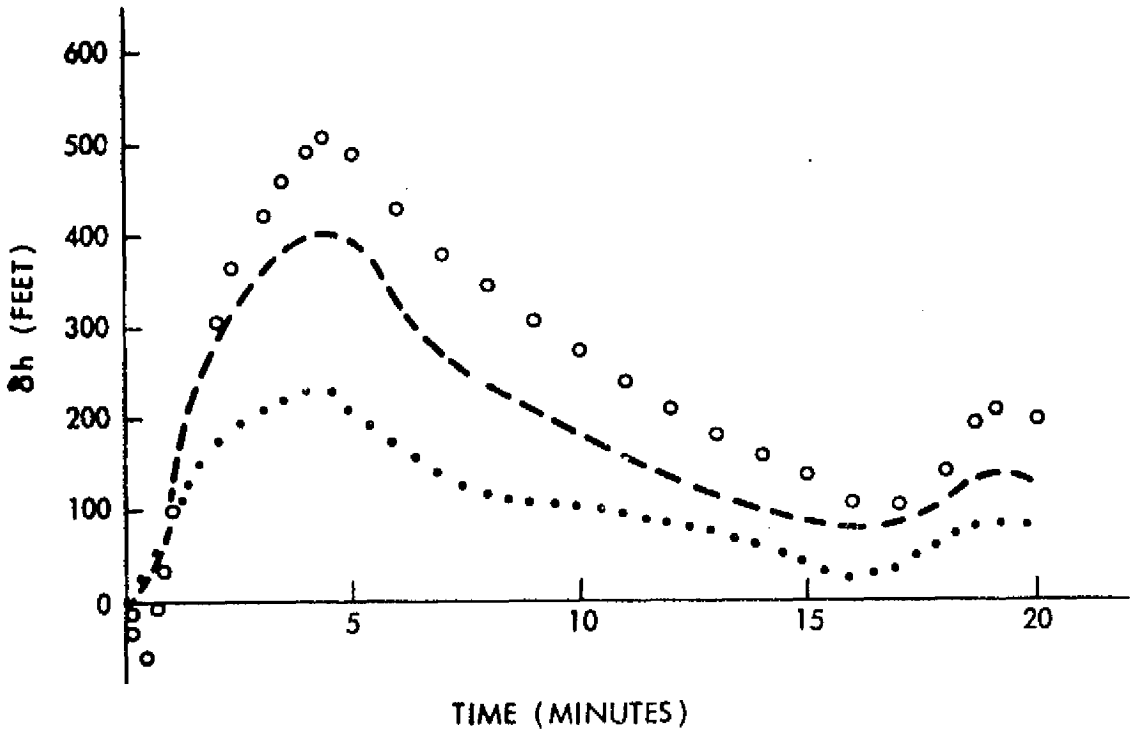

Fig. 5-17 Deviation in Altitude - δh

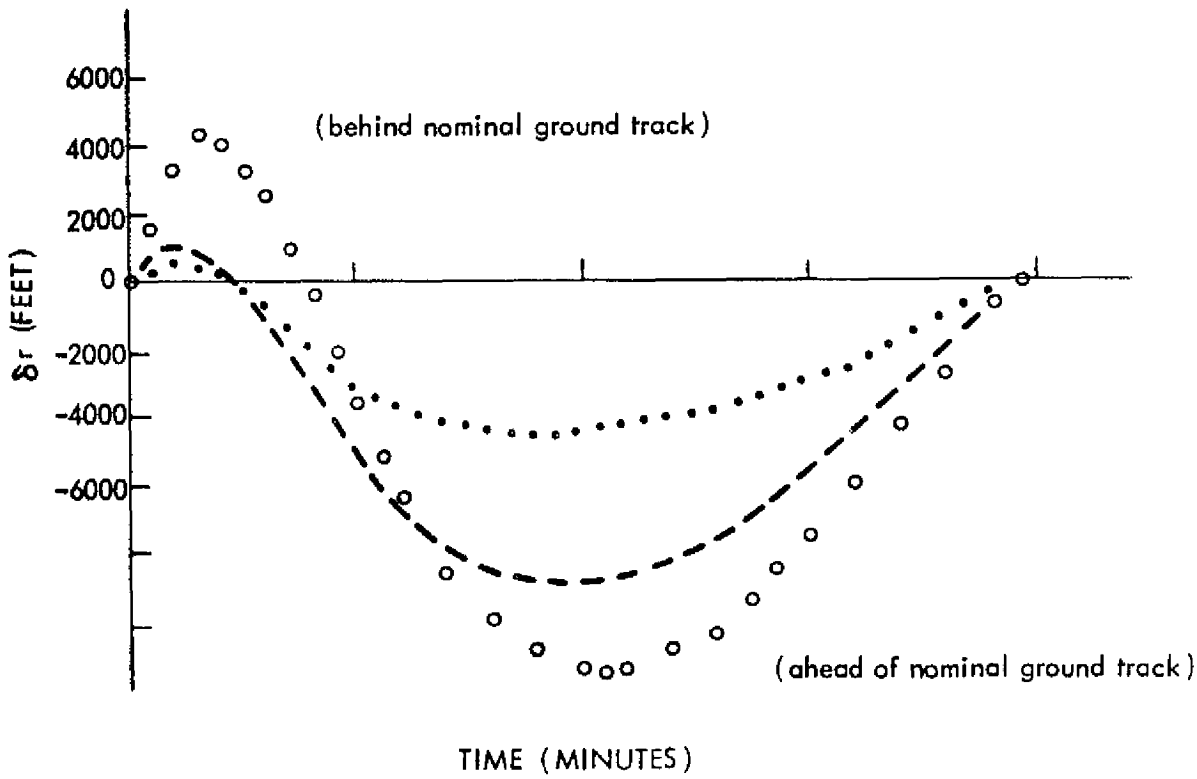

Fig. 5-18 Deviation in Range - δr

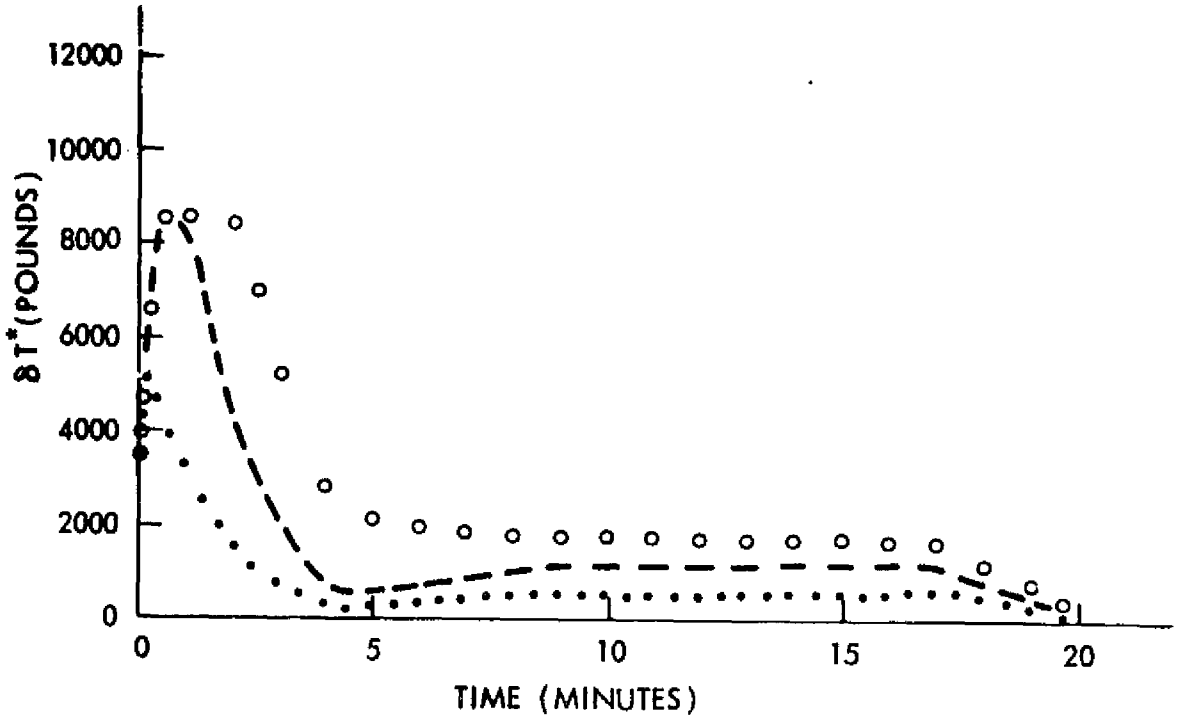

Fig. 5-19 Deviation in Thrust - δT^*

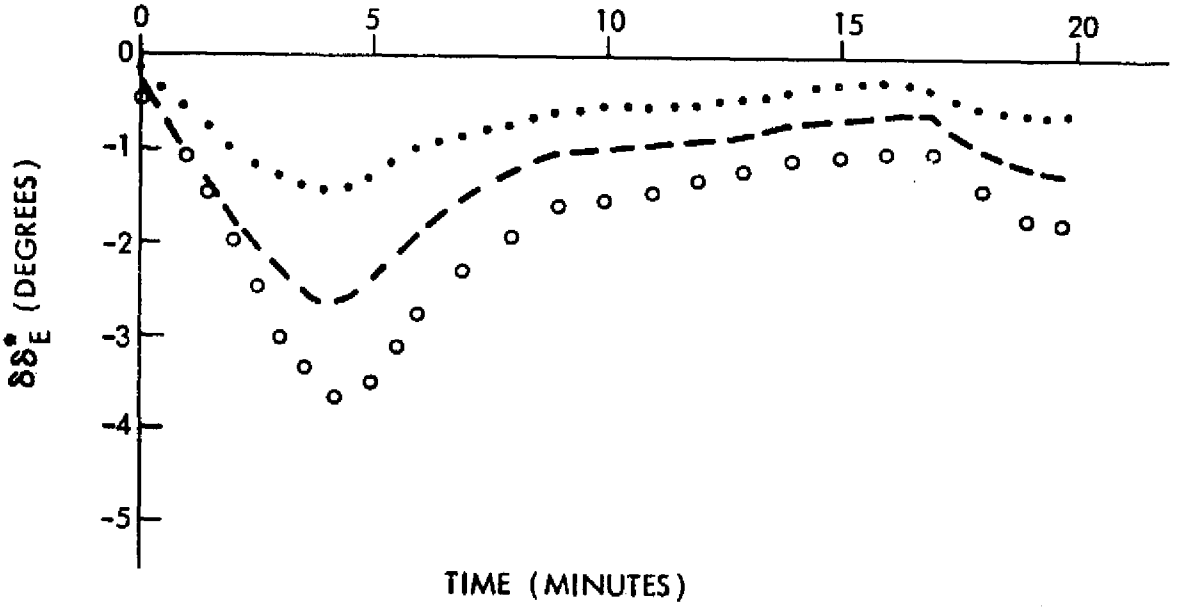

Fig. 5-20 Deviation in Elevator Deflection - $\delta\delta_E{}^*$

in pitch rate, δq, is basically indistinguishable for each head-wind disturbance and has a mean value of approximately zero. Although the deviation in pitch rate appears to be "noisy," it is actually a deterministic deviation.

5.5.1 ACCURACY ACHIEVED

The objective of the control regulator is to get the aircraft to the IAF at the assigned time. For each head-wind condition, the initial deviation in the forward velocity state is equal to the magnitude of the head-wind. The controller senses this initial deviation and increases thrust to increase the airspeed. Meanwhile, the aircraft has fallen behind schedule while it was flying at airspeeds below its adjusted nominal. Therefore, in order to compensate for the distance lost, the controller increases the aircraft's airspeed even further. It is important to understand the control regulator's action concerning this speed control. The regulator uses over 50% of its total additional thrust within the first 5 minutes of the flight. The additional thrust after 5 minutes into the flight stays approximately at a constant level until decreasing toward zero at the terminal time. The effect of using the additional thrust in this manner is to put the aircraft ahead of schedule along its ground track early in the flight by using large amounts of additional thrust while at high altitude and then letting the aircraft slowly approach the nominal schedule

while using smaller amounts of thrust at lower altitudes. The effect of this action on the deviation in range is depicted in Figure 5-18.

The advantage of this type of control action lies in fuel conservation since more thrust can be achieved at higher altitudes than can be achieved at lower altitudes for the same fuel flow.

The effect of the exogenous feedback solution component can be seen from the data presented in Table 5-2. When the exogenous component is included in the feedback solution, the control regulator achieves the desired 4-D navigation accuracy at the terminal time. For a 15 knot head-wind, the aircraft is 17 feet ahead and 76 feet too high of the desired point at the terminal time. The aircraft is 20 feet behind and 151 feet too high for a 30 knot head-wind, and 41 feet behind and 212 feet too high for a 45 knot head-wind at the terminal time. These errors in aircraft position at the terminal time are certainly acceptable since actual position measuring equipment errors are greater than those errors produced by the 4-D navigation system designed here. In addition, the aircraft is traveling at speeds that could cover the distance errors in less than a second.

However, without incorporating the exogenous component in the feedback solution, the aircraft is approximately 1 nautical mile, 2 nautical miles, and 3 nautical miles behind at the

TABLE 5-2

EFFECT OF EXOGENOUS FEEDBACK COMPONENT

Time	0		T1		T2		T3		ATA	
Feedback Solution	With/Without Exogenous Component		With/Without Exogenous Component		With/Without Exogenous Component		With/Without Exogenous Component		With/Without Exogenous Component	
Wind = 15 knot head-wind										
δu (ft./sec.)	-25.3	-25.3	17.8	-1.5	.6	-2.2	-10.	-6.6	-10.	-7.9
δw (ft./sec.)	0	0	-7.3	-4.	-3.2	-2.9	-2.3	-2.3	-2.3	-2.5
δq (rad./sec.)	-.0001	0	-.0003	-.0003	.0002	.0002	-.0025	.0013	-.0003	-.0003
$\delta\theta$ (rad.)	0	0	-.0138	-.0076	-.0046	-.0047	-.0028	-.001	-.004	-.004
δh (ft.)	0	0	230.5	166.	110.	91.	33.	51.	76.	86.
δr (ft.)	0	0	-2385	2583	4447.	3204.	-1677	4765	-17	6045
δT (lbs.)	3244	0	141	320	555	743	639	732	129	87
$\delta\delta_E$ (deg.)	-.14	0	-1.43	-.82	-.54	-.62	-.35	-.52	-.67	-.72
Wind = 30 knot head-wind										
δu (ft./sec.)	-50.7	-50.7	38.7	-3.2	1.1	-4.4	-21.3	-13.5	-18.7	-16.5
δw (ft./sec.)	0	0	-14.7	-7.9	-6.6	-5.5	-3.2	-4.61	-4.4	-4.9
δq (rad./sec.)	-.0001	0	-.0004	-.0003	.0001	.0006	.003	.001	.0001	-.0004
$\delta\theta$ (rad.)	0	0	-.0265	-.0147	-.0078	-.0075	-.0057	-.0079	-.013	-.01
δh (ft.)	0	0	407	312	209	169	68	71	151	158
δr (ft.)	0	0	-3375	5031	-8740	6406	-3463	9938	20	12256
δT (lbs.)	3244	0	532	675	1152	1470	1228	1408	191	202
$\delta\delta_E$ (deg.)	-.29	0	-2.7	-1.55	-1.1	-.89	-.48	-.7	-2	-1.3
Wind = 45 knot head-wind										
δu (ft./sec.)	-76	-76	55.9	-3.6	10.3	-6.7	-29.8	-21.8	-28.9	-24.3
δw (ft./sec.)	0	0	-21.1	-11.9	-10.3	-9	-1.6	-8.9	-6.9	-7.3
δq (rad./sec.)	-.0002	0	-.0006	-.0005	.0005	-.0006	.0136	-.0015	-.0006	-.0004
$\delta\theta$ (rad.)	0	0	-.0363	-.0212	-.0118	-.0103	-.0046	-.0027	-.0155	-.0151
δh (ft.)	0	0	509	447	304	256	117	139	212	225
δr (ft.)	0	0	-1899	7765	-10601	9201	-4662	14587	41	17956
δT (lbs.)	3244	0	2279	1047	1863	2159	1752	2046	370	302
$\delta\delta_E$ (deg.)	-.43	0	-3.7	-2.2	-1.6	-1.45	-1	-1.2	-1.8	-1.9

terminal time for 15, 30, and 45 knot head-winds respectively. These errors are obviously not acceptable for precise 4-D navigation since the time required to travel the lost distance is too great--for example, it would take approximately 45 seconds to make up for the distance lost in a 30 knot head-wind after reaching the IAF at a speed of 250 KIAS.

Although it was desired that the aircraft reach the IAF at speeds not exceeding 250 KIAS, slightly higher speeds resulted. The aircraft was approximately traveling at 257, 267, and 275 KIAS upon reaching the IAF in the presence of 15, 30, and 45 knot head-winds respectively. The reason for the slightly higher indicated airspeeds is that the nominal forward velocity was adjusted for the winds, and thus increased beyond the nominal 250 KIAS at the terminal time. Although the terminal time airspeeds do not greatly exceed the 250 KIAS requirement, there are two possible methods to remedy this situation. One possibility is to adjust the nominal forward velocity to account for the wind, yet maintaining a 250 KIAS nominal velocity near the terminal time regardless of the wind. This approach would satisfy the 250 KIAS speed limit imposed by the FAA for flight below 10,000 feet, but would not allow certain groundspeeds to be achieved which are the speeds used in determining the route-time profile. A second possibility is to impose a groundspeed speed limit for strategically controlled aircraft utilizing four-dimensional navigation so that precise

time-controlled navigation is ensured.

The total forward velocity response and total thrust response for feedback solutions both with and without the exogenous component in the presence of a 30 knot head-wind are indicated in Figures 5-21 and 5-22. It can be seen that the aircraft's forward velocity never reaches the desired nominal velocity adjusted for the wind and subsequently continuously falls behind schedule when the exogenous component of the feedback solution is not used.

From the total thrust response curve it can be seen that the thrust stays relatively constant between times T1 and T3. In addition, the total thrust is not allowed to exceed its maximum allowable value for each altitude and Mach number. At 35,000 feet, the controller is just inside the thrust saturation limit for a 30 knot head-wind, but is limited by the saturation limit for a 45 knot head-wind. This is also evident on the thrust deviations curves in Figure 5-19. When the total thrust applied in the nonlinear simulation is limited by the saturation limit, less control is applied than that desired by the feedback law. Therefore, the controller senses larger errors in the states over a longer period of time. However, the experimental results from the real-time simulations have shown that these errors are eventually corrected for by "delayed" additional control and effectively do not affect the accuracy of the 4-D navigation system at the terminal time.

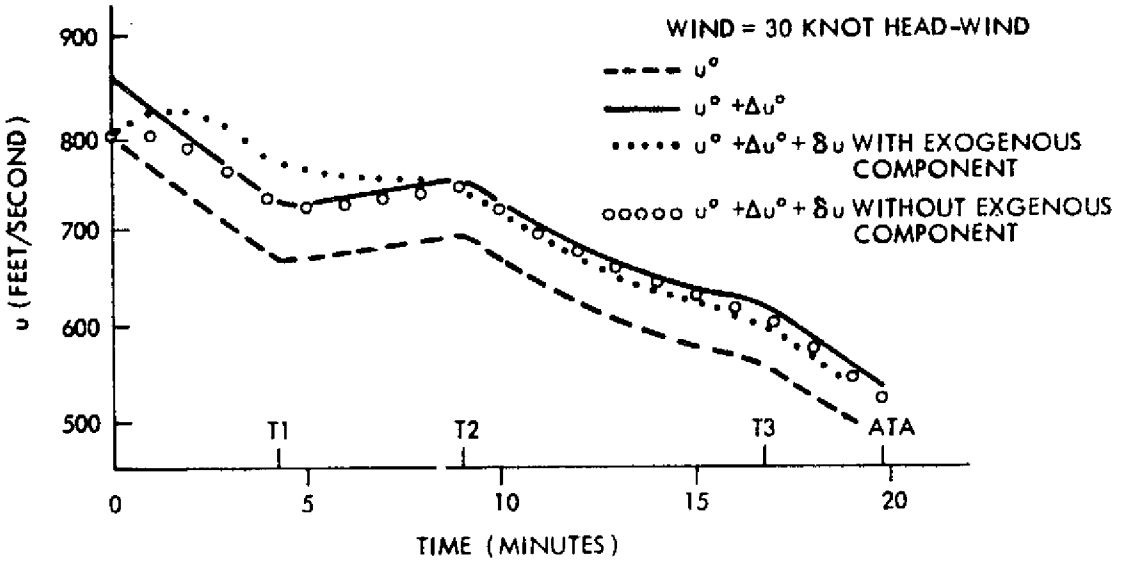

Fig. 5-21 Forward Velocity Response

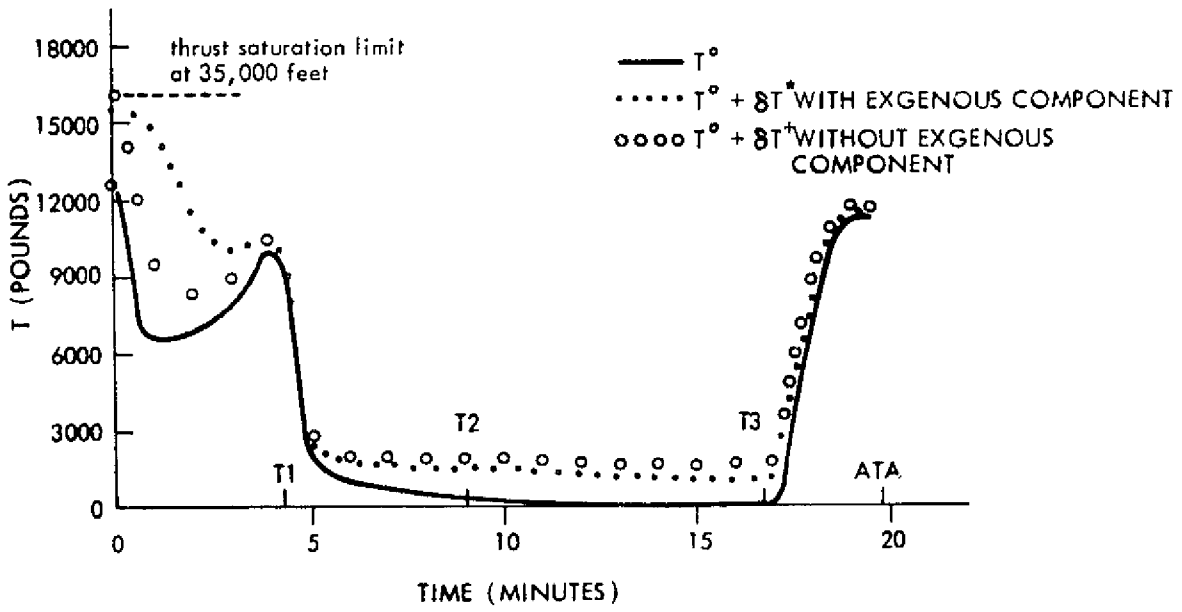

Fig. 5-22 Thrust Response

5.5.2 COMPARISON OF EXOGENOUS FEEDBACK COMPONENT SOLUTIONS

We can now postulate the differences in the system's response to each of the two methods for determining the exogenous feedback components which were briefly described in section 5-4. The first method, which is designed to minimize the overall additional thrust needed to compensate for the winds, results in exogenous feedback components that decay to zero at the terminal time. The effect of this method of solution can be seen by comparing the exogenous thrust component in Figure 5-11 with the deviation in thrust depicted in Figure 5-19. It is apparent that the feedback gains are working "hard" to initially increase the additional thrust control and then decrease it. This results in an initial addition to the exogenous thrust component followed by a partial cancellation of it which results in the deviations of thrust as depicted in Figure 5-19. As previously pointed out, this action minimizes the overall additional thrust, thus minimizing the additional fuel consumed. However, this result is achieved by making the aircraft fly faster at higher altitudes, thus initially placing it ahead of its ground track schedule.

The second method of determining the exogenous feedback components by solving for the additional control needed at each instance in time to compensate for the head-winds in order to follow the adjusted nominal state trajectories would not result

in exogenous components that decay to zero. It can be speculated that the feedback gains would not exhibit the strong time-variation previously required to add and subtract control from the exogenous control components. Subsequently, the aircraft would remain closer to its nominal ground track position, but would do so at the expense of increasing overall additional thrust during the flight. The additional thrust would result from greater control needed at lower altitudes in order to adhere to the nominal ground track as opposed to the first method where less thrust is needed at lower altitudes since the aircraft is further along its nominal ground track, and thus allowed to gradually "fall" behind to its nominal ground track position at the terminal time.

Therefore, the first method of determining the exogenous feedback control components results in overall less control than the second method, but does not remain as close to the nominal ground track as the second method. However, in either case, the desired accuracy at the terminal time can be achieved.

CHAPTER VI

ACCOMPLISHMENTS, RECOMMENDATIONS AND CONCLUSION

The objective of this research was to design and simulate a four-dimensional navigation controller to be used by air carriers in a strategic air traffic control system. A complete automatic time-controlled navigation system for aircraft is a complex system that must satisfy requirements imposed by the FAA and air traffic controllers, be within the performance capabilities of the aircraft, and be acceptable to the pilot. In this study, only the descent phase of flight was considered. It was felt that the greatest need for such a concept was within this phase of flight, where derandomization of aircraft in time could be most easily accomplished.

6.1 ACCOMPLISHMENTS

The accomplishments of this study can be summarized as follows:

1. A strategic control descent profile for aircraft arriving at Logan International Airport was designed. In addition, a strategy was devised for determining possible times of arrival at the IAF and for generating the corresponding route-time profile for each arrival time.

2. Using a mathematical model for the Boeing 707-320B aircraft, a linear feedback control solution was designed to assist the pilot to navigate along a fixed linear strategic descent profile.

3. A linear feedback control solution was derived for strategic four-dimensional aircraft navigation in the vertical plane in the presence of known along-track wind disturbances. The feedback solution is composed of two parts--one part dependent upon the deviations in the states and another part dependent upon the exogenous wind variables.

4. The linear feedback control solution for time-controlled navigation was simulated and tested on the complete nonlinear aircraft model in the presence of 15, 30, and 45 knot head-winds. The experimental results showed that the feedback controller preserved the accuracy required at the terminal time to ensure a successful 4-D navigation system.

6.2 RECOMMENDATIONS

Many important aspects of time-controlled navigation can be considered in further research. The basic recommendation is that research and development should be continued toward the capability to implement 4-D navigation control systems. The specific recommendations that the author feels are particularly related to this study are the following:

1. Examine methods for increasing aircraft descent gradient capabilities which would be desirable in order to adapt to certain environmental conditions. Such methods may include varying the slope of the descent path, thus increasing the number of route-time profiles that an aircraft is capable of executing under such conditions. In addition, the effects of spoilers and flaps on the aircraft's gradient capabilities can be considered.

2. Consider a design incorporating all aircraft states and controls. This will allow 4-D navigation to include turns and to be extended down to the runway threshold.

3. Consider thrust and actuator dynamics in the design of the controller. The present study only includes thrust dynamics as provided by the cockpit simulator hardware in real-time simulation, but no such dynamics are included for the corrective control produced by the feedback law. The effects of control saturation on the system can also be examined.

4. Consider a complete wind model that includes cross winds, gusts, and wind shear. Determine a method for estimating the mean winds along the entire descent path as well as a method for using measured winds as real-time input into the system.

5. The system designed in this study is completely deterministic. In reality, the actual system will be beset with noises and inaccuracies in observing the states as well as unknown winds and pilot error. Therefore, a stochastic system employing optimum filters might be designed in view of these considerations. The robustness of the linear feedback controller on the nonlinear simulation was gratifying in this trial study.

6. Most importantly, the practicability and physical implementation of such a system should be analyzed. It may be possible to reduce the number of states and/or feedback gains in the system without significant loss in acceptable system response and performance.

6.3 CONCLUSION

The single most important conclusion to be drawn from this research study is that the design of a time-controlled navigation system is feasible. Overall, the potential benefits of a strategic air traffic control system utilizing a 4-D navigation controller implemented by the airborne guidance system are as follows:

1. Increased air traffic control system capacity.

2. Continued operation in the event of ground system failure.

3. A reduction in controller/communication workload.

4. A reduction in flight time and delays.

5. More precise aircraft guidance and control resulting in increased safety in the airways system.

6. More efficient energy management resulting in a reduction in airline operating costs and fuel savings.

7. Ease of extension of system into the near-terminal area and adaptation to area navigation.

APPENDIX A

EVALUATION OF CONTINOUS-TIME/DISCRETE-TIME LINEAR SYSTEM MATRICES AND OPTIMAL FEEDBACK LAW

As described in Chapter IV, the continuous-time linearized aircraft system is expressed by:

$$\delta \underline{x}(t) = \underline{A}(t)\delta \underline{x}(t) + \underline{B}(t)\delta \underline{u}(t) + \underline{D}(t)\delta \underline{w}(t) \qquad \text{A-1}$$

The equivalent discrete-time linearized system is:

$$\delta \underline{x}_{k+1} = \underline{F}_k \delta \underline{x}_k + \underline{G}_k \delta \underline{u}_k + \underline{H}_k \delta \underline{w}_k \qquad \text{A-2}$$

The nominal state, control, and wind values, and the corresponding $\underline{A}_k$, $\underline{B}_k$, $\underline{D}_k$, $\underline{F}_k$, $\underline{G}_k$, and $\underline{H}_k$ matrices are presented here for the initial time (k=0) and the time immediately preceding the terminal time (k=T-1).

The nominal values at time k=0 and k=T-1 are presented in Table A-1.

TABLE A-1

NOMINAL VALUES

	Nominal Values		
Time	k=0	k=T-1	
States			Units
u	804.0	481.6	ft./sec.
w	11.0	21.5	ft./sec.
q	0.0	0.0	rad./sec.
θ	0.84	2.84	deg.
h	35000.0	10000.0	ft.
r	125.4	0.19	n. mi.
Controls			
T	12166.0	11122.5	lbs.
δ_E	-4.32	-0.52	deg.
Winds			
w_v	0.0	0.0	knots
w_h	-15.0	-15.0	knots (head-wind)

The continuous-time linear system matrices evaluated at time k=0, and the corresponding discrete-time linear system matrices are:

$$\underline{A}_o = \begin{bmatrix} -0.00414 & 0.05196 & -10.99040 & -32.19657 & 0.00007 & 0.0 \\ -0.10315 & -0.81116 & 803.99660 & -0.47206 & 0.00115 & 0.0 \\ 0.00007 & -0.00016 & -1.53043 & 0.0 & 0.0 & 0.0 \\ 0.0 & 0.0 & 1.0 & 0.0 & 0.0 & 0.0 \\ 0.01466 & -0.99989 & 0.0 & 804.07130 & 0.0 & 0.0 \\ -0.99989 & -0.01466 & 0.0 & 0.79753 & 0.0 & 0.0 \end{bmatrix} \qquad \text{A-3}$$

$$\underline{B}_o = \begin{bmatrix} 0.00014 & -0.00760 \\ 0.0 & 0.55583 \\ 0.0 & 0.02974 \\ 0.0 & 0.0 \\ 0.0 & 0.0 \\ 0.0 & 0.0 \end{bmatrix} \qquad \text{A-4}$$

$$\underline{D}_o = \begin{bmatrix} 0.0 & 0.0 \\ 0.0 & 0.0 \\ 0.0 & 0.0 \\ 0.0 & 0.0 \\ -1.0 & 0.0 \\ 0.0 & -1.0 \end{bmatrix} \qquad \text{A-5}$$

$$\underline{F}_o = \begin{bmatrix} 0.97276 & 0.06007 & -27.58448 & -95.15870 & 0.00032 & 0.0 \\ -0.07036 & 0.05726 & 73.86335 & 7.26394 & 0.00144 & 0.0 \\ 0.00005 & -0.00001 & -0.00298 & -0.00349 & 0.0 & 0.0 \\ 0.00012 & -0.00010 & 0.60162 & 0.99574 & 0.0 & 0.0 \\ 0.33406 & -1.17621 & 679.50980 & 2398.76550 & 0.99766 & 0.0 \\ -2.96182 & -0.13724 & 26.83525 & 145.83422 & -0.00048 & 1.0 \end{bmatrix} \qquad \text{A-6}$$

$$\underline{G}_o = \begin{bmatrix} 0.00042 & -0.94005 \\ -0.00002 & 15.73744 \\ 0.0 & 0.01784 \\ 0.0 & 0.04390 \\ 0.00005 & 18.77365 \\ -0.00064 & 0.51299 \end{bmatrix} \qquad \text{A-7}$$

$$\underline{H}_o = \begin{bmatrix} -0.00044 & 0.0 \\ -0.00295 & 0.0 \\ -0.0 & 0.0 \\ -0.0 & 0.0 \\ -2.99714 & 0.0 \\ 0.00046 & -3.0 \end{bmatrix} \qquad \text{A-8}$$

The continuous-time linear system matrices evaluated at time k=T-1, and the corresponding discrete-time linear system matrices are:

$$\underline{A}_{T-1} = \begin{bmatrix} -0.00523 & 0.10339 & -21.32225 & -32.17441 & 0.00001 & 0.0 \\ -0.11106 & -0.86153 & 481.70050 & -1.28396 & 0.00098 & 0.0 \\ 0.00052 & -0.00007 & -2.23353 & 0.0 & 0.0 & 0.0 \\ 0.0 & 0.0 & 1.0 & 0.0 & 0.0 & 0.0 \\ 0.03987 & -0.99920 & 0.0 & 482.16750 & 0.0 & 0.0 \\ -0.99920 & -0.03987 & 0.0 & -2.09776 & 0.0 & 0.0 \end{bmatrix} \qquad \text{A-9}$$

$$\underline{B}_{T-1} = \begin{bmatrix} 0.00014 & -0.02151 \\ 0.0 & 0.48601 \\ 0.0 & 0.02603 \\ 0.0 & 0.0 \\ 0.0 & 0.0 \\ 0.0 & 0.0 \end{bmatrix} \qquad \text{A-10}$$

$$\underline{D}_{T-1} = \begin{bmatrix} 0.0 & 0.0 \\ 0.0 & 0.0 \\ 0.0 & 0.0 \\ 0.0 & 0.0 \\ -1.0 & 0.0 \\ 0.0 & -1.0 \end{bmatrix} \qquad \text{A-11}$$

$$\underline{F}_{T-1} = \begin{bmatrix} 0.94220 & 0.10951 & -22.74816 & -94.38282 & 0.00026 & 0.0 \\ -0.00685 & 0.06864 & 24.97519 & 1.31934 & 0.00104 & 0.0 \\ 30.00022 & 0.00002 & -0.00420 & -0.01851 & 0.0 & 0.0 \\ 0.00057 & 0.00001 & 0.43522 & 0.97549 & 0.0 & 0.0 \\ 0.54402 & -1.04948 & 325.67850 & 1428.55970 & 0.99782 & 0.0 \\ -2.92484 & -0.27611 & 21.59476 & 139.22302 & -0.00041 & 1.0 \end{bmatrix} \qquad \text{A-12}$$

$$\underline{G}_{T-1} = \begin{bmatrix} 0.00042 & -0.78630 \\ -0.00001 & 6.13034 \\ 0.0 & 0.01141 \\ 0.0 & 0.02930 \\ 0.00009 & 7.66325 \\ -0.00063 & 0.33018 \end{bmatrix} \qquad \text{A-13}$$

$$\underline{H}_{T-1} = \begin{bmatrix} -0.00032 & 0.0 \\ -0.00219 & 0.0 \\ 0.0 & 0.0 \\ 0.0 & 0.0 \\ -2.99743 & 0.0 \\ 0.00038 & -3.0 \end{bmatrix} \qquad \text{A-14}$$

The optimal discrete-time linear feedback law derived in Chapter IV is of the form:

$$\delta \underline{u}_k^* = \underline{K}_k \delta \underline{x}_k + \underline{f}_k(\delta \underline{w}_k) \qquad \text{A-15}$$

where

$$\underline{K}_k = [\underline{R}_k + \underline{G}_k' \, \underline{P}_{k+1} \underline{G}_k]^{-1} \, [S_k' + \underline{G}_k' \, \underline{P}_{k+1} \underline{F}_k] \qquad \text{A-16}$$

$$\underline{f}_k(\delta \underline{w}_k) = -[\underline{R}_k + \underline{G}_k' \, \underline{P}_{k+1} \underline{G}_k]^{-1} \underline{G}_k' [\underline{P}_{k+1} \underline{H}_k \delta \underline{w}_k + \underline{N}_{k+1} \delta \underline{v}_k] \qquad \text{A-17}$$

The solution to the discrete-time matrix Riccati equation as described by equation 4-109, and the resulting feedback gain matrix and exogenous component matrix as described by equations A-16 and A-17 respectively, are shown here for the initial time interval and for the time interval immediately preceding the terminal time. For time $0 \leq t < 3$ seconds,

$$\underline{P}_o = \begin{bmatrix} 8.5665 & 0.1444 & -10.6871 & -56.0111 & 0.2888 & -0.0263 \\ -0.3059 & 0.5248 & -18.9996 & -65.1130 & -0.0303 & 0.0009 \\ 47.1494 & -18.9161 & 14761.6250 & 45993.6250 & 12.5613 & -0.1113 \\ 108.5043 & -66.4665 & 46219.8750 & 155543.2500 & 43.9428 & -0.2136 \\ 0.3171 & -0.0130 & 9.7914 & 36.2019 & 0.0338 & -0.0010 \\ -0.0782 & -0.0013 & 0.0586 & 0.2967 & -0.0030 & 0.0010 \end{bmatrix} \qquad \text{A-18}$$

$$\underline{K}_o = \begin{bmatrix} -90.9235 & -1.7603 & 183.6018 & 719.0338 & -3.2967 & 0.2919 \\ -0.0013 & 0.0062 & -13.0380 & -26.0862 & -0.0044 & -0.000014 \end{bmatrix} \quad \text{A-19}$$

$$\underline{f}_o(\delta \underline{w}_o) = \begin{bmatrix} 3469.7345 \\ -0.1430 \end{bmatrix} \quad \text{A-20}$$

For time $1180 \leq t < T = 1183$ seconds,

$$\underline{P}_{T-1} = \begin{bmatrix} 1.8670 & 0.0947 & -13.3580 & -59.6059 & 0.0422 & -0.0001 \\ 0.0355 & 0.5260 & -8.3979 & -35.3482 & -0.0143 & -0.0 \\ -12.4917 & -9.1209 & 3979.7030 & 12982.0940 & 4.4608 & -0.0015 \\ -57.2423 & -38.9512 & 13272.5780 & 54583.2500 & 19.7873 & 0.0078 \\ 0.0498 & -0.0113 & 3.9560 & 17.9359 & 0.0217 & 0.0 \\ -0.0004 & -0.0 & 0.0069 & 0.0297 & -0.0 & 0.0 \end{bmatrix} \quad \text{A-21}$$

$$\underline{K}_{T-1} = \begin{bmatrix} -13.7231 & -1.2326 & 147.1748 & 764.3848 & -0.4423 & 0.0010 \\ 0.0063 & 0.0112 & -13.9509 & -38.5792 & -0.0102 & -0.000009 \end{bmatrix} \quad \text{A-22}$$

$$\underline{f}_{T-1}(\delta \underline{w}_{T-1}) = \begin{bmatrix} 0.1502 \\ -0.0004 \end{bmatrix} \quad \text{A-23}$$

APPENDIX B

COMPUTER PROGRAMS

The functions of the computer programs used in this study are briefly described here for future researchers. All possible aircraft times of arrival at the IAF and the corresponding route-time profiles are computed by "ATA" and "RTP" respectively. These programs use the route-time profile generation strategy as described in Chapter II along with the aircraft velocity profile depicted in Figure 2-6. The times of arrival and route-time profiles computed are strictly applicable to the descent route depicted in Figure 2-1 for the aircraft's boundary conditions as shown in Figure 2-7.

The complete nonlinear aircraft model of the Boeing 707-320B is included in "NV". The basic structure of this program was created by Arye Ephrath for precision approach landings in zero-visibility conditions [23]. The program provides a real-time simulation of the nonlinear equations of motion as presented in Chapter III. The nominal values of the states and controls are recorded every 3 seconds and stored in data files by "NV" for any flight executed by the pilot in the cockpit simulator. These data files are used as inputs to "AB" where the linearized continuous-time system matrices are evaluated for each 3 second interval. These matrices are then stored in data files which are in turn used as inputs for "FGH" where the

discrete-time linear system matrices are computed and stored. Using the output data files from "FGH," the Riccati equation and driving function are solved in "RIC." Using the pre-programmed weighting matrices along with a specified wind as input, the optimal linear feedback solution is solved. The feedback gains and exogenous components to be used by the control regulator are stored on data files created by "RIC." These data files along with those containing the values of the nominal states and controls are used as input for "REG" where the linear feedback solution is implemented on the complete nonlinear aircraft model. The feedback gains and exogenous components are updated every 3 seconds. The aircraft is "flown" automatically in "REG" using the nominal control values combined with the control correction values determined by the feedback law as inputs to the nonlinear aerodynamic equations. Both "NV" and "REG" provide a real-time simulation of the aircraft's aerodynamics using the nonlinear equations of motion.

The remainder of this appendix contains the listings of the computer programs used in this study. For further explanation of the coding of the program, see reference [24]. In addition, an explanation of several of the computational subroutines called in "FGH" and "RIC" is provided in reference [25].

```
      PROGRAM ATA
C
C***  THIS PROGRAM COMPUTES ALL POSSIBLE TIMES OF ARRIVAL AT THE
C***  IAF USING A STANDARD DAY VELOCITY PROFILE FOR A BOEING 707-320B
C
      WRITE(10,100)
  100 FORMAT(3X,"IDV",3X,"TRANSITION",3X,"ACC35",3X,"ACC10",4X,"TIME",
     15X,"TIME",5X,"TIME",5X,"TIME")
      WRITE(10,200)
  200 FORMAT(10X,"ALTITUDE",20X,"AT WP1",3X,"AT WP2",3X,"AT WP3",3X,"AT
     1IAF",//)
      DELT=0.
      DELTT=0.
C
C***  INITIAL AND FINAL TRUE AIRSPEEDS ALONG DESCENT ROUTE PROFILE
C
      V0=476.
      VF=280.
C
C***  MAXIMUM AND MINIMUM TRUE AIRSPEEDS FOR THE ENTRY FIX,
C***  INITIAL APPROACH FIX, AND CRITICAL ALTIUDES
C
      VMAX35=496.
      VMAX25=517.
      VMAX10=415.5
      VMIN35=346.
      VMIN10=228.5
C
C***  HORIZONTAL RANGE DISTANCES BETWEEN WAYPOINTS ALONG DESCENT ROUTE
C
      D1=31.78
      D2=31.45
      D3=47.17
      D4=15.
C
C***  DELV1 = VMAX35 - INITIAL DESCENT VELOCITY(IDV)
C***  H2 = TRANSITION ALTITUDE
C
      DELV1=0.
      H2=25000.
  203 CONTINUE
      T1=(D1/((V0+VMAX35-DELV1)/2.))*60.
      A=0.
      T2=0.
      DD=0.
      VA=VMAX35-DELV1
      VB=VA
```

ORIGINAL PAGE IS
OF POOR QUALITY

```
      T=.001
      H=35000.
      RMACH=VA/(661.-(.002434*H))
60    D=.5*A*T*T+VA*T
      H=H-318.*D
      VA=VB
      VB=RMACH*(661.-(.002434*H))
      A=(VB-VA)/T
      T2=T2+(T*60.)
      DD=DD+D
      IF(H-H2)61,61,60
61    A=0.
      T3=0.
      DD=0.
      VA=VB
      VB=VA
      RIAS=(656.-(.0091*H2))*RMACH
62    D=.5*A*T*T+VA*T
      H=H-318.*D
      VA=VB
      VB=RIAS*(661.-(.002434*H))/(656.-(.0091*H))
      A=(VB-VA)/T
      T3=T3+(T*60.)
      DD=DD+D
      IF(H-10000.)63,63,62
63    CONTINUE
      T4=(D4/((VF+VB)/2.))*60.
      ATA=(T1+T2+T3+T4)
      ACC=((VMAX35-DELV1)*(VMAX35-DELV1)-V0*V0)/(2.*D1)
      DEC=(VF*VF-VB*VB)/(2.*D4)
      ACCA=ACC*6080./(3600.*3600.)
      DECE=DEC*6080./(3600.*3600.)
      TT22=T1+T2
      TT33=T1+T2+T3
      RIDV=VMAX35-DELV1
      WRITE(10,21)RIDV,H2,ACCA,DECE,T1,TT22,TT33,ATA
      IF(DELV1-150.)24,201,24
24    DELV1=DELV1+5.
      GO TO 203
201   IF(H2-35000.)202,20,202
202   H2=H2+1000.
      GO TO 203
21    FORMAT(1X,F6.1,F10.1,2X,2F8.3,4F9.3)
20    CONTINUE
      CALL EXIT
      END
```

ORIGINAL PAGE IS
OF POOR QUALITY

```
      PROGRAM RTP
C
C***  THIS PROGRAM COMPUTES THE ROUTE-TIME PROFILE FOR A
C***  PARTICULAR ATA AS COMPUTED IN THE PROGRAM "ATA"
C
C***  THE PROGRAMMED INPUTS ARE: RIDV = IDV
C***                             H2 = TRANSITION ALTITUDE
C***  T1 = TIME AT WP1; T2 = TIME AT WP2; T3 = TIME AT WP3
C***  ATA = ASSIGNED TIME OF ARRIVAL AT IAF
C
      RIDV=396.
      DELV1=496.-RIDV
      H2=25000.
      T1=4.373/60.
      T2=(9.053/60.)-T1
      T3=(16.793/60.)-T1-T2
      ATA=19.736
C
C***  INITIAL AND FINAL TRUE AIRSPEEDS ALONG DESCENT ROUTE PROFILE
C
      V0=476.
      VF=280.
C
C***  MAXIMUM AND MINIMUM TRUE AIRSPEEDS FOR ENTRY FIX,
C***  INITIAL APPROACH FIX, AND CRITICAL ALTITUDES
C
      VMAX35=496.
      VMAX25=517.
      VMAX10=415.5
      VMIN35=346.
      VMIN10=228.5
      TTT=0.
      H0=35000.
      HH=H0
      HF=10000.
C
C***  HORIZONTAL RANGE DISTANCES BETWEEN WAYPOINTS ALONG DESCENT ROUTE
C
      D1=31.78
      D2=31.45
      D3=47.17
      D4=15.
      WRITE(10,100)
  100 FORMAT(2X,"TIME",4X,"ALTITUDE",5X,"RANGE",6X,"TAS",7X,"IAS",6X,
     1"MACH",6X,"DH/DT",//)
      FLAG1=0.
      FLAG2=0.
      FLAG3=0.
      FLAG4=0.
      T=0.
   16 CONTINUE
```

```
      ACC=((VMAX35-DELV1)*(VMAX35-DELV1)-V0*V0)/(2.*D1)
      IF(T-T1)2,2,3
2     V=ACC*T+V0
      D=ACC*T*T/2.+V0*T
      H=H0
      GO TO 10
3     CONTINUE
5     IF(T-T1-T2)6,6,7
6     IF(FLAG3)95,96,95
96    IF(FLAG1-1.)66,68,66
66    FLAG1=1.
      J=0.
      RA=0.
      RT2=0.
      RDD=0.
      VA=VMAX35-DELV1
      VB=VA
      RH=35000.
      RMACH=VA/(661.-(.002434*RH))
      RT=.001
68    CONTINUE
40    IF(J-10)80,10,80
80    J=J+1
      RD=.5*RA*RT*RT+VA*RT
      RH=RH-318.*RD
      VA=VB
      VB=RMACH*(661.-(.002434*RH))
      RA=(VB-VA)/RT
      RT2=RT2+RT
      RDD=RDD+RD
      T=T1+RT2
      H=RH
      D=D1+RDD
      V=VA
      IF(RH-H2)41,41,40
7     CONTINUE
102   CONTINUE
95    CONTINUE
41    IF(FLAG4)97,98,97
98    IF(FLAG2)90,91,90
91    FLAG2=1.
      FLAG3=1.
      K=0.
      RA=0.
      RT3=0.
      RDD=0.
      VA=VB
      VB=VA
      RH=H2
      RIAS=(656.-(.0091*H2))*RMACH
```

ORIGINAL PAGE IS
OF POOR QUALITY

```
90  CONTINUE
42  IF(K-10)92,10,92
92  K=K+1
    RD=.5*RA*RT*RT+VA*RT
    RH=RH-318.*RD
    VA=VB
    VB=RIAS*(661.-(.002434*RH))/(656.-(.0091*RH))
    RA=(VB-VA)/RT
    RT3=RT3+RT
    RDD=RDD+RD
    T=T1+T2+RT3
    H=RH
    D=D1+D2+RDD
    V=VA
    IF(RH-10000.)43,43,42
101 CONTINUE
43  CONTINUE
    FLAG4=1.
97  CONTINUE
9   CONTINUE
11  DEC=(VF*VF-VB*VB)/(2.*D4)
    V=DEC*(T-T1-T2-T3)+VB
    D=DEC*(T-T1-T2-T3)*(T-T1-T2-T3)/2.+VB*(T-T1-T2-T3)+D1+D2+D3
    H=HF
    IF(D-125.4)202,14,14
202 CONTINUE
    GO TO 10
10  TT=T*60.
    DH=(H-HH)/(TT-TTT)
    TTT=TT
    HH=H
    R=125.4-D
    RRMACH=V/(661.-(.002434*H))
    RRIAS=(656.-(.0091*H))*RRMACH
    WRITE(10,15)TT,H,R,V,RRIAS,RRMACH,DH
15  FORMAT(1X,F5.2,2X,4F10.2,F9.3,F12.2)
    T=T+.01
    J=0.
    K=0.
    GO TO 16
14  CONTINUE
    TT=ATA
    H=HF
    R=0.
    V=VF
    RIAS=250.
    RMACH=.44
    DH=0.
    WRITE(10,15)TT,H,R,V,RIAS,RMACH,DH
    CALL EXIT
    END
```

```
      PROGRAM NV
C
C***  THIS PROGRAM INCLUDES THE COMPLETE NONLINEAR AERODYNAMICS
C***  FOR THE BOEING 707-320B AIRCRAFT MODEL
C
C***  THE NOMINAL VALUES OF CERTAIN AIRCRAFT STATES AND CONTROLS
C***  ARE RECORDED AND STORED IN DATA FILES AND ATEXT FILES
C***  FOR ANY FLIGHT EXECUTED BY THE PILOT IN THE COCKPIT SIMULATOR
C
C***  FUNCTION SWITCH 3 STORES LAST SET OF NOMINAL VALUES AFTER STOP
C***  FUNCTION SWITCH 4 RESETS INITIAL CONDITIONS
C***  FUNCTION SWITCH 8 STARTS PROGRAM
C***  FUNCTION SWITCH 12 STOPS PROGRAM
C***  FUNCTION SWITCH 16 DISPLAYS FLIGHT CONDITIONS AND PARAMETERS AT
C***  TERMINAL TIME OR AT STOPACTION
C
      GLOBAL ITIME,NF
      IMPLICIT FRACTION (F)
      LOGICAL CONE
      REAL FLAPS
L       OTSERRORS=SHORT
      DIMENSION IBUFF(208)
      COMMON/RELAX/SCORD,SSPAN,SAREA,P,Q,ROW,RMACH,DPP,DQQ,DRR,SPALF
      COMMON/WORK/UVEL,VVEL,WVEL,VTOT,UDTT,VDTT,WDTT,VTOD
      COMMON/EXTRA/DDFIE,DDTET,DDSY,RFIE,RTET,RSY,STTET,CTTET,SFIE,CFIE
      COMMON/MORE/SSY,CSY
      COMMON/CNTRL/T,FLAPS,CTETA,CPHI,CXI,GEAR,SPBRK,TPOS
      COMMON/CNTRL/BTETA,BPHI,BXI
      COMMON/PRMTR/V,XI,BETAG,DT
      COMMON/PRMTR/ALPHA,BETA,PHI,VX,VY,VZ,THETA,A,XM,Y,R,RIAS
      COMMON/FRAC/FV,FBNK,FPICH,FA,FVZ,FHDG,FADF,FVOR,FCPICH
      COMMON/FRAC/FER,FHER,DME(6),ALT(7)
      COMMON/FD/ADF,VOR,EPS,HER,RAD
      COMMON/OUT/UU(100),WW(100),QQ(100),TEET(100),HH(100),RANGE(100)
      COMMON/OUT/TP(100),EE(100),XX(70),YY(70),HHH(70),TOTXX,LOC1,LOC2,
     1TOTT(100),TH(100),DIST
      DATA TMRKR1/0.4815/,TMRKR2/0.068/,TMRKR/0.0076/
      DATA TNGSA/-0.052933/,RAD/57.296/
      DATA SCORD/34148./,SSPAN/219354./,SAREA/1505./
      ENTRY NF
1     CONTINUE
C
C***  INITIALIZE ALL VALUES
C
      CTIM=210.
      TOTXX=0.
      LOC1=0
      LOC2=0
      SPALF=0.
      DDFIE=0.
      DDTET=0.
      DDSY=0.
```

ORIGINAL PAGE IS
OF POOR QUALITY

```
      RFIE=0.
      RTET=.84/RAD
      RSY=53.07/RAD
      STTET=SIN(.015)
      CTTET=COS(.015)
      SFIE=0.
      CFIE=1.
      SSY=.79937
      CSY=.600839
      XI=53.07
      PHI=0.
      FBNK=0.0F
      ALPHA=2.84
      BETAG=0.
      BETA=0.
      DRNG=2550.
      IOM=IMM=IIM=0
      JJFF=0
      XM=-150.26
      Y=-239497.19
      VOR=53.07
      ADF=49.69
      V=476.
      VTOT=804.
      VTOD=0.
      UVEL=VTOT
      VVEL=0.
      WVEL=11.0
      UDTT=0.
      VDTT=0.
      WDTT=0.
      VX=764.65
      VY=243.45
      VZ=0.
      P=0.
      Q=0.
      R=0.
      DPP=0.
      DQQ=0.
      DRR=0.
      THETA=ALPHA-2.
      DIST=SQRT((XM+31.0826)**2+(Y/6080.2+.50366)**2)
      A=35000.
      IALT1=3
      IALT2=5
      IALT3=0
      IALT4=0
      IALT5=0
      LABEL(ALT)
      ZSET(0.0F)
      MOVE(.61F,.39F)
      WRITE(16,9011)IALT1,IALT2,IALT3,IALT4,IALT5
9011  FORMAT(2I1,"$S",1X,3I1)
      ENDLIST
```

```
      LABEL(DME)
      ZSET(0.F)
      MOVE(-0.34F,-0.01434F)
      WRITE(16,555)DIST
      ENDLIST
      XFEET=XM*6080.2
      EPS=ATAN((Y+3062.35)/((XM+31.0816)*6080.2))
      HER=A-XFEET*(-0.052933)
      BTETA=BPHI=BXI=0.
      CALL SAMPLE
      BTETA=CTETA+2.1
      BPHI=CPHI
      BXI=CXI
      CALL RTOF
C
C***  START THE DISPLAY
C
A           JPSR $GRAFX
A                $DIALS
A                5
C
C***  INITIALIZE DATA-UPDATE CLOCK
C
    2 ITIME=1
C
C***  ENTER WAIT LOOP IF SWITCH 8 (START) IS NOT ON
C
      IF(.NOT.SWITCH(8))GO TO 2
C
C***  EXECUTE UNLESS SWITCH 12 (FREEZE) IS ON
C
    6 IF(TOTXX-CTIM)851,852,852
  852 OPEN(21,0,2,0IBUFF,'VALUE1')
C
C***  STORES RECORDED NOMINAL VALUES IN DATA AND ATEXT FILES
C
      WRITE(21)LOC1,(UU(I),WW(I),QQ(I),TEET(I),HH(I),RANGE(I),TH(I),
     1TP(I),EE(I),TOTT(I),I=1,LOC1)
      CLOSE(21)
      OPEN(20,0,2,0IBUFF,'ATEXT1')
      WRITE(20,2020)LOC1,(UU(I),WW(I),QQ(I),TEET(I),HH(I),RANGE(I),
     1TH(I),TP(I),EE(I),TOTT(I),I=1,LOC1)
 2020 FORMAT(1X,I4,/,170(1X,F6.1,F5.1,F8.4,F8.4,F7.0,F7.2,F8.1,F7.3,
     1F8.3,F8.2,/))
      CLOSE(20)
```

```
C
C***  STORE RECORDED PATH VALUES IN DATA AND ATEXT FILES
C
      OPEN(21,0,2,$IBUFF,'PATH1')
      WRITE(21)LOC2,(XX(I),YY(I),HHH(I),I=1,LOC2)
      CLOSE(21)
      OPEN(20,0,2,$IBUFF,'ATEXT2')
      WRITE(20,2121)LOC2,(XX(I),YY(I),HHH(I),I=1,LOC2)
 2121 FORMAT(1X,I4,/,70(1X,2F12.2,F10.0,/))
      CLOSE(20)
      LOC1=0
      LOC2=0
      CTIM=CTIM+210.
      ITIME=1
 851  CONTINUE
C
C***  AFTER SWITCH 3 HAS BEEN PRESSED, PRESENTLY RECORDED NOMINAL
C***  VALUES AND PATH VALUES ARE STORED
C
      IF(SWITCH(3))GO TO 852
      IF(.NOT.SWITCH(12))GO TO 3
C
C***  AFTER SWITCH 12 HAS BEEN PRESSED, EXIT IF SWITCH 16 IS ON...
C
    7 IF(SWITCH(16))GO TO 4
C
C***  OR INITIALIZE VALUES IF SWITCH 4 (IC) IS ON...
C
      IF(SWITCH(4))GO TO 5
C
C***  OR START EXECUTION AGAIN IF SWITCH 8 IS ON...
C
      IF(SWITCH(8))GO TO 6
C
C***  OR INITIALIZE DATA-UPDATE CLOCK AND ENTER A WAITING LOOP
C
      ITIME=1
      GO TO 7
    5 CONTINUE
C
C***  STOP THE DISPLAY AND GO BACK TO INITIAL VALUES
C
A   JPSR $NHALT
A   NOOP
      GO TO 1
```

```
C
C***  START EXECUTION OF A NEW DATA-UPDATE CYCLE:
C***  COMPUTE DT (=TIME IN SECS OF PREVIOUS CYCLE)
C***  AND INITIALIZE DATA-UPDATE CLOCK
C
    3 TIME=ITIME
      ITIME=0
      DT=TIME/120.
      CALL DYNNF
      XFEET=XM*6080.2
      IF(XFEET.EQ.0.)XFEET=1.
      YMILE=Y/6080.2
      HER=A-XFEET*TNGSA
      IF(XM.EQ.-31.0826)XM=-31.0827
      EPS=ATAN((YMILE+.50366)/(31.0826+XM))
      IF(XM.EQ.-5.4896)XM=-5.4895
C
C***  VOR, ADF AND DME INFORMATION
C
      ADF=35.-ATAN(YMILE/(-XM-5.4896))*RAD
      IF(XM.GT.-5.4896)ADF=ADF+180.
      IF(XM.EQ.-31.0826)XM=-31.0816
      VOR=35.-ATAN((YMILE+.50366)/(-31.0826-XM))*RAD
      IF(XM.GT.-31.0826)VOR=VOR+180.
      ADF=AMOD(ADF,360.)
      VOR=AMOD(VOR,360.)
      CALL RTOF
      DIST=SQRT((XM+31.0826)**2+(YMILE+.50366)**2)
      LABEL(DME)
      ZSET(0.0F)
      MOVE(-0.34F,-0.01434F)
      WRITE(16,555)DIST
555   FORMAT("$",F5.1)
      ENDLIST
      RALT=A/10000.
      IALT1=RALT
      RALT=10.*(RALT-IALT1)
      IALT2=RALT
      RALT=10.*(RALT-IALT2)
      IALT3=RALT
      RALT=10.*(RALT-IALT3)
      IALT4=RALT
      RALT=10.*(RALT-IALT4)
      IALT5=RALT
      LABEL(ALT)
      ZSET(0.0F)
      MOVE(.61F,.39F)
      WRITE(16,9012)IALT1,IALT2,IALT3,IALT4,IALT5
9012  FORMAT(2I1,"$",1X,3I1)
      ENDLIST
```

ORIGINAL PAGE IS
OF POOR QUALITY

```
      CONE=.FALSE.
      IOM=IMM=IIM=0
      IF(EPS.LE.0.05.AND.EPS.GT.-0.05)CONE=.TRUE.
C
C***  TURN OUTER MARKER LIGHT ON
C
      IF(ABS(XM+5.4896).LE.TMRKR1.AND.CONE)IOM=1
C
C***  TURN MIDDLE MARKER LIGHT ON
C
      IF(ABS(XM+0.7896).LE.TMRKR2.AND.CONE)IMM=1
C
C***  TURN INNER MARKER LIGHT ON
C
      IF(ABS(XM+0.1896).LE.TMRKR.AND.   CONE )IIM=1
      CALL BEACONS(IOM,IMM,IIM,JJFF)
C
C***  EXIT IF ALTITUDE=0
C
      IF(A)4,4,6
    4 CONTINUE
C
C***  STOP THE DISPLAY, TURN ALL LIGHTS OFF
C
A        JPSR $NHALT
      XFF=XM*6080.2+1153.
      KDT=1./DT
C
C***  SHOW PARAMETERS AT TERMINAL TIME OR AT STOPACTION ON CRT SCREEN
C
      WRITE(25,2000)
      WRITE(25,2001)TOTXX,RIAS,XI
      WRITE(25,2002)VZ
      WRITE(25,2003)UVEL,WVEL,Q,THETA,A,DIST,TPOS,T,CTETA
2000  FORMAT(/////27X,"PARAMETERS AT TERMINAL TIME OR AT STOPACTION"//)
2001  FORMAT(27X,"TOTAL FLIGHT TIME       ",F15.0," SEC."/
     1        27X,"INDICATED AIRSPEED       ",3X,F7.1," KNOTS"/
     2        27X,"HEADING                  ",10X,F5.1," DEG.")
2002  FORMAT(27X,"VERTICAL SPEED           ",F15.1," FPM")
2003  FORMAT( /27X,"FORWARD VELOCITY U     ",10X,F7.1," FT./SEC."/
     1          27X,"DOWNWARD VELOCITY W   ",10X,F7.1," FT./SEC."/
     2          27X,"PITCH RATE            ",13X,F7.4," RAD./SEC."/
     4          27X,"PITCH ANGLE           ",13X,F7.4," DEG."/
     5          27X,"ALTITUDE              ",10X,F6.0," FT."/
     6          27X,"RANGE                 ",11X,F6.1," NAUT. MI."/
     727X,"THROTTLE POSITION     ",14X,F6.4,/,27X,"THRUST",25X,F8.1,
     8" LBS.",/,27X,"ELEVATOR POSITION     ",13X,F5.2," DEG.")
      EXIT
      END
```

```
      SUBROUTINE SAMPLE
C
C***  SUBROUTINE TO SAMPLE COCKPIT CONTROLS
C
      GLOBAL SPBRK,FLAPS,THRUST
      IMPLICIT FRACTION(F)
      REAL FLAPS
      COMMON/RELAX/SCORD,SSPAN,SAREA,P,Q,ROW,RMACH,DPP,DQQ,DRR,SPALF
      COMMON/PRMTR/V,XI,BETAG,DT
      COMMON/PRMTR/ALPHA,BETA,PHI,VX,VY,VZ,THETA,A,XM,Y,R,RIAS
      COMMON/CNTRL/T,FLAPS,CTETA,CPHI,CXI,GEAR,SPBRK,TPOS
      COMMON/CNTRL/BTETA,BPHI,BXI
A           ADEPT
            FPRI
            MD07'F 0
            0;0;0
            MD07'F 10
            0;0
            S5MD FSPBRK
            MD07'F 20
            0;0
            S5MD FT1
            MD07'F 40
            0;0
            S5MD FT2
            MD07'F 100
            0;0
            S5MD FT3
            MD07'F 200
            0;0
            S5MD FT4
            MD07'F 0
            0;0;0
            MD07'H C1
            0;0;0
            MD07'L; 1!H1
            0;0
            S5MD FFLAPS
            MD07'L; 1!H2
            0;0
            S5MD FYOKE
            MD07'L; 1!H4
            0;0
            S5MD FWHEEL
            MD07'L; 1!H10
            0;0
            S5MD FPEDL
            MD07'H C1
            0;0;0
            UPRI
```

```
            MDAR MASK
            S6AR'A'F
            ARAR'H'F
            JPLS DOWN
            MDAR ZERO
            ARMD FGEAR
            JUMP BACK
DOWN:       MDAR ONE
            ARMD FGEAR
            JUMP BACK
MASK:       00100!H0
ZERO:       0!H0
ONE:        0!H37777
FGEAR:      0
FSPBRK:     0
FT1:        0
FT2:        0
FT3:        0
FT4:        0
C1:         0!H00001
FFLAPS:     0
FYOKE:      0
FWHEEL:     0
FPEDL:      0
BACK:       NOOP
MASKUP:10000
MASKDN:04000
      MDAR MASKUP
            S6AR'A'F
            JPLS SWUP
            MDAR MASKDN
            S6AR'A'F
            JPLS SWDN
            JUMP SWEN
SWUP: NOOP
FORTRAN
      BTETA=BTETA+.05
A         ADEPT
      JUMP SWEN
SWDN: NOOP
FORTRAN
      BTETA=BTETA-.05
A         ADEPT
SWEN: NOOP
```

```
FORTRAN
C
C***  MACH NUMBER
C
      IF(A-36089.)9004,9004,9005
9004  RMACH=V/(661.-(.002434*A))
      GO TO 9006
9005  RMACH=V/573.
9006  CONTINUE
C
C***  INDICATED AIRSPEED IN KNOTS
C
      RIAS=(656.-(.0091*A))*RMACH
      SPBRK=FTOR(FSPBRK)*187.5
      IF(RIAS-189.)9007,9007,9008
9008  SPMAX=60.-(.283*(RIAS-189.))
      SPBRK=AMIN1(SPBRK,SPMAX)
9007  CONTINUE
      FLAPS=AMAX2(0.0F,FFLAPS)*128.315
      IF(FLAPS-SPALF)9001,9002,9003
9001  FLAPS=SPALF-.4175
      GO TO 9002
9003  FLAPS=SPALF+.4175
9002  SPALF=FLAPS
      CTETA=(-FTOR(FYOKE)*18.75-BTETA)*2.0
      CPHI=(-FTOR(FWHEEL)*42.5-BPHI/1.85)*1.85
      CXI=(FTOR(FPEDL)*20.5-BXI/2.65)*2.65
C
C***  THRUST COMPUTATIONS
C
      THRUST=FTOR(FT1+FT2)+FTOR(FT3+FT4)
      TPOS=(THRUST-.3727)/1.1761
      TPOS=AMAX1(TPOS,0.)
      TPOS=AMIN1(1.0,TPOS)
      IF(A-10000.)820,821,821
820   RMAXT=13800.-.28125*A+(.3117*A-7800.)*RMACH
      RIDLT=1000.-2000.*RMACH
      GO TO 822
821   RMAXT=13800.-.28125*A
     1+(.12*(A-10000.)-3125.)*RMACH
      RIDLT=1000.+(.05*(A-10000.)-2000.)*RMACH
822   RIDLT=AMAX1(RIDLT,0.)
      T=(RIDLT+(RMAXT-RIDLT)*TPOS*TPOS)*4.
206   GEAR=FTOR(FGEAR)
      RETURN
      END
```

ORIGINAL PAGE IS
OF POOR QUALITY

```
      SUBROUTINE BEACONS(IOM,IMM,IIM,JJFF)
C
C***  SUBROUTINE TO OPERATE MARKER-BEACONS' LIGHTS
C
      IF(IOM.OR.IMM.OR.IIM)9,10
9     CONTINUE
      JJFF=JJFF+1
      GO TO (8,8,6,10),JJFF
8     CONTINUE
      IF(IOM)1,4
 4    IF(IMM)2,5
5     IF(IIM)3,6
C
C***  NONE OF THE LIGHTS SHOULD BE ON:
C***  TURN THEM ALL OFF
C
10    JJFF=0
6     CONTINUE
A     ADEPT
      MDAR BCN
      ARIC'A'F
      JUMP .+2
BCN:77277!H57777
      NOOP
FORTRAN
      GO TO 7
1     CONTINUE
A     MDAR OUTER
A     ARIC'O
      GO TO 7
2     CONTINUE
A     MDAR MIDLE
A     ARIC'O
      GO TO 7
3     CONTINUE
A     MDAR INNER
A     ARIC'O
      GO TO 7
A     ADEPT
OUTER:20000
MIDLE:00400!H
INNER:00100!H
FORTRAN
7     CONTINUE
      RETURN
      END
```

```
      SUBROUTINE DYNNF
C
C***  DYNAMICS-COMPUTING SUBROUTINE
C
      GLOBAL DVZ,DT,MP,APP,DP,DQ,DR,P,Q,R
      GLOBAL CXI,CPHI,CTETA,ALPHA,BETA
      GLOBAL UVEL,VVEL,WVEL,RVX,RVY,RVZ,UDOT,WDOT,VDOT,VTOT
      GLOBAL THETA,PHI,XI,L,D,SFOR
      GLOBAL LLL,MMM,NNN,RFIE,RTET,RSY,V,RX,RY,RZ
      REAL L,FLAPS,LLL,MMM,NNN
      COMMON/RELAX/SCORD,SSPAN,SAREA,P,Q,ROW,RMACH,DPP,DQQ,DRR,SPALF
      COMMON/WORK/UVEL,VVEL,WVEL,VTOT,UDTT,VDTT,WDTT,VTOD
      COMMON/EXTRA/DDFIE,DDTET,DDSY,RFIE,RTET,RSY,STTET,CTTET,SFIE,CFIE
      COMMON/MORE/SSY,CSY
      COMMON/CNTRL/T,FLAPS,CTETA,CPHI,CXI,GEAR,SPBRK,TPOS
      COMMON/CNTRL/BTETA,BPHI,BXI
      COMMON/PRMTR/V,XI,BETAG,DT
      COMMON/PRMTR/ALPHA,BETA,PHI,VX,VY,VZ,THETA,A,XM,Y,R,RIAS
      COMMON/FD/ADF,VOR,EPS,HER,RAD
      COMMON/OUT/UU(100),WW(100),QQ(100),TEET(100),HH(100),RANGE(100)
      COMMON/OUT/TP(100),EE(100),XX(70),YY(70),HHH(70),TOTXX,LOC1,LOC2,
     1TOTT(100),TH(100),DIST
      CALL SAMPLE
      V2=VTOT*VTOT
C
C***  ATMOSPHERIC DENSITY
C
      ROW=.2378E-2+(A*((A/(1.806E12))-(.66584E-7)))
      RLPAS=FLAPS-6.
      RLAPS=RLPAS-8.
      RLPAA=AMAX1(RLPAS,0.)
      RLAPP=AMAX1(RLAPS,0.)
      RDFP=AMIN1(RLPAA,1.0)
      CLT=((4.584+RMACH*(5.387*RMACH-2.22)+(1.081)*RDFP)*((WVEL/VTOT)+
     1.0331))-.0055*CTETA+RLPAA*.01432
C
C***  LIFT
C
      L=ROW*V2*SAREA*CLT
      IF(RMACH-.845)811,811,812
811   IF(RMACH-.8)813,813,814
813   IF(RMACH-.7)815,815,816
815   CDM=.012
      GO TO 818
812   CDM=-.1089+.1455*RMACH
      RK=-.6411+.8333*RMACH
      GO TO 819
814   CDM=-.01735+.0371*RMACH
      RK=-.13608+.2356*RMACH
      GO TO 819
816   CDM=.0097+.0033*RMACH
818   RK=.0524
819   CONTINUE
```

```
C
C***  DRAG
C
      D=ROW*V2*SAREA*(CDM+RK*(CLT*CLT)+.0105*GEAR+RLPAA*.0018+.833E-3*
     1SPBRK)
C
C***  SIDE FORCE
C
      SFOR=ROW*1505.*VTOT*(-.917*VVEL-.004*VTOT*CXI)
      DFIE=P+(SFIE*STTET/CTTET)*Q+(CFIE*STTET/CTTET)*R
      DTET=CFIE*Q-SFIE*R
      DSY=(SFIE/CTTET)*Q+CFIE*R/CTTET
      RFIE=RFIE+((3.*DFIE-DDFIE)*DT/2.)
      RTET=RTET+((3.*DTET-DDTET)*DT/2.)
      RSY=RSY+((3.*DSY-DDSY)*DT/2.)
      DDFIE=DFIE
      DDTET=DTET
      DDSY=DSY
C
C***  EULER ANGLES
C
      PHI=RFIE*RAD
      THETA=RTET*RAD
      XI=RSY*RAD
      STTET=SIN(RTET)
      CTTET=COS(RTET)
      SFIE=SIN(RFIE)
      CFIE=COS(RFIE)
      SSY=SIN(RSY)
      CSY=COS(RSY)
C
C***  ROLLING, PITCHING, AND YAWING MOMENTS
C
      LLL=ROW*VTOT*(VTOT*SSPAN*(-.1719*VVEL/VTOT+.00113*CPHI-.0002*CXI)
     1-(.60745E7*P))
      MMM=ROW*VTOT*(VTOT*SCORD*(.048-(.955*WVEL/VTOT)+.009*CTETA+
     1RLAPP*(-.0033))-(.128E8*Q))
      NNN=ROW*VTOT*(VTOT*SSPAN*(.115*VVEL/VTOT+.0011*CXI)-(.23978E7*R))
      DP=(((LLL/.382E7))-R*Q*(.856)+P*Q*(.0974))
      DQ=(((MMM/.485E7))+P*R*(.336)-((P*P)-(R*R))*(.0767))
      DR=(((NNN/.812E7))-P*Q*(.127)-R*Q*(.0458))
C
C***  ANGULAR VELOCITIES IN BODY AXES
C
      P=P+((3.*DP-DPP)*DT/2.)
      Q=Q+((3.*DQ-DQQ)*DT/2.)
      R=R+((3.*DR-DRR)*DT/2.)
      DPP=DP
      DQQ=DQ
      DRR=DR
```

```
C
C***  AERODYNAMIC ANGLES
C
      ALPHA=RAD*WVEL/VTOT
      BETA=RAD*VVEL/VTOT
      BETAG=BETA
      BET1=1.-((VVEL*VVEL)/(2.*VTOT*VTOT))
      CON1=-1/(6987.*VTOT)
      UDOT=(CON1*(UVEL*BET1*D+(UVEL*VVEL/VTOT)*SFOR-WVEL*L))-
     1(Q*WVEL-R*VVEL)-32.2*STTET+T/6987.
      VDOT=(CON1*(VVEL*D-VTOT*BET1*SFOR))-(R*UVEL-P*WVEL)+32.2*CTTET*
     1SFIE
      WDOT=(CON1*(WVEL*BET1*D+(WVEL*VVEL/VTOT)*SFOR+UVEL*L))-
     1(P*VVEL-Q*UVEL)+32.2*CTTET*CFIE
      VTOT=SQRT(UVEL*UVEL+VVEL*VVEL+WVEL*WVEL)
      Y=VTOT/1.69
C
C***  LINEAR VELOCITIES IN BODY AXES
C
      UVEL=UVEL+((3.*UDOT-UDTT)*DT/2.)
      VVEL=VVEL+((3.*VDOT-VDTT)*DT/2.)
      WVEL=WVEL+((3.*WDOT-WDTT)*DT/2.)
      UDTT=UDOT
      VDTT=VDOT
      WDTT=WDOT
C
C***  LINEAR VELOCITIES IN VEHICLE AXES
C
      RVX=CTTET*CSY*UVEL+(SFIE*STTET*CSY-CFIE*SSY)*VVEL+(SFIE*SSY+
     1CFIE*CSY*STTET)*WVEL
      RVY=CTTET*SSY*UVEL+(CFIE*CSY+SFIE*STTET*SSY)*VVEL+(CFIE*STTET*SSY
     1-SFIE*CSY)*WVEL
      RVZ=-STTET*UVEL+SFIE*CTTET*VVEL+CFIE*CTTET*WVEL
      VZ=-60.*RVZ
      VX=.5735*RVY+.81915*RVX
      VY=.81915*RVY-.5735*RVX
C
C***  EARTH COORDINATE SYSTEM POINTS
C
      XM=XM+(VX/6080.2)*DT
      Y=Y+VY*DT
      A=A+VZ*DT/60.
      XI=AMOD(XI,360.)
      PHI=AMOD(PHI,360.)
      THETA=AMOD(THETA,360.)
      A=AMAX1(A,0.)
```

ORIGINAL PAGE IS
OF POOR QUALITY

```
C
C***  RECORD NOMINAL VALUES OF STATES AND CONTROLS EVERY 3 SECONDS
C***  RECORD EARTH POSITION VALUES EVERY 5 SECONDS
C
      TOTXX=TOTXX+DT
      TINT=3.
      IF(AMOD(TOTXX,TINT).GT.DT)GO TO 101
      LOC1=LOC1+1
      UU(LOC1)=UVEL
      WW(LOC1)=WVEL
      QQ(LOC1)=Q
      TEET(LOC1)=RTET
      HH(LOC1)=A
      RANGE(LOC1)=DIST
      TH(LOC1)=T
      TP(LOC1)=TPOS
      EE(LOC1)=CTETA
      TOTT(LOC1)=TOTXX
 101  CONTINUE
      TINT=5.
      IF(AMOD(TOTXX,TINT).GT.DT)GO TO 102
      LOC2=LOC2+1
      XX(LOC2)=XM*6080.2
      YY(LOC2)=Y
      HHH(LOC2)=A
 102  CONTINUE
      RETURN
      END
```

```
      SUBROUTINE RTOF
C
C***  SUBROUTINE TO CONVERT DATA REAL-TO-FRACTION
C
      GLOBAL TRIG,FPICH1,FPCH1
      IMPLICIT FRACTION (F)
      COMMON/PRMTR/V,XI,BETAG,DT
      COMMON/PRMTR/ALPHA,BETA,PHI,VX,VY,VZ,THETA,A,XM,Y,R,RIAS
      COMMON/FRAC/FV,FBNK,FPICH,FA,FVZ,FHDG,FADF,FVOR,FCPICH
      COMMON/FRAC/FER,FHER,DME(6),ALT(7)
      COMMON/FD/ADF,VOR,EPS,HER,RAD
      FV=(200.-AMOD(RIAS,400.))/200.
      FBNK1=PHI/360.
      FBNK=FBNK1+FBNK1
      FPICH1=-THETA/360.
      FPICH=FPICH1+FPICH1
      IF(A.LT.0.)A=0.
      FA=(500.-AMOD(A,1000.))/500.
      FVZ=-FMIN1(1.,AMAX1(VZ/4000.,-1.))
      FHDG1=AMOD((XI-BETAG),360.)/360.
      FHDG=FHDG1+FHDG1
      FADF1=-ADF/360.
      FADF=FADF1+FADF1
      FVOR1=-VOR/360.
      FVOR=FVOR1+FVOR1
      ERR=EPS*RAD-18.07
      TEMPP=AMAX1(ERR,-5.0)
      ERR=AMIN1(5.0,TEMPP)
      FER=ERR*0.12
      IF(XM.EQ.0.)XM=0.0001
      AHER=HER*RAD/(XM*6080.2)
      TEMPP=AMAX1(AHER,-0.7)
      TEMP=AMIN1(0.7,TEMPP)
      FHER=TEMP*0.22857
      RETURN
      END
```

```
      IMAGE DIALS
C
C***  SUBROUTINE TO DISPLAY THE INSTRUMENT PANEL
C
      INTEGER $FTIMX
      IMPLICIT FRACTION(F)
      COMMON/FRAC/FV,FBNK,FPICH,FA,FVZ,FHDG,FADF,FVOR,FCPICH
      COMMON/FRAC/FER,FHER,DME(6),ALT(7)
      LINKAGE PTR(8),LYNE(4),PNTR(20)
      LINKAGE GSI(9),LOCI(5),ADFN(18),VORN(10),HDNG(5)
C
C***  ADD FTIMX TO ITIME. TO UPDATE THE DATA-UPDATE CLOCK
C
      $ITIME=$ITIME+$FTIMX
      POSCHAR(0.2417F,-0.01434F,-0.3F,"9S53")
      POSCHAR(DME)
      POSCHAR(ALT)
      LDY(0.F)
      TABLE2D(HDNG)
      LDX(-0.75F)
      LDY(0.49F)
      LSCL(0.275F)
      LRZ(FV)
      TABLE2D(PNTR)
      LDX(0.71F)
      LDY(0.52F)
      LSCL(0.28F)
      LRZ(FA)
      TABLE2D(PNTR)
      LDX(0.71826F)
      LDY(-0.20575F)
      LSCL(0.285F)
      LRZ(FVZ-0.5F)
      TABLE2D(PNTR)
      LDX(0.F)
      LDY(-0.323F)
      LSCL(0.33F)
      LRZ(FHDG)
      TABLE2D($CCARD)
      ROTZ(-0.100388F)
A            2DT BUG
      ROTZ(-0.19444F)
      DX(FER)
      TABLE2D(LYNE)
      LRZ(FHDG)
      LDX(-0.745F)
      LDY(-0.212F)
      LSCL(0.275F)
      ROTZ(FADF)
      TABLE2D(ADFN)
      ROTZ(FVOR-FADF)
      TABLE2D(VORN)
      LRZ(FHDG)
      TABLE2D($CCARD)
      LDX(0.F)
```

```
LDY(0.66F)
LSCL(0.32F)
LRZ(FBNK)
TABLE2D(PTR)
LSCL(1.0F)
ROTX(FPICH)
LAI(16B,1.0F)
LAI(17B,0.5F)
TABLE3D($HRZON)
RETURN
DATA2D(LYNE)
ZSET(0.0F)
LINE(0.F,0.43F,0.F,-0.5286F)
ENDLIST
ENDDATA
DATA2D(PNTR)
ZSET(0.0F)
MOVE(0.0F,-0.5F)
DRAW(-0.02F,-0.56F)
DRAW(-0.02F,-0.74F)
DRAW(0.0F,-0.8F)
DRAW(0.02F,-0.74F)
DRAW(0.02F,-0.56F)
DRAW(0.0F,-0.5F)
DRAW(0.0F,-0.26F)
DRAW(0.04F,-0.2F)
DRAW(0.04F,0.0F)
DRAW(0.06F,0.1F)
DRAW(-0.06F,0.1F)
DRAW(-0.04F,0.0F)
DRAW(-0.04F,-0.2F)
DRAW(0.0F,-0.26F)
MOVE(0.0F,0.0F)
DRAW(0.0F,0.0F)
ENDLIST
ENDDATA
DATA2D(GSI)
ZSET(0.0F)
MOVE(-0.3F,0.55F)
DRAW(-0.36F,0.59F)
DRAW(-0.3F,0.63F)
MOVE(-0.3F,-0.30F)
DRAW(-0.36F,-0.34F)<
DRAW(-0.3F,-0.38F)
ENDLIST
ENDDATA
DATA2D(LOCI)
ZSET(0.0F)
MOVE(-0.04F,0.16F)
DRAW(0.0F,0.12F)
DRAW(0.04F,0.16F)
ENDLIST
ENDDATA
DATA2D(ADFN)
ZSET(0.0F)
```

```
      MOVE(-0.1F,0.5F)
      DRAW(-0.1F,-0.7F)
      DRAW(0.0F,-0.8F)
      DRAW(0.1F,-0.7F)
      DRAW(0.1F,0.5F)
      DRAW(-0 14F,0.5F)
      DRAW(0.0F,0.8F)
      DRAW(0.14F,0.5F)
      DRAW(0.1F,0.5F)
      MOVE(0.0F,0.9F)
      DRAW(0.0F,0.8F)
      MOVE(0.0F,0.0F)
      DRAW(0.0F,0.0F)
      MOVE(0.0F,-0.8F)
      DRAW(0.0F,-0.9F)
      ENDLIST
      ENDDATA
      DATA2D(VORN)
      ZSET(0.0F)
      MOVE(0.0F,0.8F)
      DRAW(-0.04F,0.6F)
      DRAW(-0.04F,-0.8F)
      DRAW(0.04F,-0.8F)
      DRAW(0.04F,0.6F)
      DRAW(0.0F,0.8F)
      MOVE(0.0F,0.9F)
      DRAW(0.0F,-0.9F)
      ENDLIST
      ENDDATA
A     ADEPT
BUG: 0
    1631224426;1631221261;1314423345;1631224427
    2000026743;1146211662;1146215461;0631414431
    0767613244;1146215461;6631462316;6314655465
    6000013054;6000013055;6000013055;7000005462
    7000005463;7000005463;1000072314;1000072315
    1000072315;2000064022;2000064023;1777764023
FORTRAN
      DATA2D(PTR)
      ZSET(0.F)
      MOVE(0.F,0.8333F)
      DRAW(-0.15F,0.6667F)
      DRAW(0.15F,0.6667F)
      DRAW(0.0F,0.8333F)
      ENDLIST
      ENDDATA
      DATA2D(HDNG)
      ZSET(0.0F)
      MOVE(-0.015F,0.03625F)
      DRAW(0.F,0.0025F)
      DRAW(0.015F,0.03625F)
      ENDLIST
      ENDDATA
      RETURN
      END
```

```
      PROGRAM AB
C
C***  THIS PROGRAM COMPUTES THE LINEARIZED EQUATIONS WHICH DESCRIBE THE
C***  CONTINUOUS-TIME A AND B MATRICES EVERY 3 SECONDS
C
C***  THE PROGRAM USES THE DATA FILES CONTAINING THE NOMINAL STATE
C***  AND CONTROL VALUES PRODUCED BY "NV" AS INPUT
C***  THE COMPUTED A AND B MATRICES ARE STORED IN DATA AND ATEXT FILES
C
      REAL L
      DIMENSION IBUFF(208),UU(100),WW(100),QQ(100),TEET(100),HH(100),
     1RANGE(100),TH(100),TP(100),EE(100),TOTT(100),A(100,6,6),
     2B(100,6,2)

      WRITE(10,100)
  100 FORMAT(1X,"ENTER 2-DIGIT NUMBER OF VALUE FILES IN OCTAL",/)
      READ(10,101)NUM
  101 FORMAT(O2)
      DO 4 J=1,NUM
      OPEN(21,0,2,$IBUFF,'VALUE1')
      REWIND 21
      IF(J-1)2,3,2
 2    DO 3 K=2,J
      SKIPFILE 21
 3    CONTINUE
      READ(21)LOC1,(UU(I),WW(I),QQ(I),TEET(I),HH(I),RANGE(I),TH(I),
     1TP(I),EE(I),TOTT(I),I=1,LOC1)
      CLOSE(21)
      DO 102 KL=1,50
 102  CONTINUE
      DO 1 I=1,LOC1
      UVEL=UU(I)
      WVEL=WW(I)
      Q=QQ(I)
      THETA=TEET(I)
      AA=HH(I)
      RANG=RANGE(I)
      THRUST=TH(I)
      TPOS=TP(I)
      CTETA=EE(I)
      VTOT=SQRT(UVEL*UVEL+WVEL*WVEL)
      V2=VTOT*VTOT
      ROW=.2373E-2+(AA*((AA/(1.806E12))-(.66584E-7)))
      RMACH=VTOT/(1.69*(661.-(.002434*AA)))
      CLMM=(4.584+RMACH*(5.387*RMACH-2.22))
      CLT=CLMM*((WVEL/VTOT+.0331)-.0055*CTETA
      L=ROW*V2*1505.*CLT
```

```
      IF(RMACH-.845)811,811,812
811   IF(RMACH-.8)813,813,814
813   IF(RMACH-.7)815,815,816
815   CDM=.012
      GO TO 818
812   CDM=-.1089+.1455*RMACH
      RK=-.6411+.8333*RMACH
      GO TO 819
814   CDM=-.01735+.0371*RMACH
      RK=-.13608+.2356*RMACH
      GO TO 819
816   CDM=.0097+.0033*RMACH
818   RK=.0524
819   CONTINUE
      CDCD=((WVEL/VTOT)+.0331)*((10.774/(1.69*(661.-.002434*AA)))-2.22/
     1VTOT)/(1.69*(661.-.002434*AA))
      D=ROW*V2*1505.*(CDM+RK*(CLT*CLT))
      DDDU=2.*UVEL*D/V2
      DDDW=2.*WVEL*D/V2
      DLDU=1505.*ROW*(-.0055*CTETA*2.*UVEL+(CLMM*UVEL*(.0662+(WVEL/VTOT
     1)))+V2*UVEL*CDCD)
      DLDW=1505.*ROW*(-.0055*CTETA*2.*WVEL+(CLMM*(VTOT+WVEL*(.0662+(
     1WVEL/VTOT))))+V2*WVEL*CDCD)
      DRDH=.002378*((2.*AA/65536)-1.835)/65536.
      DCLDH=1505.*ROW*V2*(.002434)*(.0331+(WVEL/VTOT))*(((10.774*V2)/(
     11.69*(661.-.002434*AA)))-2.22*VTOT)/(1.69*(661.-.002434*AA)*(661.
     2-.002434*AA))
      DTTD=((-2000.+.05*(AA-10000.))*(1.-TPOS*TPOS)+(-3125.+.12*(AA-
     110000.))*TPOS*TPOS)/(1.69*VTOT*(661.-.002434*AA))
      DTDU=4.*UVEL*DTTD
      DTDW=4.*WVEL*DTTD
      DTDH=4.*(VTOT+(1.-TPOS*TPOS)*(.05+((.002434)*(-2000.+.05*(AA-1000
     10.))/(661.-.002434*AA)))/(1.69*(661.-.002434*AA))+(-.28125+VTOT*(
     2.12+((.002434*(-3125.+.12*(AA-10000.))/(661.-.002434*AA))))/(1.69
     3*(661.-.002434*AA)))*TPOS*TPOS)
      RMMM=V2*(1505.)*(22.69)*(.048-.955*WVEL/VTOT+.009*CTETA)+752.5*
     1516.84*VTOT*(-32.7)*Q
      R1=(1505.)*ROW*22.69*(.048+.009*CTETA)
      R2=752.5*ROW*516.84*(-32.7)
      DMDU=2.*UVEL*R1+(UVEL*WVEL/VTOT)*(-.955)+R2*Q*UVEL/VTOT
      DMDW=2.*WVEL*R1+(VTOT+WVEL*WVEL/VTOT)*(-.955)+R2*Q*WVEL/VTOT
      DMDQ=VTOT*R2
```

```
 A(I,1,1)=(D*(((UVEL*UVEL/V2)-1.)/VTOT)-L*(WVEL*UVEL/(V2*VTOT))
1-(UVEL/VTOT)*DDDU+(WVEL/VTOT)*DLDU+DTDU)/6988.
 A(I,1,2)=(D*(UVEL*WVEL/(V2*VTOT))-(((WVEL*WVEL/V2)-1.)/VTOT)*L
1-(UVEL/VTOT)*DDDW+(WVEL/VTOT)*DLDW+DTDW)/6988.-Q
 A(I,1,3)=-WVEL
 A(I,1,4)=-32.2*COS(THETA)
 A(I,1,5)=((-(UVEL/VTOT)*D/ROW+(WVEL/(VTOT*ROW))*L)*DRDH
1+DTDH+(WVEL/VTOT)*DCLDH)/6988.
 A(I,1,6)=0.

 A(I,2,1)=((UVEL*WVEL/(V2*VTOT))*D+(((UVEL*UVEL/V2)-1.)/VTOT)*L
1-(WVEL/VTOT)*DDDU-(UVEL/VTOT)*DLDU)/6988.+Q
 A(I,2,2)=((((WVEL*WVEL/V2)-1.)/VTOT)*D+(UVEL*WVEL/(V2*VTOT))*L
1-(WVEL/VTOT)*DDDW-(UVEL/VTOT)*DLDW)/6988.
 A(I,2,3)=UVEL
 A(I,2,4)=-32.2*SIN(THETA)
 A(I,2,5)=((-(WVEL/VTOT)*D/ROW-(UVEL/VTOT)*L/ROW)*DRDH
1-(UVEL/VTOT)*DCLDH)/6988.
 A(I,2,6)=0.

 A(I,3,1)=DMDU/.485E7
 A(I,3,2)=DMDW/.485E7
 A(I,3,3)=DMDQ/.485E7
 A(I,3,4)=0.
 A(I,3,5)=(RMMM/(.485E7))*DRDH
 A(I,3,6)=0.

 A(I,4,1)=0.
 A(I,4,2)=0.
 A(I,4,3)=1.
 A(I,4,4)=0.
 A(I,4,5)=0.
 A(I,4,6)=0.

 A(I,5,1)=SIN(THETA)
 A(I,5,2)=-COS(THETA)
 A(I,5,3)=0.
 A(I,5,4)=UVEL*COS(THETA)+WVEL*SIN(THETA)
 A(I,5,5)=0.
 A(I,5,6)=0.

 A(I,6,1)=-COS(THETA)
 A(I,6,2)=-SIN(THETA)
 A(I,6,3)=0.
 A(I,6,4)=SIN(THETA)*UVEL-COS(THETA)*WVEL
 A(I,6,5)=0.
 A(I,6,6)=0.
```

ORIGINAL PAGE IS
OF POOR QUALITY

```
      B(I,1,1)=1./6988.
      B(I,2,1)=0.
      B(I,3,1)=0.
      B(I,4,1)=0.
      B(I,5,1)=0.
      B(I,6,1)=0.

      B(I,1,2)=WVEL*1505.*ROW*VTOT*(-.0055)/6988.
      B(I,2,2)=-UVEL*1505.*ROW*(-.0055)*VTOT/6988.
      B(I,3,2)=V2*ROW*1505.*22.69*.009/.485E7
      B(I,4,2)=0.
      B(I,5,2)=0.
      B(I,6,2)=0.

 1    CONTINUE
C
C***  THE A AND B MATRICES ARE STORED IN DATA AND ATEXT FILES
C
      OPEN(21,0,2,@IBUFF,'A-MATRIX')
      WRITE(21)LOC1,(((A(J1,J2,J3),J3=1,6),J2=1,6),J1=1,LOC1)
      CLOSE(21)
      OPEN(21,0,2,@IBUFF,'B-MATRIX')
      WRITE(21)LOC1,(((B(K1,K2,K3),K3=1,2),K2=1,6),K1=1,LOC1)
      CLOSE(21)
      OPEN(20,0,1,@IBUFF,'A-ATEXT')
      WRITE(20,2020)LOC1,(TOTT(J1),((A(J1,J2,J3),J3=1,6),J2=1,6),
     1J1=1,LOC1)
 2020 FORMAT(1X,I4,//,120(1X,F8.2,//,1X,6F12.5,/,5(1X,6F12.5,/),//))
      CLOSE(20)
      OPEN(20,0,1,@IBUFF,'B-ATEXT')
      WRITE(20,2121)LOC1,(TOTT(K1),((B(K1,K2,K3),K3=1,2),K2=1,6),
     1K1=1,LOC1)
 2121 FORMAT(1X,I4,//,120(1X,F8.2,12X,2F12.5,/,5(21X,2F12.5,/),//))
      CLOSE(20)
 4    CONTINUE
      EXIT
      END
```

```
      PROGRAM FGH
C
C***  THIS PROGRAM COMPUTES THE DISCRETE-TIME LINEAR SYSTEM F, G, AND H
C***  MATRICES USING THE DATA FILES CONTAINING THE A AND B MATRICES  AS
C***  INPUT; THE DISCRETE-TIME LINEAR SYSTEM MATRICES ARE STORED
C***  ON DATA AND ATEXT FILES
C
      DIMENSION GG(31,6,2),FF(31,6,6),HH(31,6,2)
      DIMENSION AA(73,6,6),BB(73,6,2),A(6,6),U(6,6),D(6,2),
     1X(6,6),Y(6,6),Z(6,6),EA(6,6),IBUFF(208),RE(6,6)
      COMMON/MAIN1/NDIM,DUM1(6,6)
      COMMON/INOU/KIN,KOUT
      NDIM=6
      KIN=10
      KOUT=10
      DO 200 J1=1,6
      DO 200 J2=1,2
  200 D(J1,J2)=0.
      D(5,1)=-1.
      D(6,2)=-1.
      WRITE(10,100)
  100 FORMAT(1X,"ENTER 2-DIGIT NUMBER OF A-B MATRIX PAIR FILES",/)
      READ(10,101)NUM
  101 FORMAT(O2)
      FLAG=0.
      DO 1 I=1,NUM
      LOC3=0
      KK=0
      II=I+I-1
      OPEN(21,0,2,@IBUFF,'A-MATRIX')
      REWIND 21
      IF (I-1)3,2,3
  3   DO 4 J=2,II
  4   SKIPFILE 21
  2   CONTINUE
      READ(21)LOC1,(((AA(J1,J2,J3),J3=1,6),J2=1,6),J1=1,LOC1)
      CLOSE(21)
      OPEN(21,0,2,@IBUFF,'B-MATRIX')
      REWIND 21
      DO 5 J=1,II
  5   SKIPFILE 21
      READ(21)LOC1,(((BB(K1,K2,K3),K3=1,2),K2=1,6),K1=1,LOC1)
      CLOSE(21)
```

```
      N=6
      T=3.0
      NR=6
      NC=6
      MT=0
      N1=6
      N2=6
      DO 6 K=1,LOC1
      KK=KK+1
      DO 8 L=1,6
      DO 8 LL=1,6
8     A(L,LL)=AA(K,L,LL)
      CALL MEXP(N,A,T,EA)
      DO 44 J1=1,6
      DO 44 J2=1,6
      IF(J1-J2)45,43,45
43    X(J1,J2)=1.
      RE(J1,J2)=3.
      GO TO 44
45    X(J1,J2)=0.
      RE(J1,J2)=0.
44    A(J1,J2)=AA(K,J1,J2)
      COEF=3.
      DO 46 KL=2,19
      FL=KL
      COEF=COEF*3./FL
      N3=6
      DO 48 J1=1,6
      DO 48 J2=1,6
48    Y(J1,J2)=A(J1,J2)
      CALL MMUL(X,Y,N1,N2,N3,Z)
      DO 16 J1=1,6
      DO 16 J2=1,6
      RE(J1,J2)=RE(J1,J2)+(Z(J1,J2)*COEF)
16    X(J1,J2)=Z(J1,J2)
46    CONTINUE
      DO 17 J1=1,6
      DO 17 K1=1,2
17    Y(J1,K1)=BB(K,J1,K1)
      DO 47 J1=1,6
      DO 47 J2=1,6
47    X(J1,J2)=RE(J1,J2)
      N3=2
      CALL MMUL(X,Y,N1,N2,N3,Z)
      DO 13 J1=1,6
      DO 13 J2=1,2
13    GG(KK,J1,J2)=Z(J1,J2)
      DO 66 L1=1,6
      DO 66 L2=1,6
66    FF(KK,L1,L2)=EA(L1,L2)
      CALL MMUL(RE,D,6,6,2,Z)
      DO 77 J1=1,6
      DO 77 J2=1,2
77    HH(KK,J1,J2)=Z(J1,J2)
```

```
      IF(K-30)30,33,30
   30 IF(K-60)35,33,35
   35 IF(K-90)36,33,36
   36 IF(K-LOC1)32,31,32
   33 LOC2=30
      LOC3=LOC3+30
      GO TO 34
   31 LOC2=LOC1-LOC3
   34 CONTINUE
      KK=0
C
C***  THE F, G, AND H MATRICES ARE STORED IN DATA AND ATEXT FILES
C
      OPEN(21,0,2,@IBUFF,'F-MATRIX')
      WRITE(21)LOC2,(((FF(J1,J2,J3),J3=1,6),J2=1,6),J1=1,LOC2)
      CLOSE(21)
      OPEN(21,0,2,@IBUFF,'G-MATRIX')
      WRITE(21)LOC2,(((GG(K1,K2,K3),K3=1,2),K2=1,6),K1=1,LOC2)
      CLOSE(21)
      OPEN(21,0,2,@IBUFF,'H-MATRIX')
      WRITE(21)LOC2,(((HH(K1,K2,K3),K3=1,2),K2=1,6),K1=1,LOC2)
      CLOSE(21)
      IF(I-1)5050,6060,5050
 5050 IF(I-NUM)32,7070,32
 6060 IF(FLAG)32,8080,32
 7070 IF(K-LOC1)32,8080,32
 8080 FLAG=1.
      OPEN(20,0,1,@IBUFF,'F-ATEXT')
      WRITE(20,2020)LOC2,(((FF(J1,J2,J3),J3=1,6),J2=1,6),J1=1,LOC2)
 2020 FORMAT(1X,I4,//,120(6(1X,6F12.5,/),//))
      CLOSE(20)
      OPEN(20,0,1,@IBUFF,'G-ATEXT')
      WRITE(20,2121)LOC2,(((GG(K1,K2,K3),K3=1,2),K2=1,6),K1=1,LOC2)
 2121 FORMAT(1X,I4,//,120(6(25X,2F12.5,/),//))
      CLOSE(20)
      OPEN(20,0,1,@IBUFF,'H-ATEXT')
      WRITE(20,2222)LOC2,(((HH(K1,K2,K3),K3=1,2),K2=1,6),K1=1,LOC2)
 2222 FORMAT(1X,I4,//,120(6(25X,2F12.5,/),//))
 32   CONTINUE
  6   CONTINUE
  1   CONTINUE
      EXIT
      END
```

ORIGINAL PAGE IS
OF POOR QUALITY

```
      PROGRAM RIC
C
C***  THIS PROGRAM SOLVES THE RICCATI EQUATION AND DRIVING FUNCTION
C***  THE FEEDBACK GAINS AND EXOGENOUS COMPONENTS ARE COMPUTED FOR
C***  USE IN THE FEEDBACK SOLUTION FOR EACH 3 SECOND TIME INTERVAL
C
C***  THE DATA FILES CONTAINING THE DISCRETE-TIME F, G, AND H MATRICES
C***  ARE USED AS INPUT
C
      DIMENSION FF(31,6,6),GG(31,6,2),HH(31,6,2),Q(6,6),R(2,2),S(6,6),
     1F(6,6),G(6,6),FT(6,6),GT(6,6),ST(6,6),Z(6,6),D1(6,6),D2(6,6),
     2D3(6,6),D4(6,6),W1(2,1),W2(2,1),D5(6,6)
      DIMENSION P(6,6),PP(31,6,6),GAIN(31,2,7),IBUFF(208),D6(6,6),
     1D7(6,6),H(6,6)
      COMMON/MAIN1/NDIM,DUM1(6,6)
      NDIM=6
      WRITE(10,5050)
 5050 FORMAT(1X,"ENTER HEAD-WIND IN KNOTS IN 3-DIGIT INTEGER FORMAT"/)
      READ(10,6060)NUM2
 6060 FORMAT(I3)
      WIND=NUM2
      W1(1,1)=0.
      W1(2,1)=-WIND*1.69
      W2(1,1)=0.
      W2(2,1)=-WIND*1.69
      DO 18 J=1,6
      DO 18 JJ=1,6
      S(J,JJ)=0.
      ST(J,JJ)=0.
      P(J,JJ)=0.
   18 Q(J,JJ)=0.
      DO 20 J=1,6
   20 D5(J,1)=0.
C
C***  THE STATE, CONTROL AND CROSS-TERM WEIGHTING MATRICES
C
      Q(1,1)=.72
      Q(2,2)=.5
      Q(3,3)=800.
      Q(4,4)=75.
      Q(5,5)=.88E-2
      Q(6,6)=.55E-5
      R(1,2)=0.
      R(2,1)=0.
      R(1,1)=.39E-4
      R(2,2)=.11
      S(1,1)=SQRT(Q(1,1)*R(1,1))
      S(2,1)=SQRT(Q(2,2)*R(1,1))
      S(3,2)=SQRT(Q(3,3)*R(2,2))
      S(4,2)=SQRT(Q(4,4)*R(2,2))
      S(5,2)=SQRT(Q(5,5)*R(2,2))
      S(6,1)=SQRT(Q(6,6)*R(1,1))
```

```
C
C***  THE TERMINAL TIME STATE WEIGHTING MATRIX
C
      P(1,1)=1.
      P(2,2)=Q(2,2)
      P(3,3)=Q(3,3)
      P(4,4)=Q(4,4)
      P(5,5)=.99E-2
      P(6,6)=.22E-4
      WRITE(10,100)
  100 FORMAT(1X,"ENTER 2-DIGIT OCTAL NUMBER OF F-G-H MATRIX SET FILES",
     1/)
      READ(10,101)NUM
  101 FORMAT(O2)
      DO 1 I=1,NUM
      II=3*NUM-3*I+1
      III=II+1
      OPEN(21,0,2,@IBUFF,'F-MATRIX')
      REWIND 21
      IF(II-1)3,2,3
  3   DO 4 J=2,II
  4   SKIPFILE 21
  2   CONTINUE
      READ(21)LOC2,(((FF(J1,J2,J3),J3=1,6),J2=1,6),J1=1,LOC2)
      CLOSE(21)
      OPEN(21,0,2,@IBUFF,'G-MATRIX')
      REWIND 21
      DO 5 J=1,II
  5   SKIPFILE 21
      READ(21)LOC2,(((GG(K1,K2,K3),K3=1,2),K2=1,6),K1=1,LOC2)
      CLOSE(21)
      OPEN(21,0,2,@IBUFF,'H-MATRIX')
      REWIND 21
      DO 95 J=1,III
  95  SKIPFILE 21
      READ(21)LOC2,(((HH(K1,K2,K3),K3=1,2),K2=1,6),K1=1,LOC2)
      CLOSE(21)
      DO 6 K=1,LOC2
      JK=LOC2-K+1
      DO 7 J=1,6
      DO 8 JJ=1,6
      F(J,JJ)=FF(JK,J,JJ)
  8   FT(JJ,J)=FF(JK,J,JJ)
      DO 7 JJ=1,2
      H(J,JJ)=HH(JK,J,JJ)
      G(J,JJ)=GG(JK,J,JJ)
  7   GT(JJ,J)=GG(JK,J,JJ)
      CALL MMUL(H,W1,6,2,1,Z)
      DO 77 J=1,6
  77  D6(J,1)=Z(J,1)
      CALL MMUL(P,D6,6,6,1,Z)
      DO 21 J=1,6
  21  D6(J,1)=Z(J,1)
```

```
      CALL MMUL(GT,P,2,6,6,Z)
      DO 10 J=1,2
      DO 10 JJ=1,6
   10 D1(J,JJ)=Z(J,JJ)
      CALL MMUL(D1,F,2,6,6,Z)
      DO 9 L=1,2
      DO 9 LL=1,6
    9 D1(L,LL)=ST(L,LL)+Z(L,LL)
      CALL MMUL(GT,P,2,6,6,Z)
      DO 11 J=1,2
      DO 11 JJ=1,6
   11 D2(J,JJ)=Z(J,JJ)
      CALL MMUL(D2,G,2,6,2,Z)
      DO 19 J=1,2
      DO 19 JJ=1,2
   19 Z(J,JJ)=Z(J,JJ)+R(J,JJ)
      RR=Z(1,1)*Z(2,2)-Z(1,2)*Z(2,1)
      D2(1,1)=Z(2,2)/RR
      D2(1,2)=-Z(1,2)/RR
      D2(2,1)=-Z(2,1)/RR
      D2(2,2)=Z(1,1)/RR
      D3(1,1)=D2(1,1)
      D3(1,2)=D2(1,2)
      D3(2,1)=D2(2,1)
      D3(2,2)=D2(2,2)
      CALL MMUL(D2,D1,2,2,6,Z)
C
C***  STORE FEEDBACK GAINS
C
      DO 12 J=1,2
      DO 12 JJ=1,6
      GAIN(JK,J,JJ)=-Z(J,JJ)
   12 D1(J,JJ)=Z(J,JJ)
      CALL MMUL(D3,GT,2,2,6,Z)
      DO 22 J=1,2
      DO 22 JJ=1,6
      D4(J,JJ)=Z(J,JJ)
   22 D5(J,JJ)=Z(J,JJ)
      DO 24 J=1,6
   24 D7(J,1)=D5(J,1)+D6(J,1)
      CALL MMUL(D3,D7,2,6,1,Z)
C
C***  STORE FEEDBACK GAIN[illegible] COMPONENTS
C
      DO 23 J=1,2
   23 GAIN(JK,J,7)=-Z(J,1)
      CALL MMUL(FT,P,6,6,6,Z)
      DO 13 J=1,6
      DO 13 JJ=1,6
   13 D2(J,JJ)=Z(J,JJ)
      CALL MMUL(D2,G,6,6,2,Z)
```

```
      DO 14 J=1,6
      DO 14 JJ=1,2
      D2(J,JJ)=S(J,JJ)+Z(J,JJ)
   14 D3(J,JJ)=D2(J,JJ)
      CALL MMUL(D2,D1,6,2,6,Z)
      DO 15 J=1,6
      DO 15 JJ=1,6
   15 D1(J,JJ)=Z(J,JJ)
      CALL MMUL(FT,P,6,6,6,Z)
      DO 16 J=1,6
      DO 16 JJ=1,6
   16 D2(J,JJ)=Z(J,JJ)
      CALL MMUL(D2,F,6,6,6,Z)
      DO 17 J=1,6
      DO 17 JJ=1,6
      P(J,JJ)=Q(J,JJ)+Z(J,JJ)-D1(J,JJ)
   17 PP(JK,J,JJ)=P(J,JJ)
      CALL MMUL(D3,D4,6,2,6,Z)
      DO 25 J=1,6
      D7(J,1)=D5(J,1)+D6(J,1)
      DO 25 JJ=1,6
   25 D3(J,JJ)=FT(J,JJ)-Z(J,JJ)
      CALL MMUL(D3,D7,6,6,1,Z)
      DO 26 J=1,6
   26 D5(J,1)=Z(J,1)
    6 CONTINUE
      OPEN(21,0,2,8IBUFF,'GAINS')
      WRITE(21)LOC2,(((GAIN(K1,K2,K3),K3=1,7),K2=1,2),K1=1,LOC2)
      CLOSE(21)
      IF(I-1)7171,7272,7171
 7171 IF(I-NUM)7373,7272,7373
 7272 CONTINUE
C
C***  THE RICCATI SOLUTION, FEEDBACK GAINS, AND EXOGENOUS COMPONENTS
C***  ARE STORED IN DATA AND ATEXT FILES
C
      OPEN(20,0,1,8IBUFF,'P-MATRIX')
      WRITE(20,2020)LOC2,(((PP(J1,J2,J3),J3=1,6),J2=1,6),J1=1,LOC2)
 2020 FORMAT(1X,I4,//,60(6(1X,6F12.4,/),//))
      CLOSE(20)
 7373 CONTINUE
      OPEN(20,0,1,8IBUFF,'GAINS')
      WRITE(20,2121)LOC2,(((GAIN(K1,K2,K3),K3=1,7),K2=1,2),K1=1,LOC2)
 2121 FORMAT(1X,I4,//,60(2(1X,7F10.4,/),//))
      CLOSE(20)

    1 CONTINUE
      EXIT
      END
```

ORIGINAL PAGE IS
OF POOR QUALITY

```
      PROGRAM REG
C
C***  THIS PROGRAM IMPLEMENTS THE LINEAR FEEDBACK SOLUTION ON
C***  THE COMPLETE NONLINEAR AIRCRAFT MODEL OF THE BOEING 707-320B
C
C***  THE DATA FILES CONTAINING THE NOMINAL STATE AND CONTROL VALUES
C***  AND THOSE CONTAINING THE FEEDBACK GAINS AND EXOGENOUS COMPONENTS
C***  ARE USED AS INPUTS
C
C***  FUNCTION SWITCH 4 RESETS INITIAL CONDITIONS
C***  FUNCTION SWITCH 8 STARTS PROGRAM
C***  FUNCTION SWITCH 12 STOPS PROGRAM
C***  FUNCTION SWITCH 16 DISPLAYS FLIGHT CONDITIONS AND PARAMETERS AT
C***  TERMINAL TIME OR AT STOPACTION
C
      GLOBAL ITIME,NF
      IMPLICIT FRACTION (F)
      LOGICAL CONE
      REAL FLAPS
L       OTSERRORS=SHORT
      COMMON/MORE/IBUFF(208),TP(75),EE(75),TOTT(75),QW(6,6),RW(2,2)
      COMMON/RELAX/SCORD,SSPAN,SAREA,P,Q,ROW,RMACH,DPP,DQQ,DRR,SPALF
      COMMON/WORK/UVEL,VVEL,WVEL,VTOT,UDTT,VDTT,WDTT,VTOD
      COMMON/EXTRA/DDFIE,DDTET,DDSY,RFIE,RTET,RSY,STTET,CTTET,SFIE,CFIE
      COMMON/MORE/SSY,CSY
      COMMON/CNTRL/T,FLAPS,CTETA,CPHI,CXI,GEAR,SPBRK,TPOS
      COMMON/CNTRL/BTETA,BPHI,BXI
      COMMON/PRMTR/V,XI,BETAG,DT
      COMMON/PRMTR/ALPHA,BETA,PHI,VX,VY,VZ,THETA,A,XM,Y,R,RIAS
      COMMON/FRAC/FV,FBNK,FPICH,FA,FVZ,FHDG,FADF,FVOR,FCPICH
      COMMON/FRAC/FER,FHER,DME(6),ALT(7)
      COMMON/FD/ADF,VOR,EPS,HER,RAD
      COMMON/GAINS/GAIN(31,2,7),UU(100),WW(100),QQ(100),TEET(100),JK5,
     1HH(100),RANGE(100),LOC1,LOC2,JK1,JK2,CTIM,TOTXX,JK3,DELU,DELW,
     2DELQ,DELT,DELH,DELR,DELTH,DELE,DIST,TH(100),JK4,NUM1,NUM2,WIND
      DATA TMRKR1/0.4815/,TMRKR2/0.068/,TMRKR/0.0076/
      DATA TNGSA/-0.052933/,RAD/57.296/
      DATA SCORD/34148./,SSPAN/219354./,SAREA/1505./
      ENTRY NF
      WRITE(10,5050)
 5050 FORMAT(1X,"ENTER HEAD-WIND IN KNOTS IN 3-DIGIT INTEGER FORMAT"/)
      READ(10,6060)INUM
 6060 FORMAT(I3)
      RNUM=INUM
      WIND=-RNUM*1.69
      WRITE(10,1010)
 1010 FORMAT(1X,"ENTER TOTAL NUMBER OF VALUE FILES IN OCTAL"/)
      READ(10,2020)NUM1
 2020 FORMAT(O2)
      WRITE(10,3030)
 3030 FORMAT(1X,"ENTER TOTAL NUMBER OF GAIN FILES IN OCTAL"/)
      READ(10,4040)NUM2
 4040 FORMAT(O2)
      WRITE(10,7070)
7070  FORMAT(1X,"TYPE 1 FOR EXOGENOUS COMPONENT- OTHERWISE 0"/)
```

```
      READ(10,8080)JK5
 8080 FORMAT(O1)
1     CONTINUE
C
C***  INITIALIZE ALL VALUES
C
      DO 124 I=1,6
      DO 124 J=1,6
  124 QW(I,J)=0.
      QW(1,1)=.72
      QW(2,2)=.5
      QW(3,3)=800.
      QW(4,4)=75.
      QW(5,5)=.88E-2
      QW(6,6)=.55E-5
      RW(1,1)=.39E-4
      RW(1,2)=0.
      RW(2,1)=0.
      RW(2,2)=.11
      COST=0.
      JK1=NUM1+NUM2-1
      JK2=1
      JK3=0
      JK4=-1
      LOC1=0
      LOC2=-10
      TOTXX=0.
      CTIM=0.
      DELU=0.
      DELW=0.
      DELQ=0.
      DELT=0.
      DELH=0.
      DELR=0.
      DELTH=0.
      DELE=0.
      SPALF=0.
      DDFIE=0.
      DDTET=0.
      DDSY=0.
      RFIE=0.
      RTET=.84/RAD
      RSY=53.07/RAD
      STTET=SIN(.015)
      CTTET=COS(.015)
      SFIE=0.
      CFIE=1.
      SSY=.79937
      CSY=.600839
      XI=53.07
      PHI=0.
      FBNK=0.0F
      ALPHA=2.84
      BETAG=0.
      BETA=0.
```

```
      DRNG=2550.
      IOM=IMM=IIM=0
      JJFF=0
      ETIME=TOTTX=0.
      XM=-150.26
      Y=-239497.19
      VOR=53.07
      ADF=49.69
      V=476.
      VTOT=304.
      VTOD=0.
      UVEL=VTOT
      VVEL=0.
      WVEL=11.0
      UDTT=0.
      VDTT=0.
      WDTT=0.
      VX=764.65
      VY=248.45
      VZ=0.
      P=0.
      Q=0.
      R=0.
      DPP=0.
      DQQ=0.
      DRR=0.
      THETA=ALPHA-2.
      DIST=SQRT((XM+31.0826)**2+(Y/6080.2+.50366)**2)
      TISD=DIST
      A=35000.
      IALT1=3
      IALT2=5
      IALT3=0
      IALT4=0
      IALT5=0
      LABEL(ALT`
      ZSET(0.0F)
      MOVE(.61F,.39F)
      WRITE(16,9011)IALT1,IALT2,IALT3,IALT4,IALT5
9011  FORMAT(2I1,"0S",1X,3I1)
      ENDLIST
      LABEL(DME)
      ZSET(0.F)
      MOVE(-0.34F,-0.01434F)
      WRITE(16,555)DIST
      ENDLIST
      XFEET=XM*6080.2
      EPS=ATAN((Y+3062.35)/((XM+31.0816)*6080.2))
      HER=A-XFEET*(-0.052933)
      BTETA=BPHI=BXI=0.
      CALL SAMPLE
      BTETA=CTETA+2.1
      BPHI=CPHI
      BXI=CXI
      CALL RTOF
```

```
C
C***  START THE DISPLAY
C
A            JPSR $GRAFX
A                 $DIALS
A                 5
C
C***  INITIALIZE DATA-UPDATE CLOCK
C
    2 ITIME=1
C
C***  ENTER WAIT LOOP IF SWITCH 8 (START) IS NOT ON
C
      IF(.NOT.SWITCH(8))GO TO 2
C
C***  EXECUTE UNLESS SWITCH 12 (FREEZE) IS ON
C
C***  READS FEEDBACK GAINS AND EXOGENOUS COMPONENTS
C
      IF(JK1-NUM1+1)859,859,6
  6   IF(JK3-LOC2)859,860,860
  860 OPEN(21,0,2,@IBUFF,'GAINS')
      REWIND 21
      IF(JK1)851,853,851
  851 DO 852 J1=1,JK1
  852 SKIPFILE 21
  853 READ(21)LOC2,(((GAIN(K1,K2,K3),K3=1,7),K2=1,2),K1=1,LOC2)
      CLOSE(21)
  92  JK3=0
  91  CONTINUE
      JK1=JK1-1
      ITIME=1
C
C***  READS NOMINAL STATE AND CONTROL VALUES
C
  859 IF(LOC1-JK4)854,866,866
  866 IF(JK2-NUM1-1)855,854,854
  855 OPEN(21,0,2,@IBUFF,'VALUE1')
      IF(JK2-1)856,857,856
  856 DO 858 J1=2,JK2
  858 SKIPFILE 21
  857 READ(21)LOC1,(UU(I),WW(I),QQ(I),TEET(I),HH(I),RANGE(I),TH(I),
     1TP(I),EE(I),TOTT(I),I=1,LOC1)
      CLOSE(21)
      JK4=LOC1
      JK2=JK2+1
      CTIM=CTIM+210.
      LOC1=0
      ITIME=1
  854 CONTINUE
```

ORIGINAL PAGE IS
OF POOR QUALITY

```
C
C***  THE DEVIATIONS IN THE STATES AND CONTROLS ARE PRINTED
C***  ON THE TELETYPE EVERY 6 SECONDS
C
      IF(AMOD(TOTXX,6.).GT.DT)GO TO 8181
      WRITE(10,6161)DELU,DELW,DELQ,DELT,DELH,DELR,DELTH,DELE
 6161 FORMAT(1X,F8.2,F7.2,F8.4,2X,F8.4,F10.2,F10.2,F10.2
     1,2X,F6.2)
      ITIME=1
 8181 CONTINUE
      IF(.NOT.SWITCH(12))GO TO 3
C
C***  AFTER SWITCH 12 HAS BEEN PRESSED, EXIT IF SWITCH 16 IS ON...
C
    7 IF(SWITCH(16))GO TO 4
C
C***  OR INITIALIZE VALUES IF SWITCH 4 (IC) IS ON...
C
      IF(SWITCH(4))GO TO 5
C
C***  OR START EXECUTION AGAIN IF SWITCH 8 IS ON...
C
      IF(SWITCH(8))GO TO 6
C
C***  OR INITIALIZE DATA-UPDATE [illegible] AND ENTER A WAITING LOOP
C
      ITIME=1
      GO TO 7
    5 CONTINUE
C
C***  STOP THE DISPLAY AND GO BACK TO INITIAL VALUES
C
A   JPSR $NHALT
A   NOOP
      GO TO 1
C
C***  START EXECUTION OF A NEW DATA-UPDATE CYCLE:
C***  COMPUTE DT (=TIME IN SECS OF PREVIOUS CYCLE)
C***  AND INITIALIZE DATA-UPDATE CLOCK
C
    3 TIME=ITIME
      ITIME=0
      DT=TIME/120.
      CALL DYNNF
      XFEET=XM*6080.2
      IF(XFEET.EQ.0.)XFEET=1.
      YMILE=Y/6080.2
```

```
C
C***  COST FUNCTION
C
      COST=COST+DELU*QW(1,1)*DELU+DELW*QW(2,2)*DELW+DELQ*QW(3,3)*DELQ
     1+DELT*QW(4,4)*DELT+DELH*QW(5,5)*DELH+DELR*QW(6,6)*DELR
     2+DELTH*RW(1,1)*DELTH+DELE*RW(2,2)*DELE
      HER=A-XFEET*TNGSA
      IF(XM.EQ.-31.0826)XM=-31.0827
      EPS=ATAN((YMILE+.50366)/(31.0826+XM))
      IF(XM.EQ.-5.4896)XM=-5.4895
C
C***  VOR, ADF AND DME INFORMATION
C
      ADF=35.-ATAN(YMILE/(-XM-5.4896))*RAD
      IF(XM.GT.-5.4896)ADF=ADF+180.
      IF(XM.EQ.-31.0826)XM=-31.0816
      VOR=35.-ATAN((YMILE+.50366)/(-31.0826-XM))*RAD
      IF(XM.GT.-31.0826)VOR=VOR+180.
      ADF=AMOD(ADF,360.)
      VOR=AMOD(VOR,360.)
      CALL RTOF
      DIST=SQRT((XM+31.0826)**2+(YMILE+.50366)**2)
      LABEL(DME)
      ZSET(0.0F)
      MOVE(-0.34F,-0.01434F)
      WRITE(16,555)DIST
555   FORMAT("&[illegible]",[illegible].1)
      ENDLIST
      RALT=[illegible]
      IALT[illegible]
      RALT=10.*(RALT-IALT1)
      IALT2=RALT
      RALT=10.*(RALT-IALT2)
      IALT3=RALT
      RALT=10.*(RALT-IALT3)
      IALT4=RALT
      RALT=10.*(RALT-IALT4)
      IALT5=RALT
      LABEL(ALT)
      ZSET(0.0F)
      MOVE(.61F,.39F)
      WRITE(16,9012)IALT1,IALT2,IALT3,IALT4,IALT5
9012  FORMAT(2I1,"&S",1X,3I1)
      ENDLIST
```

```
      CONE=.FALSE.
      IOM=IMM=IIM=0
      IF(EPS.LE.0.05.AND.EPS.GT.-0.05)CONE=.TRUE.
C
C***        TURN OUTER MARKER LIGHT ON
C
      IF(ABS(XM+5.4896).LE.TMRKR1.AND.CONE)IOM=1
C
C***        TURN MIDDLE MARKER LIGHT ON
C
      IF(ABS(XM+0.7896).LE.TMRKR2.AND.CONE)IMM=1
C
C***        TURN INNER MARKER LIGHT ON
C
      IF(ABS(XM+0.1896).LE.TMRKR.AND.   CONE )IIM=1
      CALL BEACONS(IOM,IMM,IIM,JJFF)
C
C***        EXIT IF ALTITUDE=0
C
      IF(A)4,4,6
    4 CONTINUE
C
C***  STOP THE DISPLAY, TURN ALL LIGHTS OFF
C
A        JPSR $NHALT
      XFF=XM*6080.2+1153.
      KDT=1./DT
C
C***  SHOW PARAMETERS AT TERMINAL TIME OR AT STOPACTION ON CRT SCREEN
C
      TSID=DIST*6080.2
      WRITE(25,2000)
      WRITE(25,2001)TOTXX,RIAS,XI
      WRITE(25,2002)VZ
      WRITE(25,2003)UVEL,WVEL,Q,THETA,A,DIST,TPOS,T,CTETA
2000  FORMAT(////27X,"PARAMETERS AT TERMINAL TIME OR AT STOPACTION"//)
2001  FORMAT(27X,"TOTAL FLIGHT TIME       ",F15.0," SECS."/
     2        27X,"INDICATED AIRSPEED      ",8X,F7.1," KNOTS"/
     3        27X,"HEADING                 ",10X,F5.1," DEG.")
2002  FORMAT(27X,"VERTICAL SPEED          ",F15.1," FPM")
2003  FORMAT( /27X,"FORWARD VELOCITY U    ",10X,F7.1," FT./SEC."/
     1          27X,"DOWNWARD VELOCITY W   ",10X,F7.1," FT./SEC."/
     2          27X,"PITCH RATE            ",13X,F7.4," RAD./SEC."/
     4          27X,"PITCH ANGLE           ",13X,F7.4," DEG."/
     5          27X,"ALTITUDE              ",10X,F6.0," FT."/
     8          27X,"RANGE                 ",11X,F6.1," NAUT. MI."/
     627X,"THROTTLE POSITION     ",14X,F6.4,/,27X,"THRUST",25X,F8.1,
     7" LBS.",/,27X,"ELEVATOR POSITION     ",13X,F5.2," DEG.")
      WRITE(25,2004)COST
 2004 FORMAT(/,27X,"COST                    ",F15.1)
      EXIT
      END
```

```
      SUBROUTINE SAMPLE
C
C***  SUBROUTINE TO SAMPLE COCKPIT CONTROLS
C
      GLOBAL SPBRK,FLAPS,THRUST
      IMPLICIT FRACTION(F)
      REAL FLAPS
      COMMON/MORE/IBUFF(208),TP(75),EE(75),TOTT(75),QW(6,6),RW(2,2)
      COMMON/RELAX/SCORD,SSPAN,SAREA,P,Q,ROW,RMACH,DPP,DQQ,DRR,SPALF
      COMMON/PRMTR/V,XI,BETAG,DT
      COMMON/PRMTR/ALPHA,BETA,PHI,VX,VY,VZ,THETA,A,XM,Y,R,RIAS
      COMMON/CNTRL/T,FLAPS,CTETA,CPHI,CXI,GEAR,SPBRK,TPOS
      COMMON/CNTRL/BTETA,BPHI,BXI
      COMMON/GAINS/GAIN(31,2,7),UU(100),WW(100),QQ(100),TEET(100),JK5,
     1HH(100),RANGE(100),LOC1,LOC2,JK1,JK2,CTIM,TOTXX,JK3,DELU,DELW,
     2DELQ,DELT,DELH,DELR,DELTH,DELE,DIST,TH(100),JK4,NUM1,NUM2,WIND
A           ADEPT
            FPRI
            MD07'F 0
            0;0;0
            MD07'F 10
            0;0
            S5MD FSPBRK
            MD07'F 20
            0;0
            S5MD FT1
            MD07'F 40
            0;0
            S5MD FT2
            MD07'F 100
            0;0
            S5MD FT3
            MD07'F 200
            0;0
            S5MD FT4
            MD07'F 0
            0;0;0
            MD07'H C1
            0;0;0
```

ORIGINAL PAGE IS
OF POOR QUALITY

```
            MD07'L; 1!H1
            0;0
            S5MD FFLAPS
            MD07'L; 1!H2
            0;0
            S5MD FYOKE
            MD07'L; 1!H4
            0;0
            S5MD FWHEEL
            MD07'L; 1!H10
            0;0
            S5MD FPEDL
            MD07'H C1
            0;0;0
            UPRI
            MDAR MASK
            S6AR'A'F
            ARAR'H'F
            JPLS DOWN
            MDAR ZERO
            ARMD FGEAR
            JUMP BACK
DOWN:       MDAR ONE
            ARMD FGEAR
            JUMP BACK
MASK:       00100!H0
ZERO:       0!H0
ONE:        0!H37777
FGEAR:      0
FSPBRK:     0
FT1:        0
FT2:        0
FT3:        0
FT4:        0
C1:         0!H00001
FFLAPS:     0
FYOKE:      0
FWHEEL:     0
FPEDL:      0
BACK:       NOOP
MASKUP:10000
MASKDN:04000
```

```
      MDAR MASKUP
            S6AR'A'F
            JPLS SWUP
            MDAR MASKDN
            S6AR'A'F
            JPLS SWDN
            JUMP SWEN
SWUP: NOOP
FORTRAN
      BTETA=BTETA+.05
A          ADEPT
      JUMP SWEN
SWDN: NOOP
FORTRAN
      BTETA=BTETA-.05
A          ADEPT
SWEN: NOOP
FORTRAN
C
C***  MACH NUMBER
C
      IF(A-36089.)9004,9004,9005
9004  RMACH=V/(661.-(.002434*A))
      GO TO 9006
9005  RMACH=V/573.
9006  CONTINUE
C
C***  INDICATED AIRSPEED IN KNOTS
C
      RIAS=(656.-(.0091*A))*RMACH
      SPBRK=FTOR(FSPBRK)*187.5
      IF(RIAS-188.)9007,9007,9008
9008  SPMAX=60.-(.283*(RIAS-188.))
      SPBRK=AMIN1(SPBRK,SPMAX)
9007  CONTINUE
      FLAPS=AMAX2(0.0F,FFLAPS)*128.315
      IF(FLAPS-SPALF)9001,9002,9003
9001  FLAPS=SPALF-.4175
      GO TO 9002
9003  FLAPS=SPALF+.4175
9002  SPALF=FLAPS
      CTETA=(-FTOR(FYOKE)*18.75-BTETA)*2.0
      CPHI=(-FTOR(FWHEEL)*42.5-BPHI/1.85)*1.85
      CXI=(FTOR(FPEDL)*20.5-BXI/2.65)*2.65
```

```
C
C***  THRUST COMPUTATIONS
C
      THRUST=FTOR(FT1+FT2)+FTOR(FT3+FT4)
      TPOS=(THRUST-.3727)/1.1761
      TPOS=AMAX1(0.,TPOS)
      CTETA=AMAX1(-20.,CTETA)
      TPOS=AMIN1(TPOS,1.0)
      CTETA=AMIN1(CTETA,20.)
      IF(A-10000.)820,821,821
  820 RMAXT=13800.-.28125*A+(.3117*A-7800.)*RMACH
      RIDLT=1000.-2000.*RMACH
      GO TO 822
  821 RMAXT=13800.-.28125*A+(.12*(A-10000.)-3125.)*RMACH
      RIDLT=1000.+(.05*(A-10000.)-2000.)*RMACH
  822 RIDLT=AMAX1(RIDLT,0.)
      T=(RIDLT+(RMAXT-RIDLT)*TPOS*TPOS)*4.
      JK6=JK3+1
      RJK5=JK5
C
C***  THRUST = NOMINAL THRUST + THRUST DEVIATION FROM FEEDBACK LAW
C***  ELEVATOR DEFLECTION = NOMINAL DEFLECTION + DEVIATION
C***  THRUST AND ELEVATOR DEFLECTION ARE NOT ALLOWED TO EXCEED LIMITS
C
   99 T=TH(LOC1+1)+GAIN(JK6,1,1)*DELU+GAIN(JK6,1,2)*DELW+GAIN(JK6,1,3)
     1*DELQ+GAIN(JK6,1,4)*DELT+GAIN(JK6,1,5)+DELH+GAIN(JK6,1,6)*DELR
     2-(GAIN(JK6,1,7)*WIND*RJK5/(15.*1.69))
      RMAXT=4.*RMAXT
      RIDLT=4.*RIDLT
      T=AMIN1(T,RMAXT)
      T=AMAX1(RIDLT,T)
      CTETA=EE(LOC1+1)+GAIN(JK6,2,1)*DELU+GAIN(JK6,2,2)*DELW+GAIN(JK6,2
     1,3)*DELQ+GAIN(JK6,2,4)*DELT+GAIN(JK6,2,5)*DELH+GAIN(JK6,2,6)*DELR
     2-(GAIN(JK6,2,7)*WIND*RJK5/(15.*1.69))
      DELTH=T-TH(LOC1+1)
      DELE=CTETA-EE(LOC1+1)
   96 CONTINUE
      CTETA=AMAX1(-20.,CTETA)
      CTETA=AMIN1(CTETA,20.)
      TMAX1=4.*RMAXT
      TMIN1=4.*RIDLT
206   GEAR=FTOR(FGEAR)
      RETURN
      END
```

```
      SUBROUTINE BEACONS(IOM,IMM,IIM,JJFF)
C
C***  SUBROUTINE TO OPERATE MARKER-BEACONS' LIGHTS
C
      IF(IOM.OR.IMM.OR.IIM)9,10
9     CONTINUE
      JJFF=JJFF+1
      GO TO (8,8,6,10),JJFF
8     CONTINUE
      IF(IOM)1,4
 4    IF(IMM)2,5
5     IF(IIM)3,6
C
C***  NONE OF THE LIGHTS SHOULD BE ON:
C***  TURN THEM ALL OFF
C
10    JJFF=0
6     CONTINUE
A     ADEPT
      MDAR BCN
      ARIC'A'F
      JUMP .+2
BCN:77277!H57777
      NOOP
FORTRAN
      GO TO 7
1     CONTINUE
A     MDAR OUTER
A     ARIC'0
      GO TO 7
2     CONTINUE
A     MDAR MIDLE
A     ARIC'0
      GO TO 7
3     CONTINUE
A     MDAR INNER
A     ARIC'0
      GO TO 7
A     ADEPT
OUTER:20000
MIDLE:00400!H
INNER:00100!H
FORTRAN
7     CONTINUE
      RETURN
      END
```

ORIGINAL PAGE IS
OF POOR QUALITY

C. 3

```
      SUBROUTINE DYNNF
C
C***  DYNAMICS-COMPUTING SUBROUTINE
C
      GLOBAL DVZ,DT,MP,APP,DP,DQ,DR,P,Q,R
      GLOBAL CXI,CPHI,CTETA,ALPHA,BETA
      GLOBAL UVEL,VVEL,WVEL,RVX,RVY,RVZ,UDOT,WDOT,VDOT,VTOT
      GLOBAL THETA,PHI,XI,L,D,SFOR
      GLOBAL LLL,MMM,NNN,RFIE,RTET,RSY,V,RX,RY,RZ
      REAL L,FLAPS,LLL,MMM,NNN
      COMMON/MORE/IBUFF(208),TP(75),EE(75),TOTT(75),QW(6,6),RW(2,2)
      COMMON/RELAX/SCORD,SSPAN,SAREA,P,Q,ROW,RMACH,DPP,DQQ,DRR,SPALF
      COMMON/WORK/UVEL,VVEL,WVEL,VTOT,UDTT,VDTT,WDTT,VTOD
      COMMON/EXTRA/DDFIE,DDTET,DDSY,RFIE,RTET,RSY,STTET,CTTET,SFIE,CFIE
      COMMON/MORE/SSY,CSY
      COMMON/CNTRL/T,FLAPS,CTETA,CPHI,CXI,GEAR,SPBRK,TPOS
      COMMON/CNTRL/BTETA,BPHI,BXI
      COMMON/PRMTR/V,XI,BETAG,DT
      COMMON/PRMTR/ALPHA,BETA,PHI,VX,VY,VZ,THETA,A,XM,Y,R,RIAS
      COMMON/FD/ADF,VOR,EPS,HER,RAD
      COMMON/GAINS/GAIN(31,2,7),UU(100),WW(100),QQ(100),TEET(100),JK5,
     1HH(100),RANGE(100),LOC1,LOC2,JK1,JK2,CTIM,TOTXX,JK3,DELU,DELW,
     2DELQ,DELT,DELH,DELR,DELTH,DELE,DIST,TH(100),JK4,NUM1,NUM2,WIND
      CALL SAMPLE
      V2=VTOT*VTOT
C
C***  ATMOSPHERIC DENSITY
C
      ROW=.2378E-2+(A*((A/(1.806E12))-(.66584E-7)))
      RLPAS=FLAPS-6.
      RLAPS=RLPAS-8.
      RLPAA=AMAX1(RLPAS,0.)
      RLAPP=AMAX1(RLAPS,0.)
      RDFP=AMIN1(RLPAA,1.0)
      CLT=((4.584+RMACH*(5.397*RMACH-2.22)+(1.081)*RDFP)*((WVEL/VTOT)+
     1.0331))-.0055*CTETA+RLPAA*.01432
C
C***  LIFT
C
      L=ROW*V2*SAREA*CLT
```

```
      IF(RMACH-.845)811,811,812
811   IF(RMACH-.8)813,813,814
813   IF(RMACH-.7)815,815,816
815   CDM=.012
      GO TO 818
812   CDM=-.1089+.1455*RMACH
      RK=-.6411+.8333*RMACH
      GO TO 819
814   CDM=-.01735+.0371*RMACH
      RK=-.13608+.2356*RMACH
      GO TO 819
816   CDM=.0097+.0033*RMACH
818   RK=.0524
819   CONTINUE
C
C***  DRAG
C
      D=ROW*V2*SAREA*(CDM+RK*(CLT*CLT)+.0105*GEAR+RLPAA*.0018+.833E-3*
     1SPBRK)
C
C***  SIDE FORCE
C
      SFOR=ROW*1505.*VTOT*(-.917*VVEL-.004*VTOT*CXI)
      DFIE=P+(SFIE*STTET/CTTET)*Q+(CFIE*STTET/CTTET)*R
      DTET=CFIE*Q-SFIE*R
      DSY=(SFIE/CTTET)*Q+CFIE*R/CTTET
      RFIE=RFIE+((3.*DFIE-DDFIE)*DT/2.)
      RTET=RTET+((3.*DTET-DDTET)*DT/2.)
      RSY=RSY+((3.*DSY-DDSY)*DT/2.)
      DDFIE=DFIE
      DDTET=DTET
      DDSY=DSY
C
C***  EULER ANGLES
C
      PHI=RFIE*RAD
      THETA=RTET*RAD
      XI=RSY*RAD
      STTET=SIN(RTET)
      CTTET=COS(RTET)
      SFIE=SIN(RFIE)
      CFIE=COS(RFIE)
      SSY=SIN(RSY)
      CSY=COS(RSY)
```

```
C
C***  ROLLING, PITCHING, AND YAWING MOMENTS
C
      LLL=ROW*VTOT*(VTOT*SSPAN*(-.1719+VVEL/VTOT+.00113*CPHI-.0002*CXI)
     1-(.60745E7*P))
      MMM=ROW*VTOT*(VTOT*SCORD*(.048-(.955*WVEL/VTOT)+.009*CTET4+
     1RLAPP*(-.0033))-(.128E8*Q))
      NNN=ROW*VTOT*(VTOT*SSPAN*(.115*VVEL/VTOT+.0011*CXI)-(.23978E7*R))
      DP=(((LLL/.382E7))-R*Q*(.856)+P*Q*(.0974))
      DQ=(((MMM/.485E7))+P*R*(.886)-((P*P)-(R*R))*(.0767))
      DR=(((NNN/.812E7))-P*Q*(.127)-R*Q*(.0458))
C
C***  ANGULAR VELOCITIES IN BODY AXES
C
      P=P+((3.*DP-DPP)*DT/2.)
      Q=Q+((3.*DQ-DQQ)*DT/2.)
      R=R+((3.*DR-DRR)*DT/2.)
      DPP=DP
      DQQ=DQ
      DRR=DR
C
C***  AERODYNAMIC ANGLES
C
      ALPHA=RAD*WVEL/VTOT
      BETA=RAD*VVEL/VTOT
      BETAG=BETA
      BET1=1.-((VVEL*VVEL)/(2.*VTOT*VTOT))
      CON1=-1/(6987.*VTOT)
      UDOT=(CON1*(UVEL*BET1*D+(UVEL*VVEL/VTOT)*SFOR-WVEL*L))-
     1(Q*WVEL-R*VVEL)-32.2*STTET+T/6987.
      VDOT=(CON1*(VVEL*D-VTOT*BET1*SFOR))-(R*UVEL-P*WVEL)+32.2*CTTET*
     1SFIE
      WDOT=(CON1*(WVEL*BET1*D+(WVEL*VVEL/VTOT)*SFOR+UVEL*L))-
     1(P*VVEL-Q*UVEL)+32.2*CTTET*CFIE
      VTOT=SQRT(UVEL*UVEL+VVEL*VVEL+WVEL*WVEL)
      V=VTOT/1.69
C
C***  LINEAR VELOCITIES IN BODY AXES
C
      UVEL=UVEL+((3.*UDOT-UDTT)*DT/2.)
      VVEL=VVEL+((3.*VDOT-VDTT)*DT/2.)
      WVEL=WVEL+((3.*WDOT-WDTT)*DT/2.)
      UDTT=UDOT
      VDTT=VDOT
      WDTT=WDOT
```

```
C
C***  LINEAR VELOCITIES IN VEHICLE AXES
C
      RVX=CTTET*CSY*UVEL+(SFIE*STTET*CSY-CFIE*SSY)*VVEL+(SFIE*SSY+
     1CFIE*CSY*STTET)*WVEL
      RVY=CTTET*SSY*UVEL+(CFIE*CSY+SFIE*STTET*SSY)*VVEL+(CFIE*STTET*SSY
     1-SFIE*CSY)*WVEL
      RVZ=-STTET*UVEL+SFIE*CTTET*VVEL+CFIE*CTTET*WVEL
      VZ=-60.*RVZ
      RAA=18.07/RAD
      VX=.5735*RVY+.81915*RVX+WIND*COS(RAA)
      VY=.81915*RVY-.5735*RVX+WIND*SIN(RAA)
C
C***  EARTH COORDINATE SYSTEM POINTS
C
      XM=XM+(VX/6080.2)*DT
      Y=Y+VY*DT
      A=A+VZ*DT/60.
      XI=AMOD(XI,360.)
      PHI=AMOD(PHI,360.)
      THETA=AMOD(THETA,360.)
      A=AMAX1(A,0.)
      TOTXX=TOTXX+DT
      TINT=3.
      IF(AMOD(TOTXX,TINT).GT.DT)GO TO 101
      IF(JK2-NUM1-1)897,797,897
  797 IF(LOC1-JK4)897,899,897
  897 CONTINUE
      LOC1=LOC1+1
  899 CONTINUE
C
C***  CALCULATION OF DEVIATIONS IN STATES
C
      DELU=UVEL-UU(LOC1)+WIND
      DELW=WVEL-WW(LOC1)
      DELQ=Q-QQ(LOC1)
      DELT=RTET-TEET(LOC1)
      DELH=A-HH(LOC1)
      DELR=(DIST-RANGE(LOC1))*6080.
      IF(JK1-NUM1+1)898,761,898
  761 IF(JK3-LOC2)898,101,898
  898 JK3=JK3+1
  101 CONTINUE
      RETURN
      END
```

ORIGINAL PAGE IS
OF POOR QUALITY

```
      SUBROUTINE RTOF
C
C***  SUBROUTINE TO CONVERT DATA REAL-TO-FRACTION
C
      GLOBAL TRIG,FPICH1,FPCH1
      IMPLICIT FRACTION (F)
      COMMON/PRMTR/V,XI,BETAG,DT
      COMMON/PRMTR/ALPHA,BETA,PHI,VX,VY,VZ,THETA,A,XM,Y,R,RIAS
      COMMON/FRAC/FV,FBNK,FPICH,FA,FVZ,FHDG,FADF,FVOR,FCPICH
      COMMON/FRAC/FER,FHER,DME(6),ALT(7)
      COMMON/FD/ADF,VOR,EPS,HER,RAD
      FV=(200.-AMOD(RIAS,400.))/200.
      FBNK1=PHI/360.
      FBNK=FBNK1+FBNK1
      FPICH1=-THETA/360.
      FPICH=FPICH1+FPICH1
      IF(A.LT.0.)A=0.
      FA=(500.-AMOD(A,1000.))/500.
      FVZ=-FMIN1(1.,AMAX1(VZ/4000.,-1.))
      FHDG1=AMOD((XI-BETAG),360.)/360.
      FHDG=FHDG1+FHDG1
      FADF1=-ADF/360.
      FADF=FADF1+FADF1
      FVOR1=-VOR/360.
      FVOR=FVOR1+FVOR1
      ERR=EPS*RAD-18.07
      TEMPP=AMAX1(ERR,-5.0)
      ERR=AMIN1(5.0,TEMPP)
      FER=ERR*0.12
      IF(XM.EQ.0.)XM=0.0001
      AHER=HER*RAD/(XM*6080.2)
      TEMPP=AMAX1(AHER,-0.7)
      TEMP=AMIN1(0.7,TEMPP)
      FHER=TEMP*0.22357
      RETURN
      END
```

```
      IMAGE DIALS
C
C***  SUBROUTINE TO DISPLAY THE INSTRUMENT PANEL
C
      INTEGER $FTIMX
      IMPLICIT FRACTION(F)
      COMMON/FRAC/FV,FBNK,FPICH,FA,FVZ,FHDG,FADF,FVOR,FCPICH
      COMMON/FRAC/FER,FHER,DME(6),ALT(7)
      LINKAGE PTR(8),LYNE(4),PNTR(20)
      LINKAGE GSI(8),LOCI(5),ADFN(18),VORN(10),HDNG(5)
C
C***  ADD FTIMX TO ITIME, TO UPDATE THE DATA-UPDATE CLOCK
C
      $ITIME=$ITIME+$FTIMX
      POSCHAR(0.2417F,-0.01434F,-0.3F,"0S53")
      POSCHAR(DME)
      POSCHAR(ALT)
      LDY(0.F)
      TABLE2D(HDNG)
      LDX(-0.75F)
      LDY(0.49F)
      LSCL(0.275F)
      LRZ(FV)
      TABLE2D(PNTR)
      LDX(0.71F)
      LDY(0.52F)
      LSCL(0.28F)
      LRZ(FA)
      TABLE2D(PNTR)
      LDX(0.71826F)
      LDY(-0.20575F)
      LSCL(0.285F)
      LRZ(FVZ-0.5F)
      TABLE2D(PNTR)
      LDX(0.F)
      LDY(-0.323F)
      LSCL(0.33F)
      LRZ(FHDG)
      TABLE2D($CCARD)
      ROTZ(-0.100388F)
A            2DT BUG
      ROTZ(-0.19444F)
      DX(FER)
      TABLE2D(LYNE)
      LRZ(FHDG)
      LDX(-0.745F)
      LDY(-0.212F)
      LSCL(0.275F)
      ROTZ(FADF)
      TABLE2D(ADFN)
      ROTZ(FVOR-FADF)
      TABLE2D(VORN)
      LRZ(FHDG)
      TABLE2D($CCARD)
      LDX(0.F)
```

```
LD/(0.66F)
LSCL(0.32F)
LRZ(FBNK)
TABLE2D(PTR)
LSCL(1.0F)
ROTX(FPICH)
LAI(16B,1.0F)
LAI(17B,0.5F)
TABLE3D($HRZON)
RETURN
DATA2D(LYNE)
ZSET(0.0F)
LINE(0.F,0.43F,0.F,-0.5286F)
ENDLIST
ENDDATA
DATA2D(PNTR)
ZSET(0.0F)
MOVE(0.0F,-0.5F)
DRAW(-0.02F,-0.56F)
DRAW(-0.02F,-0.74F)
DRAW(0.0F,-0.8F)
DRAW(0.02F,-0.74F)
DRAW(0.02F,-0.56F)
DRAW(0.0F,-0.5F)
DRAW(0.0F,-0.26F)
DRAW(0.04F,-0.2F)
DRAW(0.04F,0.0F)
DRAW(0.06F,0.1F)
DRAW(-0.06F,0.1F)
DRAW(-0.04F,0.0F)
DRAW(-0.04F,-0.2F)
DRAW(0.0F,-0.26F)
MOVE(0.0F,0.0F)
DRAW(0.0F,0.0F)
ENDLIST
ENDDATA
DATA2D(GSI)
ZSET(0.0F)
MOVE(-0.3F,0.55F)
DRAW(-0.36F,0.59F)
DRAW(-0.3F,0.63F)
MOVE(-0.3F,-0.30F)
DRAW(-0.36F,-0.34F)<
DRAW(-0.3F,-0.38F)
ENDLIST
ENDDATA
DATA2D(LOCI)
ZSET(0.0F)
MOVE(-0.04F,0.16F)
DRAW(0.0F,0.12F)
DRAW(0.04F,0.16F)
ENDLIST
ENDDATA
DATA2D(ADFN)
ZSET(0.0F)
```

```
      MOVE(-0.1F,0.5F)
      DRAW(-0.1F,-0.7F)
      DRAW(0.0F,-0.8F)
      DRAW(0.1F,-0.7F)
      DRAW(0.1F,0.5F)
      DRAW(-0.14F,0.5F)
      DRAW(0.0F,0.8F)
      DRAW(0.14F,0.5F)
      DRAW(0.1F,0.5F)
      MOVE(0.0F,0.9F)
      DRAW(0.0F,0.8F)
      MOVE(0.0F,0.0F)
      DRAW(0.0F,0.0F)
      MOVE(0.0F,-0.8F)
      DRAW(0.0F,-0.9F)
      ENDLIST
      ENDDATA
      DATA2D(VORN)
      ZSET(0.0F)
      MOVE(0.0F,0.8F)
      DRAW(-0.04F,0.6F)
      DRAW(-0.04F,-0.8F)
      DRAW(0.04F,-0.8F)
      DRAW(0.04F,0.6F)
      DRAW(0.0F,0.8F)
      MOVE(0.0F,0.9F)
      DRAW(0.0F,-0.9F)
      ENDLIST
      ENDDATA
A     ADEPT
BUG: 0
    1631224426;1631221261;1314423345;1631224427
    2000026743;1146211662;1146215461;0631414431
    0767613244;1146215461;6631462316;6314655465
    6000013054;6000013055;6000013055;7000005462
    7000005463;7000005463;1000072314;1000072315
    1000072315;2000064022;2000064023;1777764023
FORTRAN
      DATA2D(PTR)
      ZSET(0.F)
      MOVE(0.F,0.8333F)
      DRAW(-0.15F,0.6667F)
      DRAW(0.15F,0.6667F)
      DRAW(0.0F,0.8333F)
      ENDLIST
      ENDDATA
      DATA2D(HDNG)
      ZSET(0.0F)
      MOVE(-0.015F,0.03625F)
      DRAW(0.F,0.0025F)
      DRAW(0.015F,0.03625F)
      ENDLIST
      ENDDATA
      RETURN
      END
```

ORIGINAL PAGE IS
OF POOR QUALITY

REFERENCES

1. Kayton, M. and W. R. Fried, editors. Avionics Navigation Systems. John Wiley and Sons, Inc., New York. 1969.

2. Report of the Department of Transportation Air Traffic Control Advisory Committee. Volumes I and II. December, 1969.

3. Strategic Control Algorithm Development, Volume I: Summary. Boeing Commercial Airplane Co., Contract DOT-TSC-538-1. August, 1974.

4. Strategic Control Algorithm Development, Volume II: Technical Report. Boeing Commercial Airplane Co., Contract DOT-TSC-538-2. August, 1974.

5. Strategic Control Algorithm Development, Volume III: Strategic Algorithm Report. Boeing Commercial Airplane Co., Contract DOT-TSC-538-3. August, 1974.

6. Corley, Charles J. A Simulation Study of Time-Controlled Aircraft Navigation. S. M. Thesis, Dept. of Electrical Engineering, M.I.T. December, 1974.

7. Hemesath, N. B., J. M. H. Bruckner, and others. Three and Four Dimensional Area Navigation Study Simulation and Systems Development. Collins Radio Co., Contract DOT-FA72WA-3123. April, 1974.

8. Connelly, Mark E. The Role of the Airborne Traffic Situation Display in Future ATC Systems. Electronic Systems Laboratory, M.I.T. Report ESL-P-483. May, 1972.

9. Etkin, Bernard. Dynamics of Atmospheric Flight. John Wiley and Sons, Inc., New York. 1972.

10. Connelly, Mark E. Simulation of Aircraft. Electronic Systems Laboratory, M.I.T. Report 7591-R-1. February,1959.

11. Dynamics of the Airframe, Volume II, Fundamentals of Design and Piloted Aircraft Flight Control Systems, BoAer Report AE-61-4, Washington, D. C. Bureau of Aeronautics, U. S. Department of the Navy. February, 1953.

12. Borden, Norman E., Jr. Jet-Engine Fundamentals. Hayden Book Co., New York. 1967.

13. The Aircraft Gas Turbine Engine and Its Operation. Pratt and Whitney Aircraft. Part No. PWA182408. May, 1974.

14. Hill, P. G. and C. R. Peterson. Mechanics and Thermodynamics of Propulsion. Addison-Wesley Publishing Co. Inc., Reading, Mass. 1965.

15. Boeing 707 Operating Manual. Pan American and American Airlines.

16. U. S. Standard Atmosphere, 1962. U. S. Government Printing Office, Washington, D. C. December, 1962.

17. Pecsvardi, Thomas. Four-Dimensional Guidance Algorithms For Aircraft In An Air Traffic Control Environment. National Aeronautics and Space Administration. Report No. NASA TN D-7829. Washington, D. C. March, 1975.

18. Vietor, Carl W. "Time, Space, and Energy Management in the Airways Traffic Control Medium," Journal of the Institute of Navigation. Volume 20, No. 2, pp. 159-169. Summer, 1973.

19. Athans, Michael. "The Discrete Time Linear-Quadratic-Gaussian Stochastic Control Problem," Annals of Economic and Social Measurement. pp. 449-491. 1/4, 1972.

20. Athans, Michael. "The Role and Use of the Stochastic Linear-Quadratic-Gaussian Problem in Control System Design," IEEE Transactions on Automatic Control. Volume AC-16, No. 6, pp. 529-552. December, 1971.

21. Bryson, A. E., Jr., and Yu-Chi Ho. Applied Optimal Control. Blaisdell Publishing Co., Waltham, Mass. 1969.

22. Brockett, Roger W. Finite Dimensional Linear Systems. John Wiley and Sons, Inc. New York, 1970.

23. Ephrath, Arye R. Pilot Performance in Zero-Visibility Precision Approach. Ph. D. Thesis, Man-Vehicle Laboratory, Dept. of Aeronautics and Astronautics, M.I.T. June, 1975.

24. Programmer's Reference Manual for the Adage Monitor and Operating System: Adage Graphics Terminal. Adage, Inc. Boston, Massachusetts.

25. Sandell, Nils R. and Michael Athans. Modern Control Theory. A Self-Study Subject. Computer Manual. Center For Advanced Engineering Study, M.I.T. 1974.